BEHAVIOUR OF HTPB-POLYURETHANE ELASTOMER MATERIAL REINFORCED WITH MICRO AND NANO PARTICLES

A THESIS SUBMITTED TO
THE GRADUATE SCHOOL OF NATURAL AND APPLIED SCIENCES
OF
MIDDLE EAST TECHNICAL UNIVERSITY

BY

EMRE ERTEN

IN PARTIAL FULFILLMENT OF THE REQUIREMENTS
FOR
THE DEGREE OF MASTER OF SCIENCE
IN
METALLURGICAL AND MATERIALS ENGINEERING

AUGUST 2022

Approval of the thesis:

BEHAVIOUR OF HTPB-POLYURETHANE ELASTOMER MATERIAL REINFORCED WITH MICRO AND NANO PARTICLES

submitted by **EMRE ERTEN** in partial fulfillment of the requirements for the degree of **Master of Science** i**n Metallurgical and Materials Engineering, Middle East Technical University** by,

Prof. Dr. Halil Kalıpçılar
Dean, Graduate School of **Natural and Applied Sciences** _____

Prof. Dr. Ali Kalkanlı
Head of the Department, **Metallurgical and Materials Eng.** _____

Prof. Dr. Cevdet Kaynak
Supervisor, **Metallurgical and Materials Eng., METU** _____

Assoc. Prof. Dr. Taner Atalar
Co-Supervisor, **Defense Res. and Dev. Institute, TUBITAK** _____

Examining Committee Members:

Prof. Dr. Necati Özkan
Polymer Science and Technology, METU _____

Prof. Dr. Cevdet Kaynak
Metallurgical and Materials Eng., METU _____

Assist. Prof. Dr. Cemal Merih Şengönül
Manufacturing Engineering, Atılım University _____

Assist. Prof. Dr. Yusuf Keleştemur
Metallurgical and Materials Eng., METU _____

Assist. Prof. Dr. Irmak Sargın
Metallurgical and Materials Eng., METU _____

Date: 29.08.2022

I hereby declare that all information in this document has been obtained and presented in accordance with academic rules and ethical conduct. I also declare that, as required by these rules and conduct, I have fully cited and referenced all material and results that are not original to this work.

Name Last name : Emre Erten

Signature :

ABSTRACT

BEHAVIOUR OF HTPB-POLYURETHANE ELASTOMER MATERIAL REINFORCED WITH MICRO AND NANO PARTICLES

Erten, Emre
Master of Science, Metallurgical and Materials Engineering
Supervisor: Prof. Dr. Cevdet Kaynak
Co-Supervisor: Assoc. Prof. Dr. Taner Atalar

August 2022, 88 pages

Hydroxyl-Terminated-Polybutadiene Polyurethane (HTPB-PU) elastomer materials are mainly used in the "liner" layer of solid propellant rocket motor cases. The required levels of mechanical and thermal properties are obtained by reinforcing this elastomer matrix with approximately 10 wt% micron-sized carbon black (mCB) particles. Therefore, the main purpose of this study was to investigate effects of mCB alone and then when used together with 3 wt% nano-sized carbon black (nCB), micron-sized zirconia ($mZrO_2$), nano-sized titania ($nTiO_2$) and silica ($nSiO_2$) on the mechanical and thermal properties of HTPB-PU elastomer matrix. The main technique used for the production of unfilled and filled HTPB-PU specimens was mechanical mixing.

Tension tests conducted at 70°C, 23°C and -40°C revealed that use of all filler combinations improved all mechanical properties of HTPB-PU elastomer matrix at all temperatures. On the other hand, compared to others, replacement of total 10 wt% mCB particles with 3 wt% nCB particles resulted in highest level of improvements. Various thermal analyses conducted for all specimen compositions indicated that use

of 10 wt% total filler content had slight influences on the thermal properties of the HTPB-PU elastomer matrix.

Keywords: Hydroxyl-Terminated-Polybutadiene (HTPB), Polyurethane (PU), Carbon Black, Zirconia, Titania, Silica

ÖZ

MİKRO VE NANO PARÇACIKLARLA GÜÇLENDİRİLMİŞ HTPB-POLİÜRETAN ELASTOMER MALZEMENİN DAVRANIŞI

Erten, Emre
Yüksek Lisans, Metalurji ve Malzeme Mühendisliği
Tez Yöneticisi: Prof. Dr. Cevdet Kaynak
Ortak Tez Yöneticisi: Doç. Dr. Taner Atalar

Ağustos 2022, 88 sayfa

Hidroksil-Sonlu-Polibütadien Poliüretan (HTPB-PU) elastomer malzemeler genel olarak katı yakıtlı roket motoru gövdelerinde "astar" tabakasında kullanılır. Gerekli mekanik ve termal özellik seviyeleri, bu elastomer matrisin ağırlıkça yaklaşık %10 mikron boyutlu karbon siyahı (mCB) parçacıkları ile güçlendirilmesiyle elde edilir. Bu nedenle, bu çalışmanın temel amacı, mCB'nin tek başına ve daha sonra ağırlıkça %3 nano boyutlu karbon siyahı (nCB), mikron boyutlu zirkonya ($mZrO_2$), nano boyutlu titanya ($nTiO_2$) ve silika ($nSiO_2$) ile birlikte kullanıldığında HTPB-PU elastomer matrisinin mekanik ve termal özellikleri üzerine etkilerini araştırmaktır. Dolgusuz ve dolgulu HTPB-PU numunelerinin üretimi için kullanılan ana teknik mekanik karıştırma yöntemidir.

70°C, 23°C ve -40°C'de yapılan çekme testleri, tüm dolgu kombinasyonlarının HTPB-PU elastomer matrisinin tüm mekanik özelliklerini tüm sıcaklıklarda arttırdığını göstermiştir. Öte yandan, diğerlerine kıyasla, toplam ağırlıkça %10 mCB parçacıklarının %3 nCB parçacıkları ile değiştirilmesi en yüksek düzeyde iyileştirme sağlamıştır. Tüm numune bileşimleri için yürütülen çeşitli termal analizler, ağırlıkça

%10 toplam dolgu içeriği kullanımının HTPB-PU elastomer matrisinin termal özellikleri üzerinde az oranlarda etkileri olduğunu göstermiştir.

Anahtar Kelimeler: Hidroksil-Sonlu-Polibütadien (HTPB), Poliüretan (PU), Karbon Siyahı, Zirkonya, Titanya, Silika

To my dear beloved wife

ACKNOWLEDGMENTS

I would like to express my deepest gratitude to my supervisor Prof. Dr. Cevdet Kaynak and co-supervisor Assoc. Prof. Dr. Taner Atalar for their guidance, advice, criticism, encouragements, and insight throughout the research.

I also wish to thank the members of examining committee, Prof. Dr. Necati Özkan, Assist. Prof. Dr. Cemal Merih Şengönül, Assist. Prof. Dr. Yusuf Keleştemur, and Assist. Prof. Dr. Irmak Sargın for their valuable criticism, suggestions, and comments to make this thesis better during the defense period.

I am excessively grateful to my principals Dr. Değer Çetin and Serhat Bilgen at Defense Research and Development Institute, TUBITAK for their support during the research and experimentation throughout the thesis. Additionally, I am grateful to all technicians of Energetic Materials Custom Production Division in Defense Research and Development Institute, TUBITAK for their technique supports and helps during the manufacturing of materials and experimentation. Moreover, the technical staff of Chemical Quality Control Laboratory, and Materials Quality Control Laboratory in the same institute are gratefully acknowledged for their technical assistance during the characterization of materials throughout the thesis. I also thank to the technical staff of Central Laboratory, METU for their assistance in SEM and BET analysis.

My utmost gratefulness is to my dearest parents who have always supported me for my works and who are the responsible of my achievements in my life. Deserving all the best, I am appreciated and indebted to them and my sister for their moral support and encouragements.

Beloved with whole of my heart, my deepest appreciation is to my wife without whom, this endeavor would not have been possible. Her support, encouragement and love have been the main driving force to accomplish this thesis.

TABLE OF CONTENTS

LIST OF TABLES

TABLES

LIST OF FIGURES

FIGURES

NOMENCLATURE

ABBREVIATIONS / SYMBOLS

ADN	**:**	Ammonium Dinitramide
AN	**:**	Ammonium Nitrate
AP	**:**	Ammonium Perchlorate
ASTM	**:**	American Society of Testing and Materials
BET	**:**	Brunauer-Emmett-Teller
CAS	**:**	Chemical Abstracts Service
CB	**:**	Carbon Black
Contn'd	**:**	Continued
CTBN	**:**	Carboxyl-Terminated Poly(Butadiene-c*o*-Acrylonitrile)
CTPB	**:**	Carboxyl-Terminated Polybutadiene
DBTL	**:**	Dibutyltin Dilaurate
DEHA	**:**	Di(2-Ethylhexyl) Adipate
DIOS	**:**	Diisooctyl Sebacate
DLS	**:**	Dynamic Light Scattering
DMA	**:**	Dynamic Mechanical Analysis
DOP	**:**	Di(2-Ethylhexyl) Phthalate
DSC	**:**	Differential Scanning Calorimetry
EPDM	**:**	Ethylene Propylene Diene Monomer
HMDS	**:**	Hexamethyl Disilazane
HT	**:**	1,2,6-hexanetriol
HTPB	**:**	Hydroxyl-Terminated Polybutadiene
HTPB-PU	**:**	Hydroxyl Terminated Polybutadiene-Polyurethane
HTPE	**:**	Hydroxyl-Terminated Polyether
HX-868	**:**	Benzene-1,3,5-tris((2-ethyl-aziridinyl)-carbonyl)
IDP	**:**	Isodecyl pelargonate
IPDI	**:**	Isophorone diisocyanate

i.e.	**:**	That is (Latin. *Id est*)
LOI	**:**	Limiting Oxygen Index
MAPO	**:**	Tris-(2-Methyl Aziridinyl) Phosphine Oxide
PBAN	**:**	Polybutadiene Acrylonitrile
POSS	**:**	Polyhedral Oligomeric Silsesquioxanes
PPG	**:**	Polypropylene Glycol
PTFE	**:**	Polytetrafluororethane
PU	**:**	Polyurethane
SEM	**:**	Scanning electron Microscopy
STANAG	**:**	Standardization Agreement
TEA	**:**	Triethanolamine
TGA	**:**	Thermogravimetric Analysis
TMA	**:**	Thermomechanical Analysis
TMP	**:**	Trimethylol Propane
US DoD	**:**	the United States Department of Defence
%	**:**	Percent
%/°C	**:**	Percent weight loss per degree Celsius
~	**:**	approximately
>	**:**	Bigger than
<	**:**	Smaller than
±	**:**	Plus minus
≥	**:**	Bigger and equal than
≤	**:**	Smaller and equal than
°C	**:**	Degree Celsius
°C/min	**:**	Degree Celsius per minute (Heating rate)
µm	**:**	micrometer
A_{BET}	**:**	Specific surface area from BET analysis
--►	**:**	Continuing Arrow
C=C	**:**	Carbon-Carbon double bond
C-C	**:**	Carbon-Carbon single bond

C-H	**:**	Carbon-Hydrogen single bon
C-N	**:**	Carbon-Nitrogen single bond
C-O	**:**	Carbon-Oxygen single bond
cps	**:**	Centipoise-second
d	**:**	Diameter
g	**:**	gram
g/cm^3	**:**	Grams per cubic centimeter
g/mol	**:**	Grams per mole
Hz	**:**	Hertz
kg	**:**	Kilogram
kJ/m^3	**:**	Kilojoule per cubic meter
kN	**:**	kilonewton
l	**:**	length
m	**:**	meter
m^2/g	**:**	Square meter per gram
mbar	**:**	Millibar
mg	**:**	Milligram
mg/kg	**:**	Milligram per kilogram
min	**:**	Minute
mL/min	**:**	Milliliters per minute
mm	**:**	Millimeter
mm/min	**:**	Millimeter per meter
mm/s	**:**	Millimeter per second
mol/cm^3	**:**	Mole per cubic centimeter
MPa	**:**	Megapascal
mPa·s	**:**	Millipascal-second
—NCO	**:**	Isocyanate group
NCO/OH	**:**	Ratio of total number of isocyanate groups and hydroxyl groups
N-H	**:**	Nitrogen-Hydrogen sing bond

nm	**:**	Nanometer
—OH	**:**	Hydroxyl group
pH	**:**	Potential of Hydrogen
rpm	**:**	Revolution per minute
$T_{5\%}$	**:**	Thermal degradation temperature at 5% weight loss
$T_{5\%}$	**:**	Thermal degradation temperature at 10% weight loss
$T_{25\%}$	**:**	Thermal degradation temperature at 25% weight loss
tan δpeak	**:**	Temperature at peak of *tan δ* curve
tan δ	**:**	Ratio of Loss Modulus to Storge Modulus in DMA
T_g	**:**	Glass Transition Temperature
T_{max}	**:**	Thermal degradation temperature at maximum weight loss
W/m·K	**:**	Watt per meter-Kelvin
wt%	**:**	Weight percent
μm/m·°C	**:**	Micrometer per meter-degree Celsius
ρ	**:**	Density

CHAPTER 1

INTRODUCTION

Ever since the invention of the wheel, human ingenuity has led to the discovery and development of various means for transportation. One of them is called “propulsion” which means to push or thrust forward, i.e. a force acting to move an object initially at rest or to change the velocity of a moving one [1, 2]. A propulsion system is a machine designed to generate thrust according to Newtons third law of action (action-reaction) by accelerating a working fluid of gas at the engine. There are four main types of propulsion systems: (i) the propeller, (ii) the turbine or jet, (iii) the ramjet, and (iv) the rocket. The first three uses surrounding air as working fluid, but in the rocket propulsion the working fluid is exhaust gases [3].

1.1 Chemical Rocket Propulsion Systems

In rocket propulsion, thrust is produced by an accelerated working fluid, the propellant, which is entirely stored within the flying vehicle. Rocket propulsion systems can be classified in several ways. Based on the source of energy utilized in the system, there are four main categories: nuclear energy, solar energy, electrical energy, and chemical energy. These energies are transferred to gaseous species and converted into kinetic energy by exerting forces at the surfaces exposed to exhaust gases which provides thrust [2].

Chemical energy originating from combustion of two chemical entities, a fuel, and an oxidizer, in the rocket engine is the most widely used type of rocket propulsion. The reaction between the fuel and the oxidizer results in formation of gaseous products and huge amount of heat. Gaseous species produced from this reaction is

heated by the heat generated and hot gases are expelled through the exit of reaction chamber, the nozzle, while exerting force to the rocket [2].

Chemical rocket propulsion systems can be classified according to the physical state of the stored propellant. These systems are (i) Liquid Propellant Rocket Engines, (ii) Solid Propellant Rocket Motors, and (iii) Hybrid Propellant Rocket Propulsion Systems. It should be appropriate to mention that, historically, the term “engine” is used for liquid propellant rocket propulsion systems while the term “motor” is used for solid propellant rocket propulsion. The difference arises from the fact that each system was developed by different research groups [2].

1.2 Solid Propellant Rocket Motors

In solid propellant rocket motors, thrust is provided by the solid propellant, or charge, which is already present within the motor. The propellant, also called the grain, is chemically formulated to include both the fuel and the oxidizer that would be burned completely [2].

There are two types of solid rocket motors based on installation of solid propellant: “cartridge-loaded” and “case-bonded”. In cartridge-loaded solid rocket motors, propellant is prepared as solid mass outside the motor and inserted into the rocket motor. This type is especially preferred for rocket motors with small dimensions and when large numbers are required. In case-bonded solid rocket motors, the propellant is prepared as slurry through chemical processes, then cast into rocket motor and solidified. They are especially used for large-sized rocket motors for longer ranges and high payload carrying capacities [2, 4].

Main components of a typical case-bonded solid rocket motors [5], as shown in Figure 1.1, are; the case, the insulator, the liner, the propellant, the igniter, and the nozzle. Igniter is a pyro-technique to initiate the burning of the solid propellant and nozzle is used to adjust pressure inside the motor and to control the expansion of exhaust gases [2]. Other parts are briefly explained below.

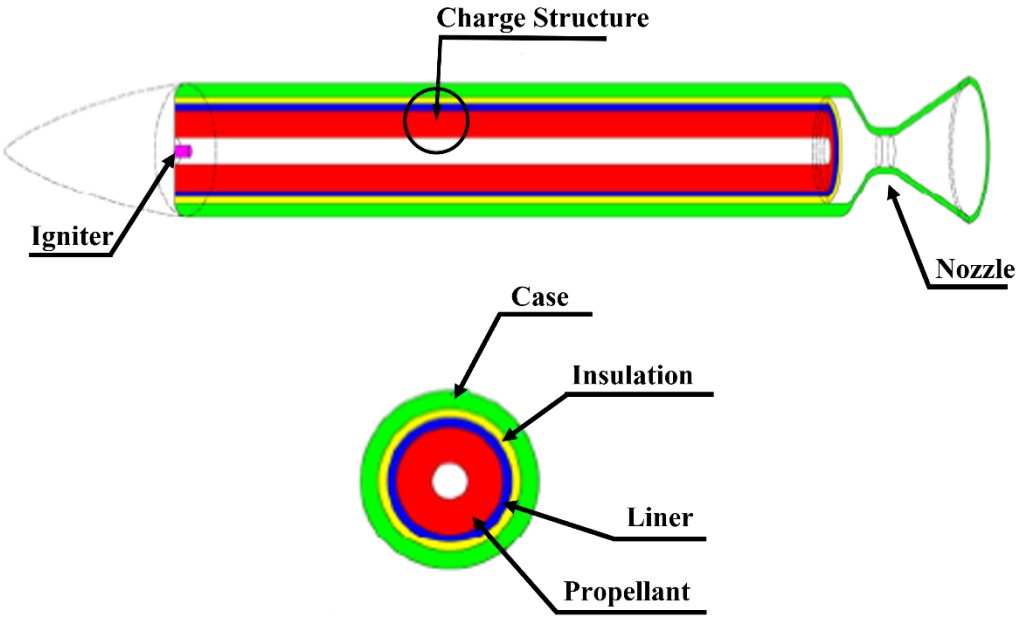

Figure 1.1 A schematic of a solid propellant rocket motor [5].

(i) Case

Case is the outer-most part of the motor acting as pressure vessel with high levels of internal pressure developed during propellant burning. Due to the very high hoop strength requirement, the materials used for the case are high strength metals with or without filament-wound composite layers [2, 6].

(ii) Insulator

Insulator is the layer applied to the inner surfaces of the motor case. Its primary function is to limit the transfer of heat generated and temperature rise during combustion of the propellant. It is made of thermally insulating adhesive materials which should be resistant to erosion of hot gases such as neoprene, butyl rubber and ethylene propylene diene monomer (EPDM) [2,7-10].

(iii) Propellant

The energetic component of the solid rocket motor is the propellant layer, once ignited, hot gases forming via chemical reactions are expelled from the nozzle providing momentum to the rocket. There are two types of materials/chemicals used for the solid propellants. One type is the mixtures of nitroglycerine and nitrocellulose which are also called double-base propellants. Other type is the mixture of (i) a synthetic binder such as polybutadiene acrylonitrile (PBAN), hydroxyl-terminated polybutadiene (HTPB), polyurethane (PU), carboxyl-terminated polybutadiene (CTPB), (ii) an oxidizer such as ammonium perchlorate (AP), ammonium nitrate (AN), ammonium dinitramide (ADN), and (iii) a powdered metallic fuel (such as aluminum) [2].

(iv) Liner

Liner is the layer between the insulator and the propellant grain to enhance bonding of these layers. It is sticky, relatively low density, flexible, non-self-burning, and rubber-like material which is applied inside the motor prior to propellant casting [2]. Since this thesis is about the liner layer, it would be discussed below in detail.

1.3 Function of the Liner Material

As stated above, “liner” is a thin adhesive layer between the “insulator” and the “propellant”. Its main function is to achieve an adequate bonding with sufficient strength to withstand all the operational and environmental stresses developed during the life of the rocket motor, so that, its structural integrity can be maintained [4, 8, 11-14]. Those stresses develop; due to (i) thermal cycling, (ii) handling and storage, (iii) inertia of the propellant especially at upper stages during acceleration, and (iv) rapid pressurization after ignition [7, 12].

Due to different chemical formulation and material characteristics of the insulator and the propellant, there exists an incompatibility and migration of chemical species across the liner which affects its characteristics and performance [7, 8, 10, 11]. Diffusion of chemical species across the liner is especially important for the adhesion quality between the insulator and the propellant. Thus, another important function of the liner material is to act as a barrier to inhibit the unwanted diffusion of mobile species from the propellant to the insulator [8, 10].

1.4 HTPB-PU Elastomer System as Liner Material

There have been various liner materials developed so far to meet the requirements of solid propellant rocket motor systems. These materials include epoxy-based resins, polyester-based resins, and polyurethane-based resins. However, low temperature properties and better aging characteristics of filled polyurethane-based resin systems have made them superior compared to their epoxy and polyester-based analogues [15]. Several prepolymers have been utilized in the formation of polyurethane-based liner material systems. Polypropylene glycol (PPG) [2], carboxyl-terminated poly(butadiene-*co*-acrylonitrile) (CTBN) [9], carboxyl-terminated polybutadiene (CTPB) [16], hydroxyl-terminated polyether (HTPE) [17], and especially hydroxyl-terminated polybutadiene (HTPB) [4-15] have been frequently used prepolymers for the production of polyurethane-based elastomeric liner material systems.

Among these systems mentioned above, hydroxyl terminated polybutadiene-polyurethane (HTPB-PU) system have been considered as one of the most ideal one due to; (i) its capability to mix with higher amounts of fillers, (ii) having better low temperature properties and aging characteristics, (iii) superior hydrolytic stability and mechanical strength compared to others [2, 7, 15, 18]. Another factor making HTPB-PU elastomer system as efficient liner material is its compatibility and better adhesion between the propellant and the liner [9, 12, 19, 20].

It is known that HTPB is also used as a binder material in many solid propellant mixtures. Thus, the use of the same chemical (i.e. HTPB) in both liner material and propellant material also diminishes the problem of concentration differences leading to migration of species at the interface. This migration problem could be very harmful for the bond quality and the material properties across the interfacial region [7, 9-12, 18-20]. Therefore, HPTB-PU elastomer system is considered as an optimum liner material system for the solid propellants having HTPB binder.

As shown in Figure 1.2(a), a urethane group can be obtained by the reaction between a hydroxyl (—OH) and an isocyanate (—NCO) reactive group. Of course, as shown in Figure 1.2(b), for the formation of a continuous macromolecule of urethane, i.e. "polyurethane", certain oligomers of "polyols" and "polyisocyanates" would be required [4, 6, 8-10, 13, 15, 18-20, 21-25].

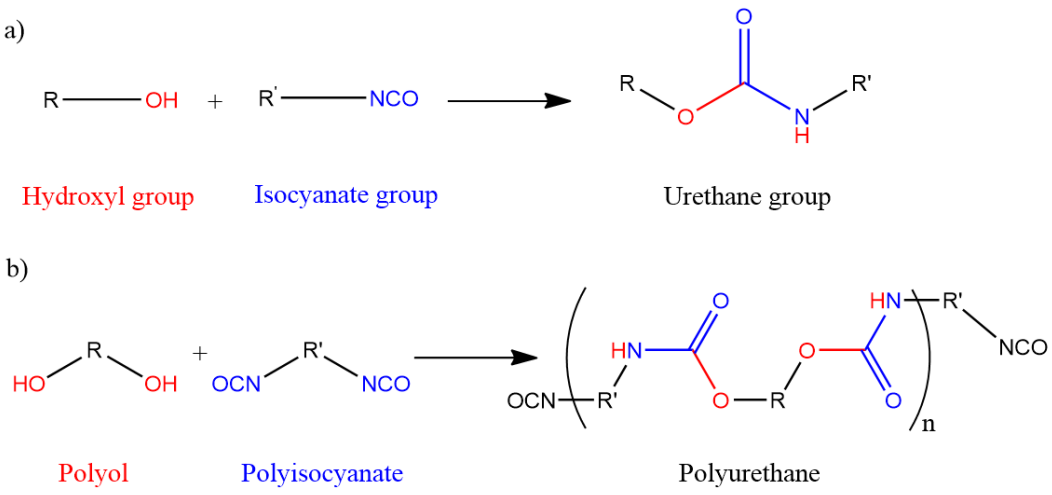

Figure 1.2 Formation of (a) urethane group via reaction of hydroxyl and isocyanate groups, and (b) polyurethane from reaction of a polyol and a polyisocyanate.

In the synthesis of HTPB-PU liner material systems, the polyol oligomer chosen is the hydroxyl-terminated polybutadiene (HTPB) as shown in Figure 1.3(a), while the polyisocyanate oligomer chosen is generally isophorone diisocyanate (IPDI) as shown in Figure 1.3(b) [4, 6-8, 10, 15, 18-21]. The resultant macromolecular structure of the HTPB-PU elastomer liner material system is shown in Figure 1.3(c).

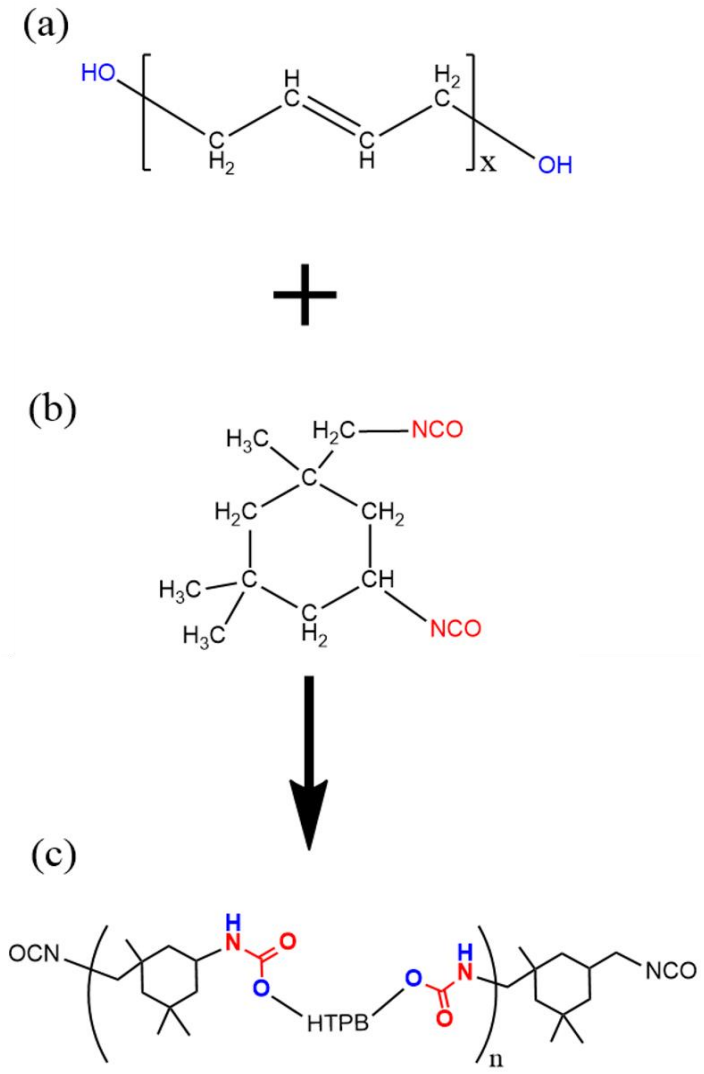

Figure 1.3 Reaction of (a) HTPB polyol and (b) IPDI polyisocyanate to form (c) HTPB-PU elastomer material.

In the preparation of HTPB-PU elastomeric liner material system, many other ingredients such as plasticizers, bonding agents, crosslinking agents, catalysts, and fillers are added. Purposes and brief details of these ingredients and importance of certain chemical group ratios are explained below.

(i) NCO/OH and Triol/Diol Ratios

NCO/OH and Triol/Diol ratios are considered as certain parameters in the design of liner material systems. NCO/OH ratio is the ratio of total number of isocyanate groups and hydroxyl groups in the system. It is stated that mechanical, thermal, and adhesive properties of liner material systems can be tailored by adjusting NCO/OH ratio of the system [20]. For example, liner materials having more isocyanate groups (NCO/OH>1) and solid propellant mixture having more hydroxyl groups (NCO/OH<1) could form a reactive bond at the liner-propellant interface [24].

Triol/Diol ratio is the ratio of the number of triol molecules (having three hydroxyl groups on single molecule) and diol molecules (having two hydroxyl groups on single molecule) in the HTPB-PU part of the system. Since this ratio is related to the crosslinking points in the system, then mechanical, thermal, and adhesive properties of the liner can also be tailored by adjusting this ratio [20, 21, 28].

(ii) Plasticizers

Plasticizers are low molecular weight liquid organic ingredients added to the liner system to enhance percent elongation at low temperatures, as well as to decrease overall viscosity of the system. [2, 10]. Being non-reactive, plasticizers can migrate from the propellant to the liner due to concentration differences across the interface. This can be inhibited by using the same type of plasticizer both in the liner material and the propellant formulations [2, 11]. Use of plasticizers also facilitates adding more amount of fillers to the liner materials, so that desired mechanical properties can be attained [19]. Isodecyl pelargonate (IDP), di(2-ethylhexyl) adipate (DEHA),

diisooctyl sebacate (DIOS), and di(2-ethylhexyl) phthalate (DOP) have been frequently used plasticizers in HTPB-PU based liner materials [8-10, 13, 20-22, 24, 25, 26].

(iii) Bonding Agents

Bonding agents, also known as bond promoters, provides enhanced adhesion between the propellant and the liner layers by physical and chemical bond formation at the interface. HX-868 [Benzene-1,3,5-tris((2-ethyl-aziridinyl)-carbonyl)], and MAPO [Tris-(2-methyl aziridinyl) phosphine oxide] are two aziridine based chemicals being the most widely used bonding agents in liner material formulations [8, 13, 20, 24, 25, 27].

(iv) Crosslinking Agents

Introduction of crosslinking agents into the HTPB-PU based liner systems can be done either by adding short polyols with functionality greater than two as the chain extender or by adding triols into the mixture [20]. Rigid polyurethanes are highly cross-linked structures while low levels of crosslinking leads to flexible structure [28]. Addition of low molecular weight triols improves crosslinking degree of the liner system and hinders migration of plasticizers from the propellant layer [8]. Trimethylol propane (TMP), triethanolamine (TEA), and 1,2,6-hexanetriol (HT) are the examples of crosslinking agents utilized in liner materials [4, 15, 18, 20, 21].

(v) Catalysts

Formation of urethane group through reaction between isocyanate and hydroxyl groups can be catalyzed by certain organometallic salts, especially tin based ones, such as dibutyltin dilaurate, stannous octoate and tin mercaptides [2]. Adding small amounts of these catalysts can be used to control the duration of reactions during the formation of HTPB-PU liner material system.

(vi) Fillers

It is known that, although use of plasticizers, bonding agents, crosslinking agents, and catalysts are significant in the performance of the liner material systems; addition of certain amount of inorganic "filler" particles into the liner material formulations is considered as one of the most critical factor for the overall performance of liner material systems, including the HTPB-PU system [4, 5, 7-10, 18-26, 29, 31-34].

Fillers might have significant influences on the mechanical properties [9, 13, 15, 18-21], thermal properties [4, 15, 18, 19,21], rheological properties [9, 13, 21, 29] of the liner material, as well as its adhesion quality with the propellant layer [4, 9, 13, 15, 18, 19]. Fillers might also decrease the level of migration of plasticizer molecules from the propellant layers [18, 23, 30].

The traditional filler materials used in the liner formulations for many years are the different size and grades of "carbon black" particles [9, 13-15,18-21]. On the other hand, use of other alternatives such as antimony trioxide, titania, silica, zirconia, and alumina, etc. are under investigation [4, 18, 19, 21, 23, 32]. These filler particles could be used either in micron or nano sized fillers [4, 5, 7-10, 18-26, 29, 31-34].

Since the main purpose of this thesis is to investigate effects of micron and nano sized carbon black particles alone and together with other alternative filler particles on the performance of HTPB-PU liner material system, the related literature would be explained in the next section.

1.5 Literature Survey on the Effects of Fillers in HTPB-PU Elastomer Materials

Literature review revealed that there are limited number of reported research investigating the effects of micro and nanoparticles on the performance of HTPB-PU based elastomer materials; which are summarized below. Several properties of these elastomer materials reported are tabulated in Table 1.1 and Table 1.2.

Quagliano *et al.* [31] studied mechanical and swelling properties of HTPB-PU based liner material filled with 5 wt% nanoclay, and 20 wt% micron-sized TiO_2, ZrO_2 and ZnO particles. Nanoclay was reactive one (Cloisite 20A) with quaternary ammonium ions. Crosslink density of unfilled HTPB-PU was found to be 1.4×10^{-4} mol/cm^3, and this value was increased two-fold with TiO_2, one-fold with ZrO_2 and ZnO, while decreased with the incorporation of nanoclay. It was stated that nanoclay particles hinder the formation of chemical and physical crosslinks. Tensile strength (1.06 MPa) and elongation at break (707%) values of unfilled HTPB-PU changed with particles of TiO_2 as 0.67 MPa and 500%, with ZrO_2 as 1.33 MPa and 186%, with ZnO as 1.81 MPa and 237%, and with nanoclay as 1.48 MPa and 636%, respectively.

Ross *et al.* [32] also studied mechanical properties, especially elastic modulus of HTPB-PU with 20 wt% fillers of TiO_2 (10-15 μm), carbon black (1.5 μm), lithopone (2-4 μm), $CaCO_3$ (1.5 μm), ZnO (0.4 μm) and 5 wt% nanoclay (Cloisite 20A). Nanoclay was further modified by adding hexamethyl disilazane (HMDS) to make hydrophobic nanoclay. Young's modulus value of unfilled HTPB-PU (0.50 MPa) changed to 1.08 MPa with TiO_2, 1.81 MPa with ZnO, 1.68 MPa with lithophone, 2.17 MPa with $CaCO_3$, 2.82 MPa with carbon black, 3.3 MPa with nanoclay, and 0.5 MPa with hydrophobic nanoclay.

Chen *et al.* [13] investigated especially effects of several fillers on the bonding behavior of HTPB-PU based liner to the propellant. Although the amount of loading level of each filler was not stated, carbon black and zinc dimethacrylate increased viscosity of the HTPB-PU liner material too much, so that, casting was not possible. Bonding strength values of the liner material with Fe_2O_3, talcum, zinc dimethacrylate, molecular sieve, magnesia, and ZnO were 0.689 MPa, 0.655 MPa, 0.592 MPa, 0.872 MPa, 0.816 MPa, and 0.716 MPa, respectively. The highest bonding strength obtained was with molecular sieve owing to its porous structure and surface hydroxyl groups interacting with the isocyanate groups present in the structure of HTPB-PU system.

Kim *et al.* [33] used three different polyhedral oligomeric silsesquioxanes (POSS) nanoparticles. The non-reactive one was octaisobutyl POSS (POSS-1), while two reactive ones were trans-cyclohexanediol isobutyl POSS (POSS-2) and 1,2-propaediol isobutyl POSS (POSS-3). Tensile strength of unfilled HTPB-PU (0.51 MPa) become 0.13 MPa with POSS-1 (50 wt%), 1.19 MPa with POSS-2 (23 wt%), and 0.97 MPa with POSS-3 (33 wt%). DSC analysis revealed that glass transition temperature of HTPB-PU was -80.4°C; this transition with POSS-1, POSS-2, and POSS-3 were -82.8°C, -80.2°C, and -82.1°C, respectively. TGA analysis showed that decomposition temperature at 5 wt% loading was decreased from 367.7°C to 281ºC with POSS-1, to 310°C with POSS-2, and to 303.3°C with POSS-3.

Grythe *et al.* [23] conducted modeling and experimental studies on the diffusion of several species from the propellant material across HTPB-PU liner material. Carbon black and TiO_2 particles were incorporated as fillers at different loadings (0 to 40 wt%) to reveal their effects on diffusion. It was stated that diffusion of molecular species was hindered by these particles due to the "obstruction effect" phenomenon. Barrier property of carbon black particles was found to be more effective than TiO_2 particles, and this behavior was attributed to the larger specific surface area and adsorbent properties of carbon black particles.

Dubois *et al.* [34] studied effects of bisphenol-A coated silica particles on the mechanical properties. Elastomer materials were obtained by mixing HTPB-PU system with treated and untreated silica particles (up to 22 wt%). It was observed that even surface coated silica particles tended to agglomerate during the mixing process at higher loadings. Low loadings of silica (e.g. 2.5 wt%) dispersed more uniformly. At this loading, untreated silica resulted in tensile strength and percent elongation at break values of 0.792 MPa and 136.6%; while surface coated silica led to 0.919 MPa and 128.5%, respectively. At higher loadings, these properties decreased considerably.

Navale *et al.* [4] investigated effects of using two different fillers together; that is, antimony trioxide (Sb_2O_3) and carbon black particles together in HTPB-PU based

liner material. Two liner compositions were prepared: one with 24 wt% Sb_2O_3 plus 10 wt% CB, and the other with 10 wt% Sb_2O_3 plus 10 wt% CB. Liner with higher Sb_2O_3 amount had better flame retardancy performance determined by limiting oxygen index (LOI) measurements. They also indicated that tensile strength of this composition (2.8-3.3 MPa) was higher than low Sb_2O_3 content composition (2.6-2.9 MPa). Interfacial performance of the liner with higher Sb_2O_3 content was also proved to be suitable at the propellant operating temperature range (-20°C and +50°C).

Kakade *et al.* [18] conducted a comprehensive study on the performance of HTPB-PU based elastomer formulations with various particles. Carbon black with different grades (N770, N550, N330) were chosen as main filler while metal oxides (TiO_2, Al_2O_3, SiO_2), silicates (talc, mica, kaolin, lithopone asbestos), organic compounds (melamine), and fire-retardant compounds (Zinc borate, sodium metaborate, $NH_4H_2PO_4$, Sb_2O_3) were incorporated as additional fillers. All fillers had particle size of 2-10 μm except carbon blacks having nanosizes. CB was used at 40 wt% loading and other fillers were used at 8 wt%. Based on tensile strength (5.6 MPa) and processability of liner formulations, N550 grade CB was chosen as the optimum one for further studies. Compared to others, Sb_2O_3 was found to be an efficient fire-retardant filler leading to also tensile strength value was of 4.9 MPa.

Benli *et al.* [21] studied performance of HTPB-PU based liners with two grades of carbon black (micron and nano sized) plus addition of SiO_2 (500 nm), Al_2O_3 (5 μm), and ZrO_2 (10 μm) particles. Tensile strength of unfilled liner was found to be 0.567 MPa. This value increased to 0.858 MPa with the addition of 10 wt% micro-carbon black and to 2.010 MPa with the addition of 10 wt% nano-carbon black. When 16 wt% of other particles were added to the liner filled with 10 wt% nano-carbon black particles, the tensile strength was determined as 2.658 MPa with SiO_2, 2.075 MPa with Al_2O_3, and 1.983 MPa with ZrO_2. Moreover, oxyacethylene ablation tests were conducted to measure erosion rate to determine relative thermal insulation effectiveness. It was stated that liner with nano-carbon black particles had lower erosion rate (0.260 mm/s) than the unfilled liner (0.467 mm/s) and the liner with micro-carbon black particles (0.324 mm/s).

Table 1.1 Several properties of HTPB-PU elastomer materials having different filler particles reported in the literature.

Main Filler	Main Filler Content (wt%)	Tensile Strength (MPa)	Tensile Modulus (MPa)	Elongation at Break (%)	Bonding Strength (MPa)	Source
No Filler	-	1.06	-	707	-	Quagliano *et. al.* (2019) [31]
TiO_2	20	0.67	-	500	-	
ZrO_2	20	1.33	-	186	-	
ZnO	20	1.81	-	237	-	
Nanoclay (Cloisite 20A)	5	1.48	-	636	-	
No Filler	-	-	0.50	-	-	Ross *et. al*. (2017) [32]
TiO_2 (10-15 um)	20	-	1.08	-	-	
ZnO (0.4 um)	20	-	1.81	-	-	
Lithophone (2-4 um)	20	-	1.68	-	-	
$CaCO_3$ (1.5 um)	20	-	2.17	-	-	
Carbon Black (1.5 um)	20	-	2.82	-	-	
Nanoclay (Cloisite 20A)	5	-	3.3	-	-	
Silanized Nanoclay (Cloisite 20A)	5	-	0.5	-	-	
Fe_2O_3	-	-	-	-	0.689	Chen *et. al.* (2014) [13]
Talcum	-	-	-	-	0.655	
Zinc Dimethacrylate	-	-	-	-	0.592	
Molecular sieve	-	-	-	-	0.872	
Magnesia	-	-	-	-	0.816	
ZnO	-	-	-	-	0.716	

Table 1.2 Several properties of HTPB-PU elastomer materials having different filler particles reported in the literature.

Main Filler	**Main Filler Content** (wt%)	**Additional Filler**	**Additional Filler Content** (wt%)	**Tensile Strength** (MPa)	**Elongation at Break** (%)	**T_g (DSC)** (°C)	**T_d (5 wt%)** (°C)	**Source**
No Filler	-	-	-	0.51	-	-80.4	367.7	Kim *et. al*. (2013) [33]
Octaisobutyl POSS	50	-	-	0.13	-	-82.8	281	
trans-cyclohexanediol isobutyl POSS	23	-	-	1.19	-	-80.2	310	
1,2-propanediol isobutyl POSS	33	-	-	0.97	-	-82.1	303.3	
SiO_2	2.5	-	-	0.792	136.6	-	-	Dubois *et. al*. (2006) [34]
Bisphenol-A coated SiO_2	2.5	-	-	0.919	128.5	-	-	
Carbon Black	10	Sb_2O_3	10	2.6-2.9	-	-	-	Navale *et. al*. (2004) [4]
Carbon Black	10	Sb_2O_3	24	2.8-3.3	-	-	-	
No Filler	-	-	-	0.567	-	-	-	Benli *et. al*. (1998) [21]
Carbon Black (300 nm)	10	-	-	0.858	-	-	-	
Carbon Black (25 nm)	10	-	-	2.010	-	-	-	
Carbon Black (25 nm)	10	SiO_2 (500 nm)	16	2.658	-	-	-	
Carbon Black (25 nm)	10	Al_2O_3 (5 um)	16	2.075	-	-	-	
Carbon Black (25 nm)	10	ZrO_2 (10 um)	16	1.983	-	-	-	
Carbon Black (N550)	48	-	-	5.60	-	-	-	Kakade *et. al*. (2001) [18]
Carbon Black (N550)	40	SiO_2 (2-10 um)	8	5.24	-	-	-	
Carbon Black (N550)	40	TiO_2 (2-10 um)	8	4.88	-	-	-	
Carbon Black (N550)	40	Sb_2O_3 (2-10 um)	8	4.92	-	-	-	
No Filler	-	-	-	0.50	250	-	-	Aslan, *MSc. Thesis* (2021) [44]
Carbon Black (300 nm)	10	-	-	0.77	260	-	-	
Carbon Black (25 nm)	10	-	-	1.75	375	-	-	
Carbon Black (25 nm)	5	Carbon Black (300 nm)	5	1.35	278	-	-	

1.6 Aim Of the Study

Although there are other applications, HTPB-PU elastomer materials are mainly used in the "liner" layer of solid propellant rocket motor cases. In this military application, the required levels of mechanical and thermal properties are obtained by reinforcing this elastomer matrix with approximately 10 wt% micron-sized carbon black (mCB) particles. As discussed in the literature survey section, other alternative fillers to replace mCB completely, or to use together with mCB particles are still under research. Today, there are limited number of reported research on the limited types of fillers. Studies on HTPB-PU elastomer material as "liner" matrix given in the literature revealed that there is no reported research to elucidate the effect of low and high temperatures on the material's mechanical properties which is important in military applications.

Therefore, from this point of view, the main purpose of this study was to investigate effects of mCB alone and then when used together with nano-sized carbon black (nCB), micron-sized zirconia ($mZrO_2$), nano-sized titania ($nTiO_2$) and silica ($nSiO_2$) on the mechanical properties of HTPB-PU elastomer matrix at three different testing temperatures: 70°C, 23°C, and -40°C. Thermal properties of HTPB-PU elastomer matrix were also investigated.

For this purpose, first of all, unfilled HTPB-PU elastomer specimens were tested and analyzed. Then, this elastomer matrix was filled with 10 wt% mCB particles alone, just like the traditional way. In order to investigate effects of nCB, $mZrO_2$, $nTiO_2$ and $nSiO_2$ fillers, certain amount of mCB were replaced with other fillers without changing the "total filler content of 10 wt%".

CHAPTER 2

EXPERIMENTAL WORK

2.1 Materials Used

(i) HTPB-PU Elastomer Used as the Matrix Material

Polyurethane (PU) based elastomer matrix materials consist of a polyol having at least two hydroxyl groups and a polyisocyanate having at least two isocyanate groups. Hydroxyl terminated polybutadiene (HTPB) is the polyol of the PU based elastomer matrix material chosen in this study. It is known that, although there are other application areas, HTPB-PU elastomer materials are the main matrix material preferred in rocket motor inner layers such as “liner” layer and/or “insulator” layer. Therefore, depending on the military application, different grades of HTPB could be chosen. In this study, used grade of HTPB is designated as R45M with CAS number of 69102-90-5; that is especially used for the “liner” layer of rocket motors.

Polyisocyanate used in this study for the synthesis of HTPB-PU matrix material was isophorone diisocyanate (IPDI). Similar to HTPB, IPDI had The United States Department of Defence (US DoD) material specification to meet the requirements of military applications.

Other chemicals used for the formation of HTPB-PU matrix material was as follows: Di(2-ethylhexyl) adipate (DEHA) is used as plasiticizer, triethanol amine (TEA) as crosslink agent, tris-(2-methyl aziridinyl) phosphine oxide (MAPO) as bonding agent, and dibutyltin dilaurate (DBTL) as catalyst. Important ratios used for the system were NCO/OH ratio as 1.1 and Triol/Diol ratio as 0.1. All the materials and

chemicals used are tabulated in Table 2.1, while certain properties of the HTPB and IPDI given in technical data sheet of their suppliers are tabulated in Table 2.2.

Table 2.1 Materials and chemicals used in the synthesis of HTPB-PU elastomer matrix material

Purpose	**Materials/Chemicals**	**Supplier**	**% Purity**
Polyol	Hydroxyl-terminated Polybutadiene (HTPB)	Cray Valley LLC, USA	≥99
Polyisocyanate	Isophorone Diisocyanate (IPDI)	Bayer, Germany	≥99.5
Plasticizer	Di(2-ethylhexyl) adipate (DEHA)	Plastifay Kimya Endüstrisi, Turkey	≥99
Crosslink Agent	Triethanol amine (TEA)	Merck, Germany	≥99
Bonding Agent	Tris-(2-methyl aziridinyl) phosphine oxide (MAPO)	Mil-Spec Industries, USA	≥99
Catalyst	Dibutyltin dilaurate (DBTL)	Merck, Germany	≥99

Table 2.2 Certain properties of the HTPB polyol and IPDI polyisocyanate given in technical data sheet of their suppliers

HTPB	• Molecular Weigth (M_n): 2800 g/mol • Having 1 wt% antioxidant (2,2'-methylene bis(4-methyl-6-*ter*-butylphenol) • Having structural isomers *trans*:*cis*:*vinyl* ratio of 0.6:0.2:0.2 • Viscosity at 30°C: 4200 cps • Glass transition temeprature: -76°C • Moisture content: < 0.1 wt% • Hydroxyl content: 2.3 groups/chain
IPDI	• NCO content: ≥ 37.5 wt% • Total chlorides: ≤ 200 mg/kg • Hydrolyzable chlorides: ≤ 200 mg/kg • Viscosity at 20°C: 10 mPa·s

(ii) Carbon Black and Metal Oxide Particles Used as the Fillers

In the first step of this thesis, effects of nano-sized carbon black (nCB) particles when used together with conventional micron-sized carbon black (mCB) particles were investigated; while in the second step effects of three metal oxide particles were studied. These particles were: micron-sized zirconia ($mZrO_2$), nano-sized titania ($nTiO_2$), and nano-sized silica ($nSiO_2$). Designations and names of these fillers with certain properties reported in the technical data sheets of their suppliers are tabulated in Table 2.3.

Table 2.3 Designations, names, and certain properties of the fillers given in technical data sheet of their supplier.

Designation	Name	Properties
mCB	Micron-sized carbon black	• Tradename/Supplier: Thermax®/Cancarb, Canada • Purity: 100% • Nitrogen surface area: 7.0-12.0 m^2/g • Ash content: max 0.20% • pH: 9.0-11.0
nCB	Nano-sized carbon black	• Tradename/Supplier: Printex®U/Orion, Luxembourg • Purity: > 99.8% • BET surface area: 92 m^2/g • Ash content: 0.02% • pH: 4.5 • Average primary particle size: 25 nm
$mZrO_2$	Micron-sized zirconia	• Supplier: Merck, Germany • Purity: 99% • Average particle size: 5 μm
$nTiO_2$	Nano-sized titania	• Supplier: Nanografi, Turkey • Purity: 99.995% • 100% anatase phase • Specific Surface Area: 220 m^2/g • Average particle size: 17 nm
$nSiO_2$	Nano-sized silica	• Supplier: Nanografi, Turkey • Purity: > 99.5% • 100% amourphous fumed silica • Specific Surface Area: 150-550 m^2/g • Average particle size: 15-35 nm

2.2 Analyses for the Particle Size Ranges and Surface Area of the Fillers

Although there are certain data about size of the fillers reported by their suppliers, it is important to confirm the data with experimental work before starting reinforcement of elastomer matrix with fillers. Therefore, for this purpose, first "Laser Diffraction" analysis and "Dynamic Light Scattering (DLS)" analyses were conducted. However, due to the problems in sample preparation and other experimental difficulties, no consistent results were obtained. Then, other possibilities were considered. For example, use of scanning electron microscopy (SEM) analysis to determine "size ranges" of the fillers; and use of Brunauer-Emmett-Teller (BET) analysis to determine "surface area" of the fillers.

(i) Scanning Electron Microscopy (SEM) Analysis

Scanning electron microscopy (SEM) was performed to get data on the size ranges and morphology of the fillers. For this purpose, 1.2 nm resolution FEI QUANTA 400F Field Emission SEM instrument was used. Before the analysis, fillers were coated with a gold-palladium alloy.

Note that, dispersion states of fillers in the HTPB-PU matrix were also studied by SEM. For this purpose, fracture surfaces of the tensile test specimens pulled at room temperature were examined.

(ii) Brunauer-Emmett-Teller (BET) Analysis

Determination of specific surface area of fillers were performed with Quantachrome Corp Autosorb-6B model instrument. Filler samples were conditioned at 90°C overnight and vacuum degassed at 65°C prior to measurements. The adsorbent gas was nitrogen, and the calculation was based on multipoint BET theory.

In this study, in order to get data on the average particle size of the fillers, results of BET analysis were also evaluated by using a mathematical model between the

"surface area" and "size" of the particles. This model has been used to determine particle size of a filler by using its specific surface area measured by BET analysis [35, 36, 37, 38]. The model is based on the idealized case where centimeter cube of a particle is fragmented into equal cubes having edge length of *l*. Total number of these cubes will be $1/l^3$. Each of these cubes will have surface area of $6l^2$. Thus, total surface area of the particles will be $(1/l^3)x(6l^2)=6/l$. If the density of the particle is ρ, then the following equation can be used to calculate the size, *d (nm)*, of the particle [38].

$$\text{Surface Area } (m^2/g) = \frac{6}{l\,(m) \times \rho(g/m^3)} \quad \Rightarrow$$

$$d\,(nm) = \frac{6000}{A_{BET}(m^2/g) \times \rho\,(g/cm^3)}$$

The equation above is also applicable to the particles with spherical shape [38]. In that case, *l* become the diamater (*d*) of the particle, ρ is the density, and surface area can be replaced with the specific surface area obtained from BET analysis (A_{BET}). It is known that many particles are irregular in shape with different sizes. Nevertheless, this equation still gives rough information about the particle size of the fillers [38]. In this study, in order to use this model density values of the fillers used were 1.80, 5.89, 3.90, and 2.20 g/cm^3 for CB, ZrO_2, TiO_2, and SiO_2, respectively.

(iii) Results of SEM and BET Analyses

SEM images given in Figure 2.1 revealed that mCB, nCB, nTiO_2, and nSiO_2 particles have rather "spherical-like" morphology, while mZO_2 particles have "irregular-prism" morphology. Size measurements on many SEM images taken at various locations indicated that size of the mCB and mZrO_2 particles were all above 100 nm, thus they are classified as "micro fillers"; while size of nCB, nTiO_2, and nSiO_2

particles were all below 100 nm, thus they classified as “nano fillers”. Details of the “size ranges” determined for each filler were tabulated in Table 2.4.

Results of the BET analyses for each particle in terms of “surface area” were given in Table 2.4. Then, the model described above was used to calculate the “size” of the particles, and the obtained values were also tabulated in Table 2.4. It is seen that “BET calculated size” of the particles were all in the “SEM size ranges” of the particles. Moreover, the data given in Table 2.4 are approximately coincide with the values reported by the suppliers of the fillers.

Table 2.4 Experimental and estimated particle size data via SEM and BET analyses.

Fillers	**SEM Particle Size Range** (nm)	**BET Surface Area** (m^2/g)	**BET Particle Size** (nm)
mCB	200-500	9.058	368
nCB	40-90	91.32	36.5
$mZrO_2$	100-350	10.79	94.4
$nTiO_2$	10-100	258.1	5.96
$nSiO_2$	20-60	140.3	19.4

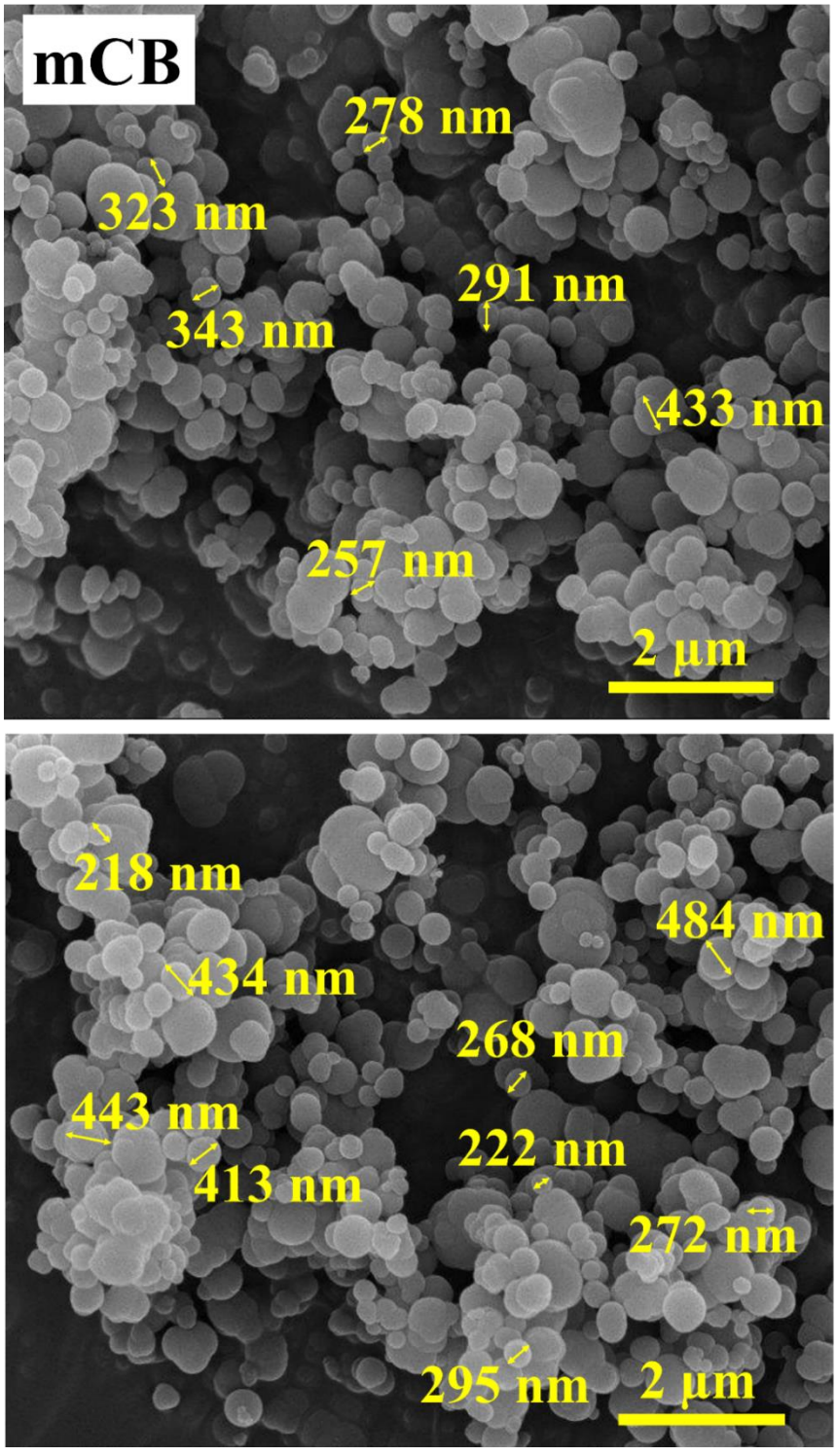

(a)

Figure 2.1 SEM images showing "particle size ranges" for the fillers; (a) mCB, (b) nCB, (c) $mZrO_2$, (d) $nTiO_2$, and (e) $nSiO_2$

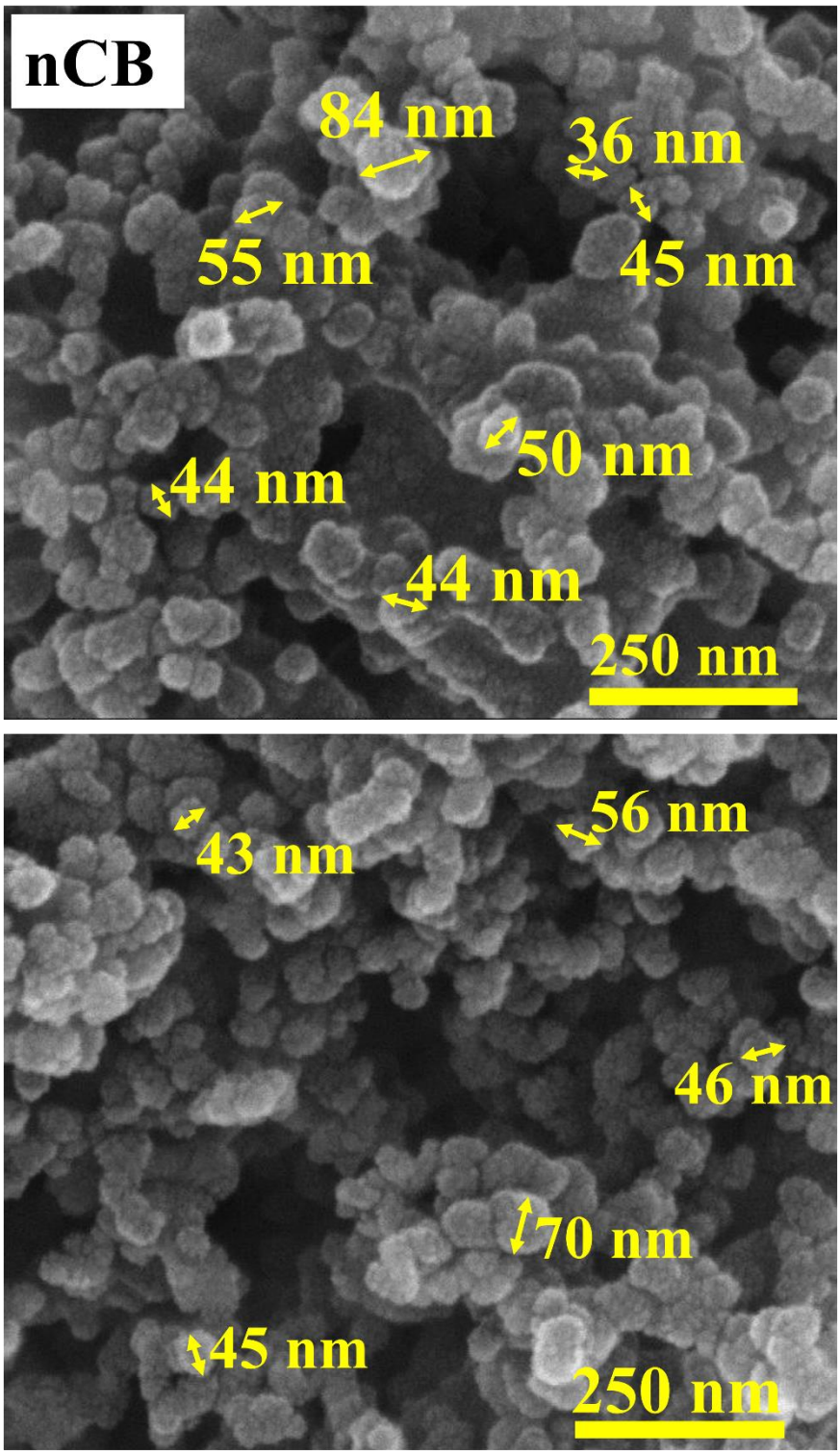

(b)

Figure 2.1 Contn'd.

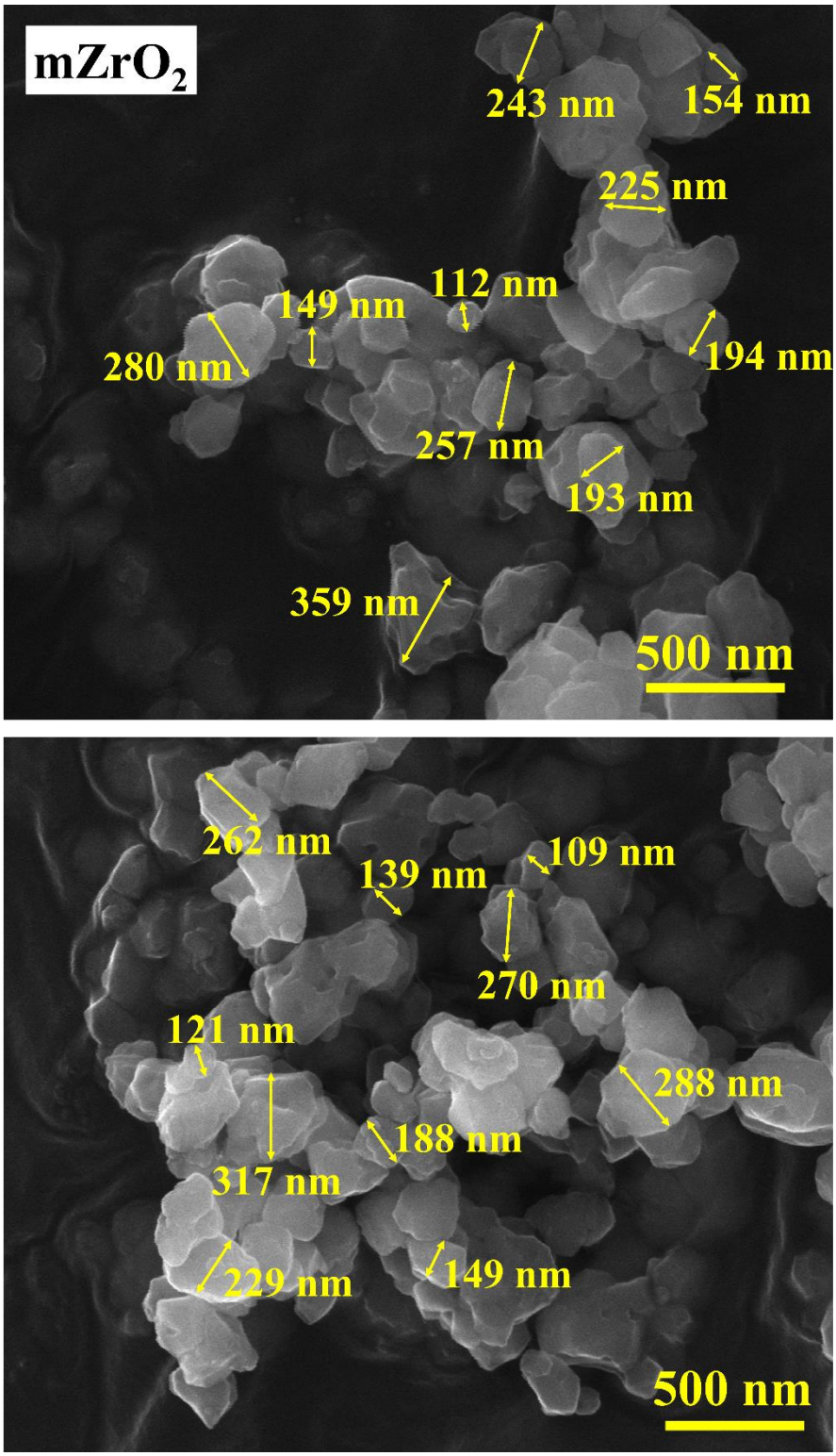

(c)

Figure 2.1 Contn'd.

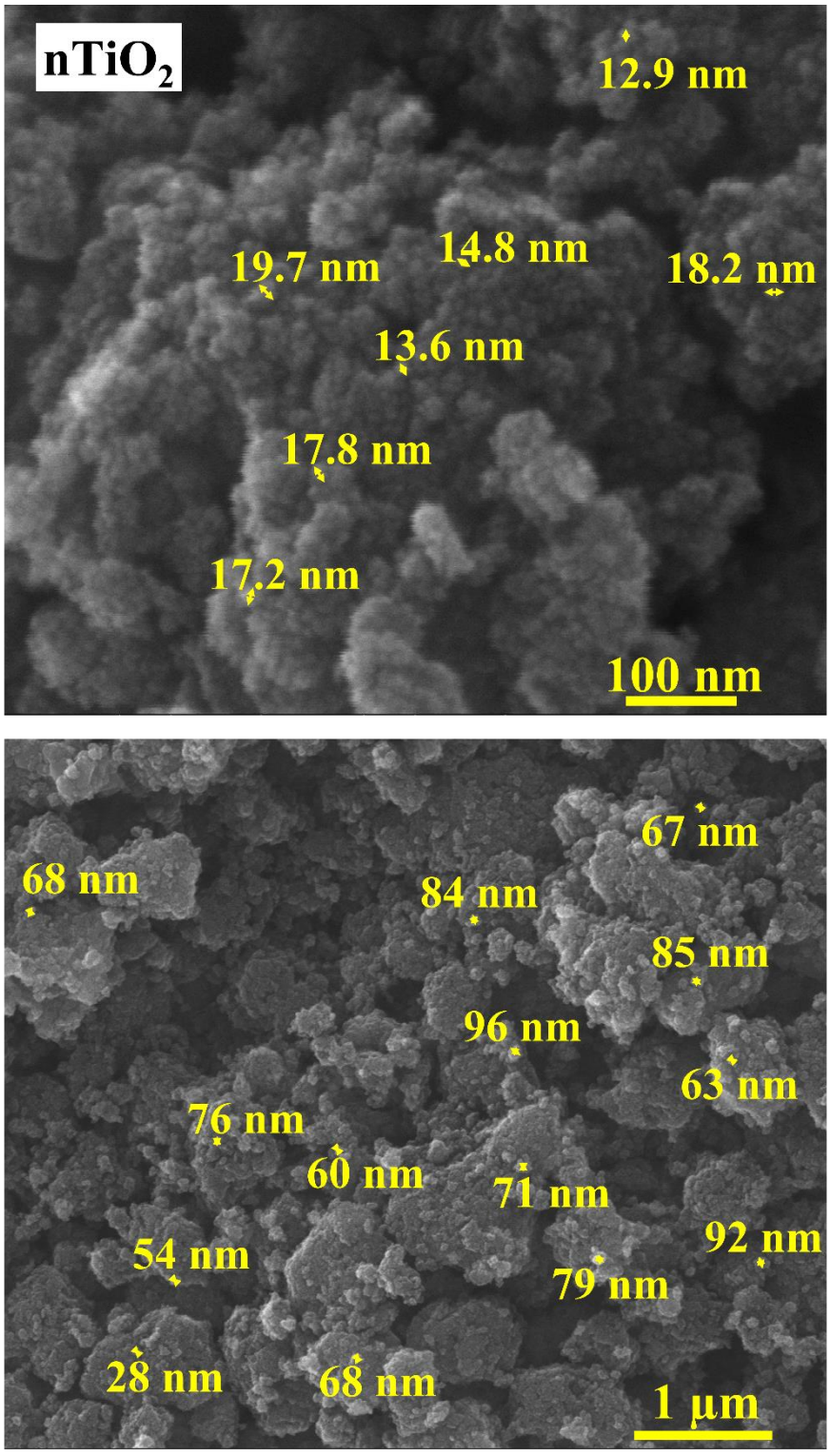

(d)

Figure 2.1 Contn'd.

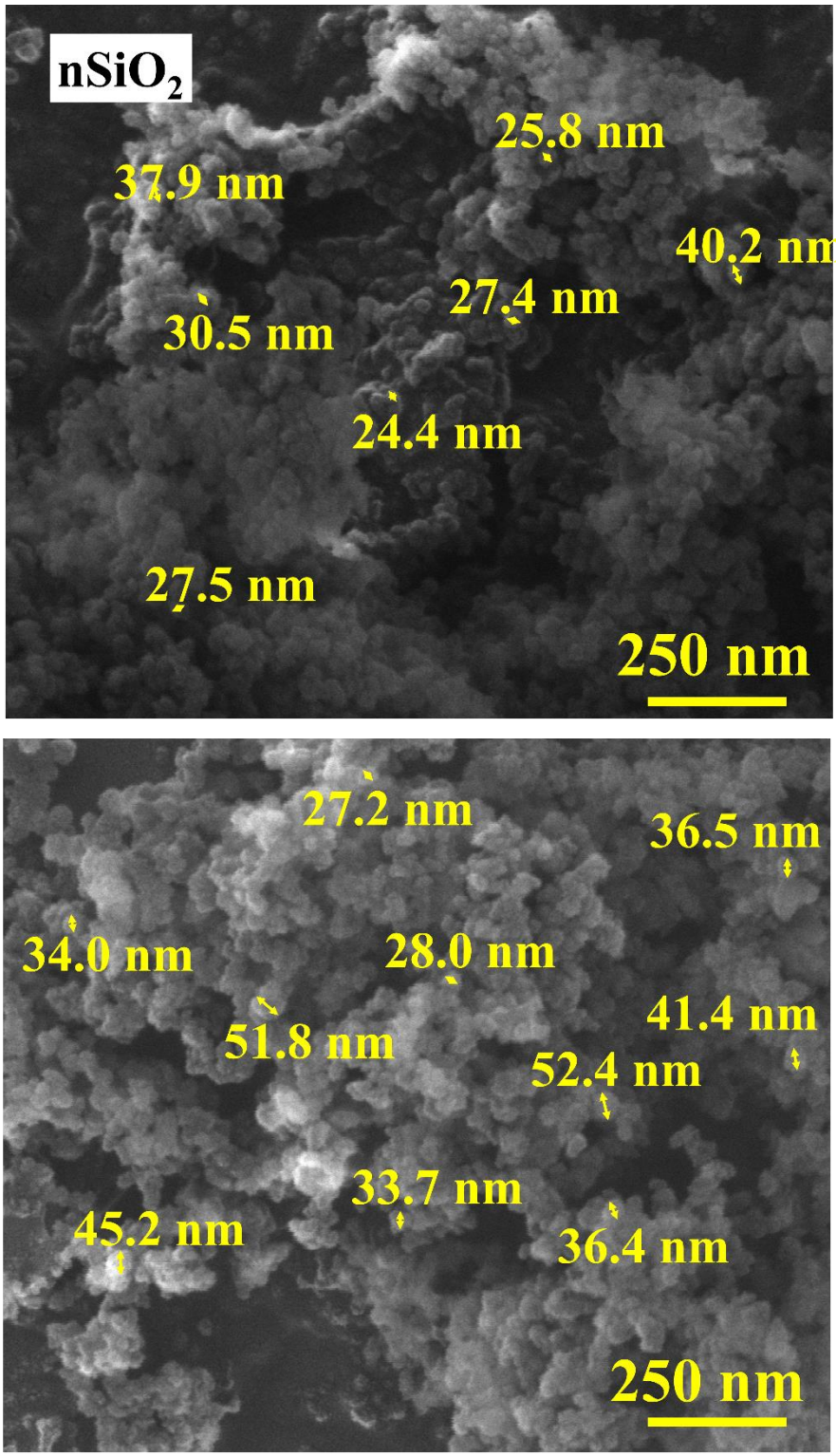

(e)

Figure 2.1 Contn'd.

2.3 Production of the Unfilled and Filled HTPB-PU Elastomer Specimens

The main technique used for the production of unfilled and filled HTPB-PU elastomer material was “mechanical mixing”. For this purpose, a mechanical stirrer (Heidolph Hei-Torque Precision 400) with three-blade impeller (made of PTFE) were utilized (Figure 2.2(a)). For each specimen formulation, amounts of the ingredients were adjusted with a precision balance, so that, 1.6 kg of the final mixture could be obtained. Details of the production steps were explained below and illustrated in Figure 2.2.

(1) Preconditioning: Before mixing, polyol (HTPB) and plasticizer (DEHA) were preconditioned at 65°C, while fillers were preconditioned at 90°C overnight.

(2) Premixing: Predetermined amount of catalyst (DBTL), crosslink agent (TEA), bonding agent (MAPO), plasticizer (DEHA), and polyol (HTPB) were weighed and added into 2-liter beaker. Then, all these chemicals were mixed for 10 min at 500 rpm and 35°C (Figure 2.2(b)).

(3) Mixing: Predetermined amount of fillers were added in a manner that, first nano-sized fillers little by little, and then micron-sized fillers in the same way. Then, the whole mixture was mechanically stirred for 90 min at 500 rpm and 35°C (Figure 2.2(c)).

(4) Final Mixing: Predetermined amount of polyisocyanate (IPDI) was added into the mixture and all ingredients stirred for 10 min at 500 rpm and 35°C (Figure 2.2(c)).

(5) Vacuum Degassing: After each mixing, entrapped air bubbles within the mixtures were removed under -880 mbar vacuum for 15 min at 500 rpm (Figure 2.2(d)).

(6) Molding: Vacuum degassed mixtures were poured into PTFE-coated rectangular molds which were preconditioned at 65°C for at least 2 hours prior to molding (Figure 2.2(e)).

(7) Curing: Poured mixtures in the mold with certain thickness were cured at 65°C for 7 days (Figure 2.2(e)).

(8) Specimen Cutting: After curing, materials in the plate form were demolded, and die-cut into certain specimen dimensions for testing (Figure 2.2(f)).

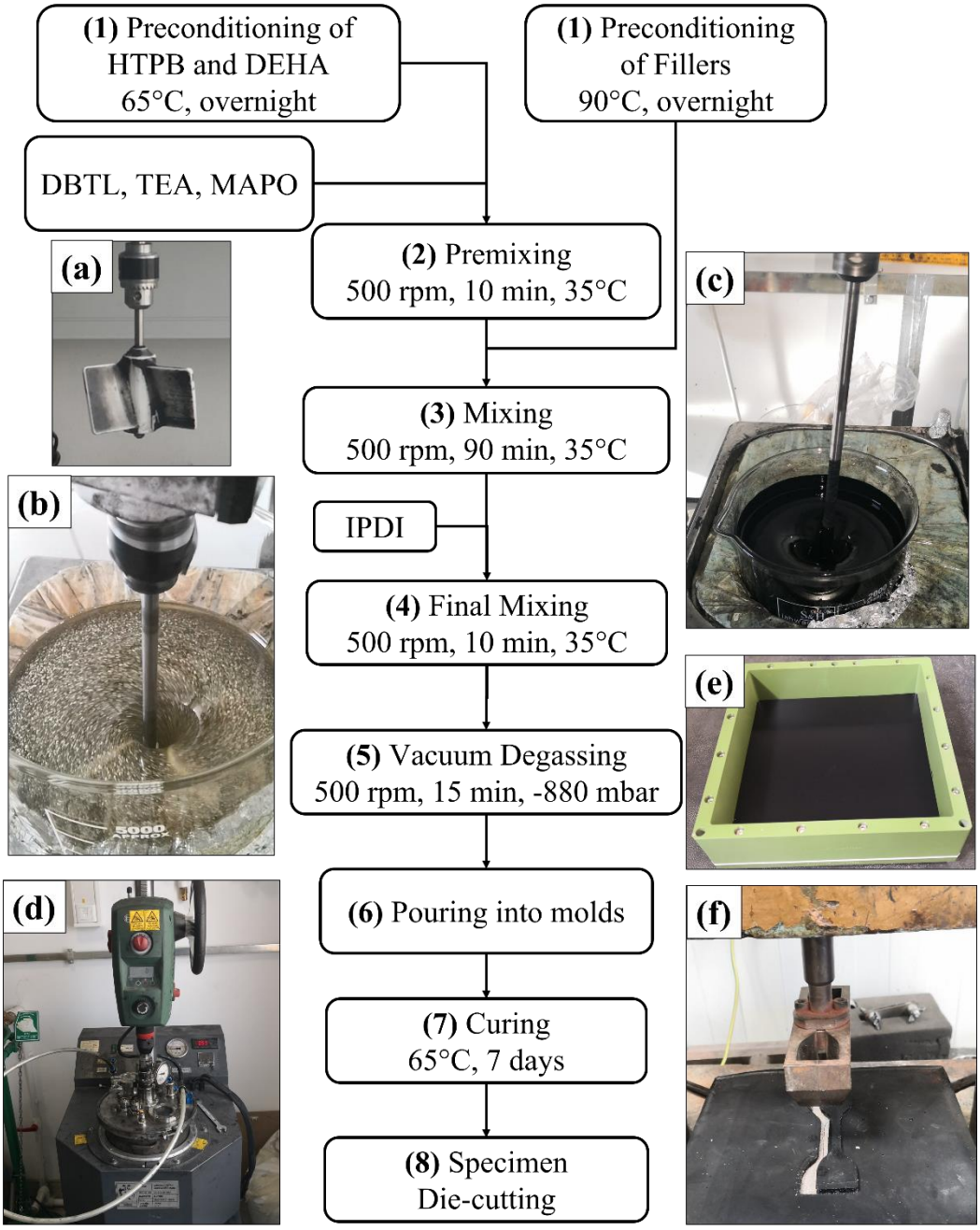

Figure 2.2 The flowchart and the images of the **s**teps used during the production of unfilled and filled HTPB-PU elastomer specimens; (a) Three-blade mechanical stirrer, (b) Premixing, (c) Mixing and Final mixing, (d) Vacuum degassing, (e) Molding and Curing, and (f) Specimen die-cutting.

2.4 Tension Tests for the Mechanical Properties of the Specimens

Tensile properties of all unfilled and filled HTPB-PU elastomer materials were obtained according to ASTM D638 standard [39]. Tests were conducted at three different temperatures: -40°C, room temperature (~23°C), and 70°C. Before testing all specimens were conditioned at desired test temperature for 150 min. Tests were performed in the chamber set to testing temperatures, except the room temperature one. Specimens were obtained from 4 mm thick cured and molded elastomer material plates by die cutting in accordance with the Type IV specimen geometry especially specified for the non-rigid plastics in the standard (Figure 2.3).

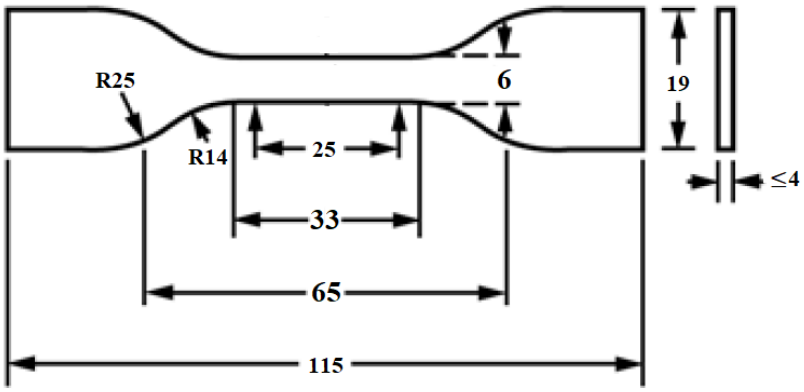

Figure 2.3. Type IV specimen geometry specified in ASTM D638 standard [39]. All numbers are in mm.

Tests were conducted by Instron 5965 Universal Testing System with 5kN load cell and wedge-action grips, under the crosshead speed of 50 mm/min. Extension for nominal strain values were determined as the change in the distance between the grips. For the specimens tested at 23°C and 70°C, tensile pulling was continued until the break (Figure 2.4(a) and (b)).

On the other hand, for the specimens tested at -40°C, the height of the testing chamber was not sufficient for breakage; so that tensile pulling was stopped at the highest position of the testing chamber (Figure 2.4(c)). That position corresponded to the strain value of 350%. Thus, for these specimens, stress value at 350% strain was taken as tensile strength of these specimens.

For each condition, at least five specimens were tested. All tensile mechanical properties determined were reported as average values with standard deviations.

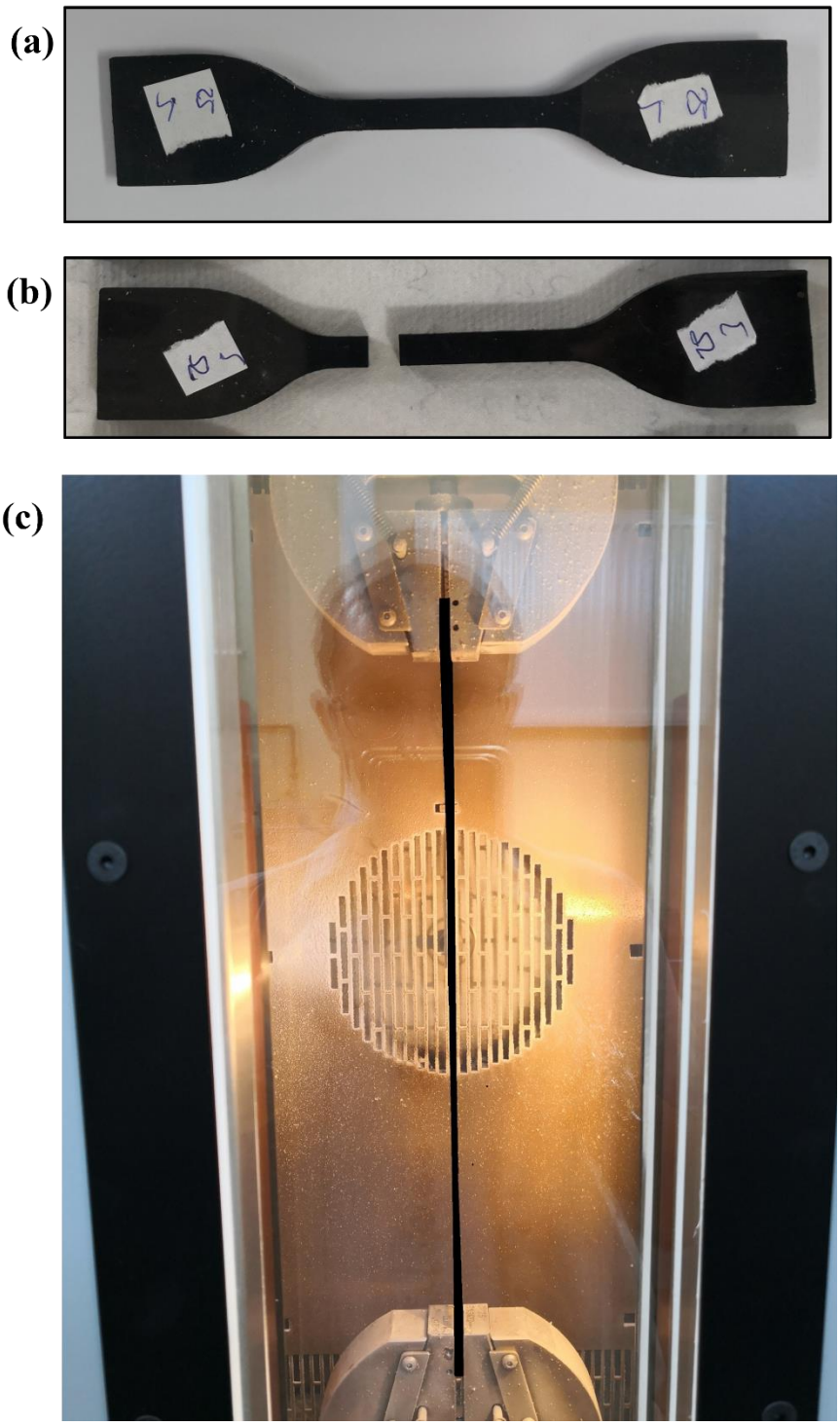

Figure 2.4 Example images of the specimens (a) before, and (b) after the tensile test at room temperature; (c) view of the unbroken tensile test specimen pulled to the highest position of the testing chamber at -40°C.

2.5 Analyses for the Thermal Properties of the Specimens

(i) Thermogravimetric Analysis (TGA)

Thermogravimetric analyses were performed to investigate thermal decomposition behavior of the specimens by using TA TGA Q500 model instrument in accordance with STANAG 4515 standard [40]. Platinum pans were loaded with 3±1 mg of samples for each measurement. Purging was with high purity nitrogen gas under 50 mL/min flow rate. Samples were first heated to 50°C, after holding for 3 min at this temperature, they were heated to 555°C with 5 °C/min heating rate. Obtained thermograms were analyzed both in terms of % weight loss and derivative curves (% weight loss per temperature, %/°C) for each decomposition step.

(ii) Differential Scanning Calorimetry (DSC)

Differential Scanning Calorimetry analyses were conducted to determine glass transition temperature of each specimen by using TA DSC2500 model instrument. Purging was again with high purity nitrogen gas under flow rate of 50 mL/min. Samples were first cooled to -100°C and kept for 10 min at this temperature. Then, they were heated to 100°C with 5°C/min heating rate. Temperature at half-height of the transition region was reported as T_g of the samples.

(iii) Dynamic Mechanical Analysis (DMA)

Dynamic Mechanical Analysis were conducted to study viscoelastic behavior of the specimens by using TA DMA850 model instrument. Bar shaped specimens were cut in dimensions of 35x5x3 mm. Heating profile applied was first cooling to -110°C, isothermally waiting for 10 min at this temperature, and heating to 70°C with 3°C/min heating rate. Loading was at tensile mode with 0.1% strain amplitude under 10 Hz frequency. Storage and loss modulus, and $tan\ \delta$ curves were recorded during the investigation.

(iv) Thermomechanical Analysis (TMA)

Thermal expansion characteristics of the specimens were observed by using TA Q400 model thermomechanical analyzer in accordance with STANAG 4525 standard [41]. Round samples with 8 mm in diameter and 3 mm in length were analyzed under high purity helium purge gas with flow rate of 100 mL/min. After measuring the height of the samples precisely at room temperature, first they were cooled down to -70°C, then heated to +100°C with 2°C/min heating rate. Changes in the dimensions of the specimens were analyzed to determine thermal expansion coefficient values between -50°C and +100°C. At least two samples were analyzed to determine the average values for each specimen.

(v) Thermal Conductivity

Thermal conductivity of the specimens was measured by using TCi Thermal Conductivity Analyzer (C-Therm). Cut specimens with 10 mm in height and 25 mm in diameter were placed on the sensor. Before that, Wakefield 120 Thermal contact agent was applied between the sample surface and the sensor. Then, 500 g of weight was placed on the equipment. Thermal conductivity values were measured at four different temperatures: 0°C, 30°C, 60°C, and 90°C.

CHAPTER 3

RESULTS AND DISCUSSION

Although there are other applications, HTPB-PU elastomers are mainly used as the base material in the “liner” layer of solid propellant rocket motor cases. In this military application, the required levels of mechanical and thermal properties are obtained by reinforcing this elastomer matrix with approximately 10 wt% micron-sized carbon black (mCB) particles. As discussed in the literature survey section, other alternative fillers to replace mCB completely, or to use together with mCB particles are still under research.

From this point of view; in the first step of this thesis, effects of nano-sized carbon black (nCB) particles,while in the second step, effects of micron-sized zirconia ($mZrO_2$), nano-sized titania ($nTiO_2$) and silica ($nSiO_2$), when used together with mCB particles were investigated.

In this first step, first of all, unfilled HTPB-PU elastomer specimens were tested and analyzed. Then, this elastomer matrix was filled with 10 wt% mCB particles, just like the traditional way. In order to investigate effects of nCB particles, certain amount of mCB particles were replaced with nCB particles without changing the “total filler content of 10 wt%”. In this respect, three formulations used were; the matrix filled with 9% mCB/ 1% nCB, 8% mCB/ 2% nCB, and 7% mCB/ 3% nCB. Results obtained from these specimens will be presented as dispersion of the fillers, then effects on the mechanical properties and finally effects on the thermal properties in the following subssections.

Note that, above 3% nCB replacement, due to the very high levels of the specific surface area of the nCB particles, the viscosity of the uncured mixture became too high leading to significant diffculties both in mechanical mixing and entrapped air

removal by vacuum degassing. Therefore, it was not possible to produce specimens for testing and analysis beyond 7% mCB/ 3% nCB formulation.

3.1 Dispersion of mCB Together with nCB in the Matrix

Scanning electron microscopy (SEM) is a powerful technique to study dispersion state of micron and nano sized fillers within a polymer matrix, as well as to explore fracture surface morphology of the specimens. SEM images given in Figure 3.1 revealed that when HTPB-PU matrix was filled with only 10 wt% mCB particles, there were no significant dispersion problem. On the other hand, when nCB particles were introduced, due to the nature of the nano-size, there were certain degree of agglomeration especially in the formulation with 3 wt% nCB.

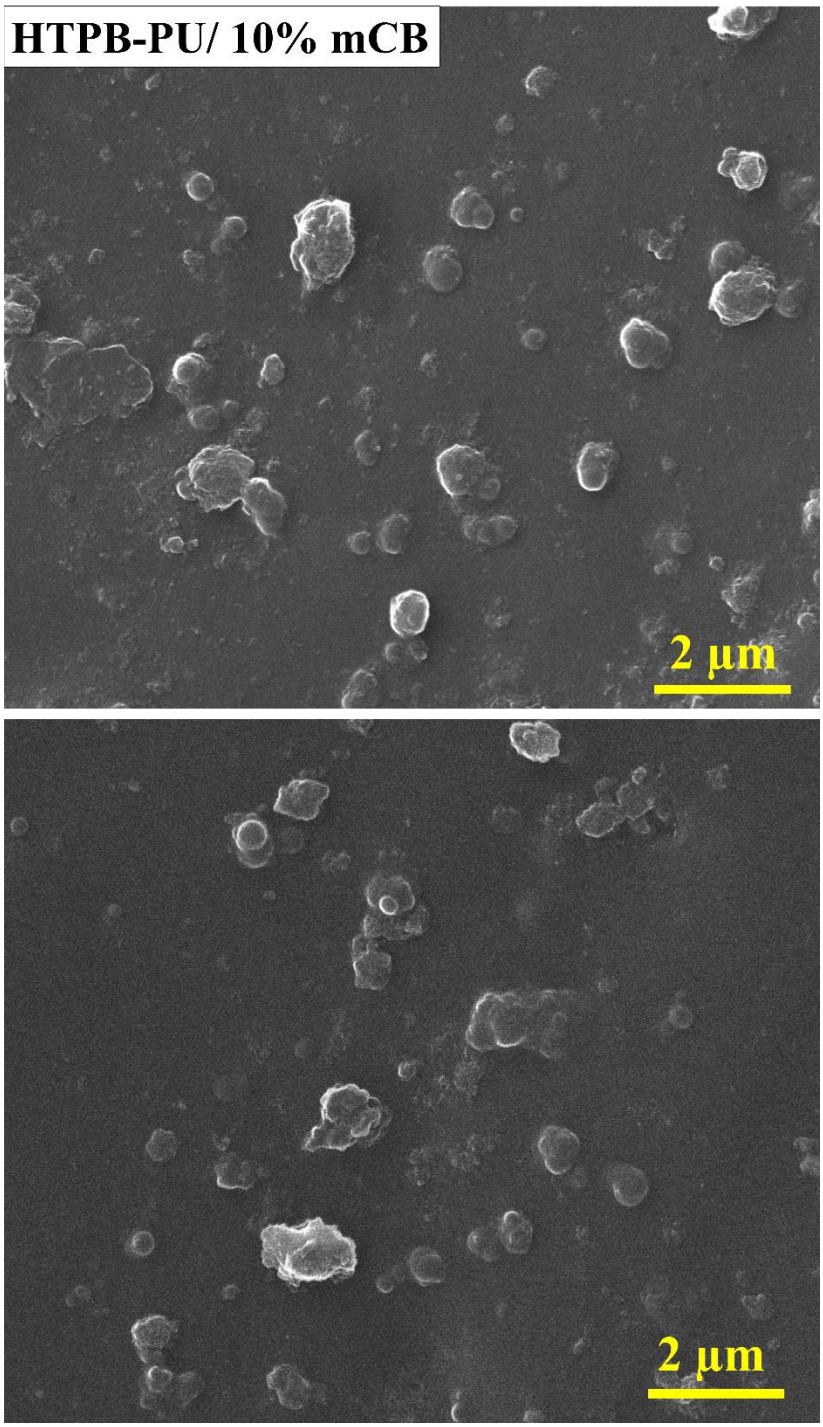

(a)

Figure 3.1 SEM images showing dispersion state of (a) 10% mCB, and (b) 8% mCB/ 2% nCB and 7% mCB/ 3% nCB in the HTPB-PU matrix.

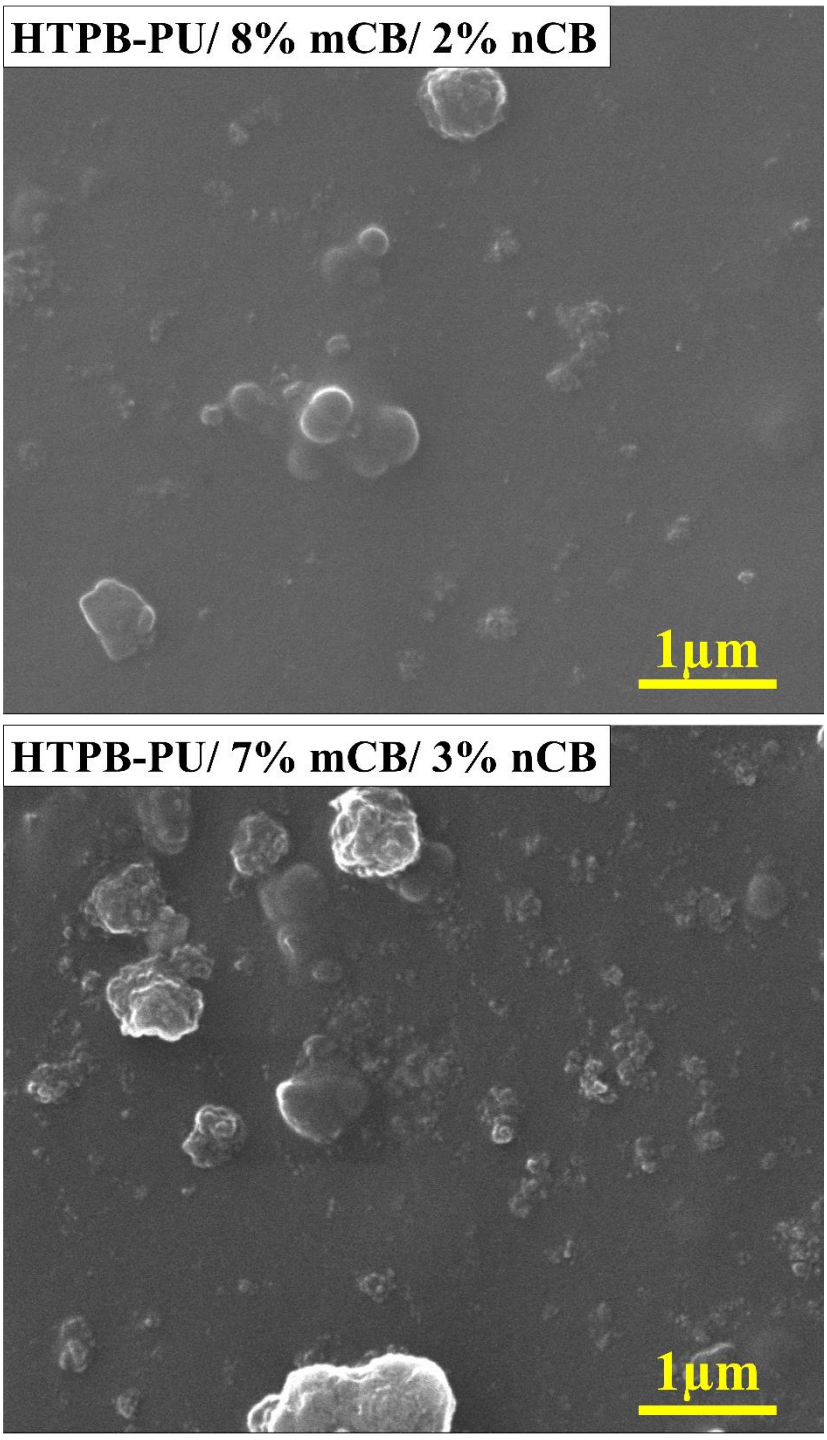

(b)

Figure 3.1 Contn'd.

3.2 Effects of nCB Replacement on the Mechanical Properties

It is known that “tension tests” are very practical and useful tests to determine “mechanical properties” of polymer materials including elastomers. By conducting “one” test, it is possible to determine “four” mechanical properties: (i) “Tensile Strength” as the highest level of stress in the curve, (ii) “Tensile Modulus” as the slope of the initial linear region of the curve, (iii) “Elongation at Break” as the final strain percent in the curve, and (iv) general “Toughness” as the area under the stress-strain curve at fracture.

Tension tests for all specimens were conducted at three different temperatures (70, 23, -40°C). 70°C and -40°C temperatures are typical temperature extremes that HTPB-PU elastomer material is exposed to during its operational lifetime. Stress-strain curves obtained from these tests were given in Figure 3.2 in detail in order to observe effects of nCB replacement on the stress-strain curves. Then, these curves were re-evaluated in order to observe effects of temperature level in Figure 3.3 by using the same stress-strain range in the x-y axes.

Then, by using the stress-strain curves for all specimen compositions at each temperature, the four mechanical properties mentioned above were determined and tabulated in Table 3.1 as the average values with standard deviations.

In order to reveal effects of nCB replacement on the Tensile Strength and Tensile Modulus of HTPB-PU matrix clearly, the data were re-used in Figure 3.4; while effects on the Elongation at Break and Toughness properties in Figure 3.5, respectively. Again, effects of temperature on these four properties were re-evaluated in Figure 3.6. All these results were discussed in the following sub-sections.

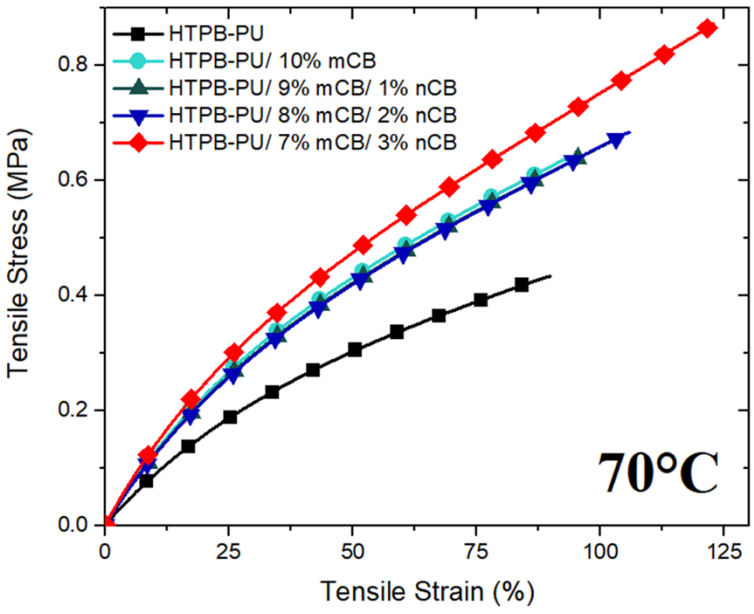

(a)

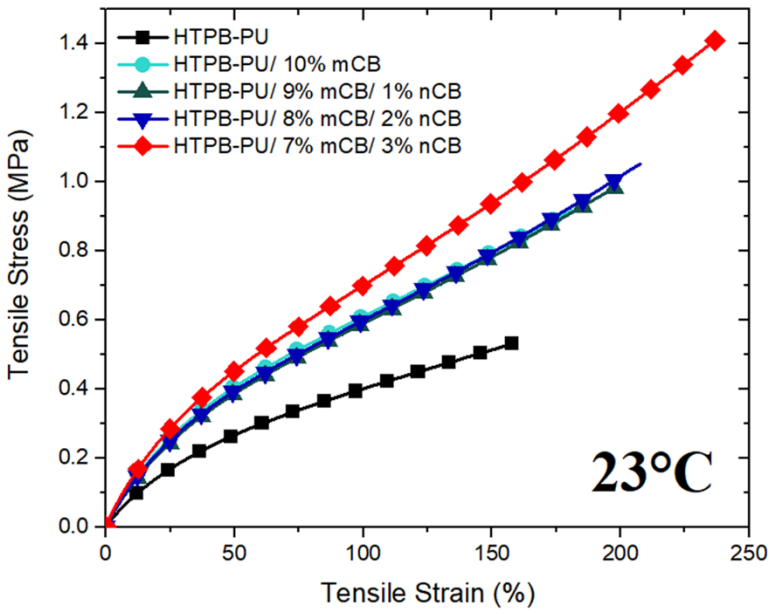

(b)

Figure 3.2 Effects of mCB and nCB replacement on the Tensile Stress versus Tensile Strain curves at (a) 70°C, (b) 23°C, and (c) -40°C.

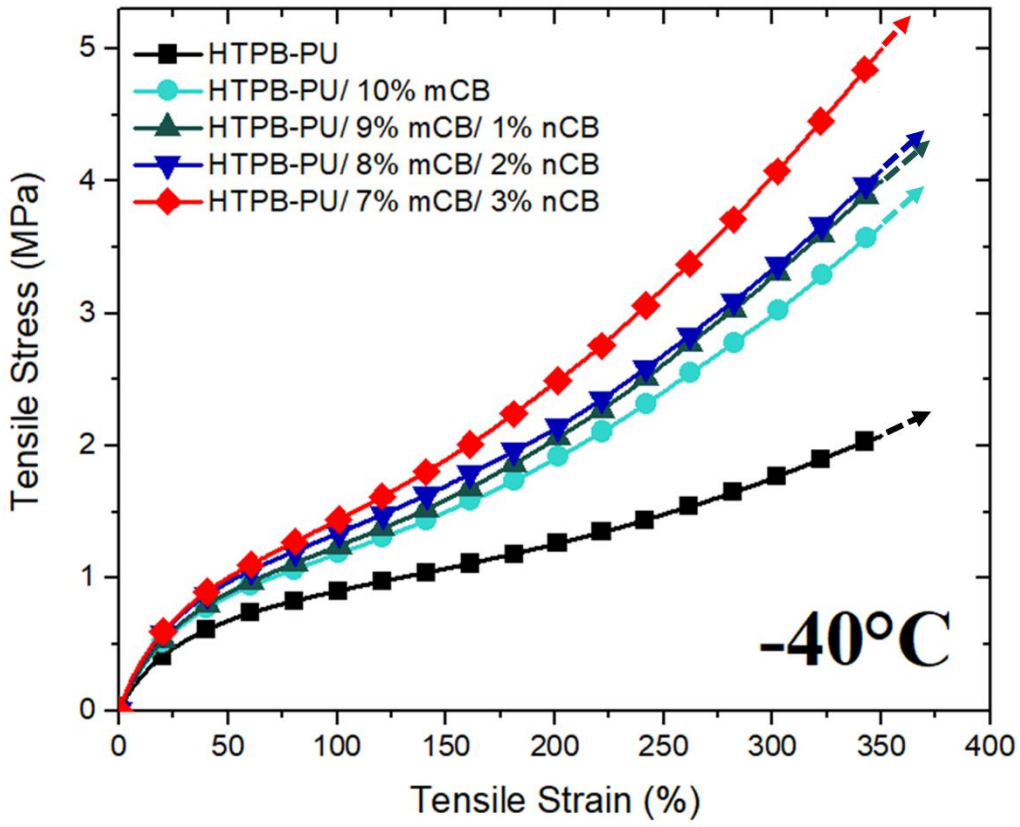

(c)

Figure 3.2 Contn'd.

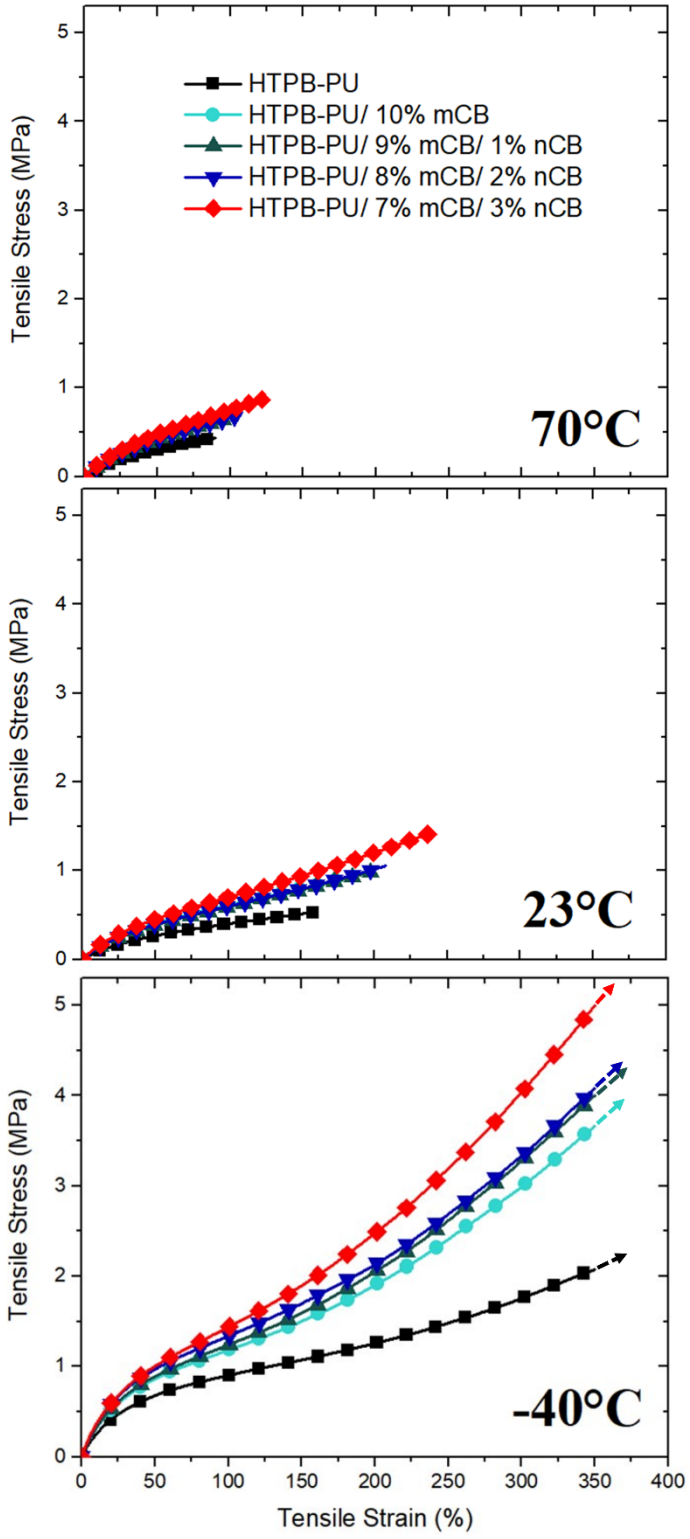

Figure 3.3 Effects of Temperature on the Tensile Stress versus Tensile Strain curves having the same ranges in the x-y axes.

Table 3.1 Mechanical properties of unfilled, mCB and nCB filled HTPB-PU elastomer material at three different testing temperatures.

Temperature (°C)	**Specimens**	**Tensile Strength** (MPa)	**Tensile Modulus** (MPa)	**Elongation at Break** (%)	**Toughness** (kJ/m^3)
70	HTPB-PU	0.43±0.02	0.93±0.02	90±9	233±38
	HTPB-PU/ 10% mCB	0.64±0.04	1.36±0.03	92±7	353±48
	HTPB-PU/ 9% mCB/ 1% nCB	0.66±0.03	1.33±0.02	103±6	410±45
	HTPB-PU/ 8% mCB/ 2% nCB	0.70±0.03	1.34±0.03	106±8	473±54
	HTPB-PU/ 7% mCB/ 3% nCB	0.87±0.05	1.50±0.02	123±9	630±73
23	HTPB-PU	0.53±0.05	0.89±0.02	155±22	508±123
	HTPB-PU/ 10% mCB	0.92±0.02	1.35±0.02	179±8	984±66
	HTPB-PU/ 9% mCB/ 1% nCB	0.98±0.02	1.33±0.02	199±6	1134±48
	HTPB-PU/ 8% mCB/ 2% nCB	1.11±0.08	1.36±0.02	208±16	1397±177
	HTPB-PU/ 7% mCB/ 3% nCB	1.42±0.08	1.53±0.03	238±12	1860±176
-40	HTPB-PU	>2.07	2.80±0.03	>350	>4910
	HTPB-PU/ 10% mCB	>3.64	3.51±0.07	>350	>7730
	HTPB-PU/ 9% mCB/ 1% nCB	>3.99	3.60±0.19	>350	>8220
	HTPB-PU/ 8% mCB/ 2% nCB	>4.08	3.68±0.12	>350	>8580
	HTPB-PU/ 7% mCB/ 3% nCB	>5.00	4.13±0.14	>350	>9610

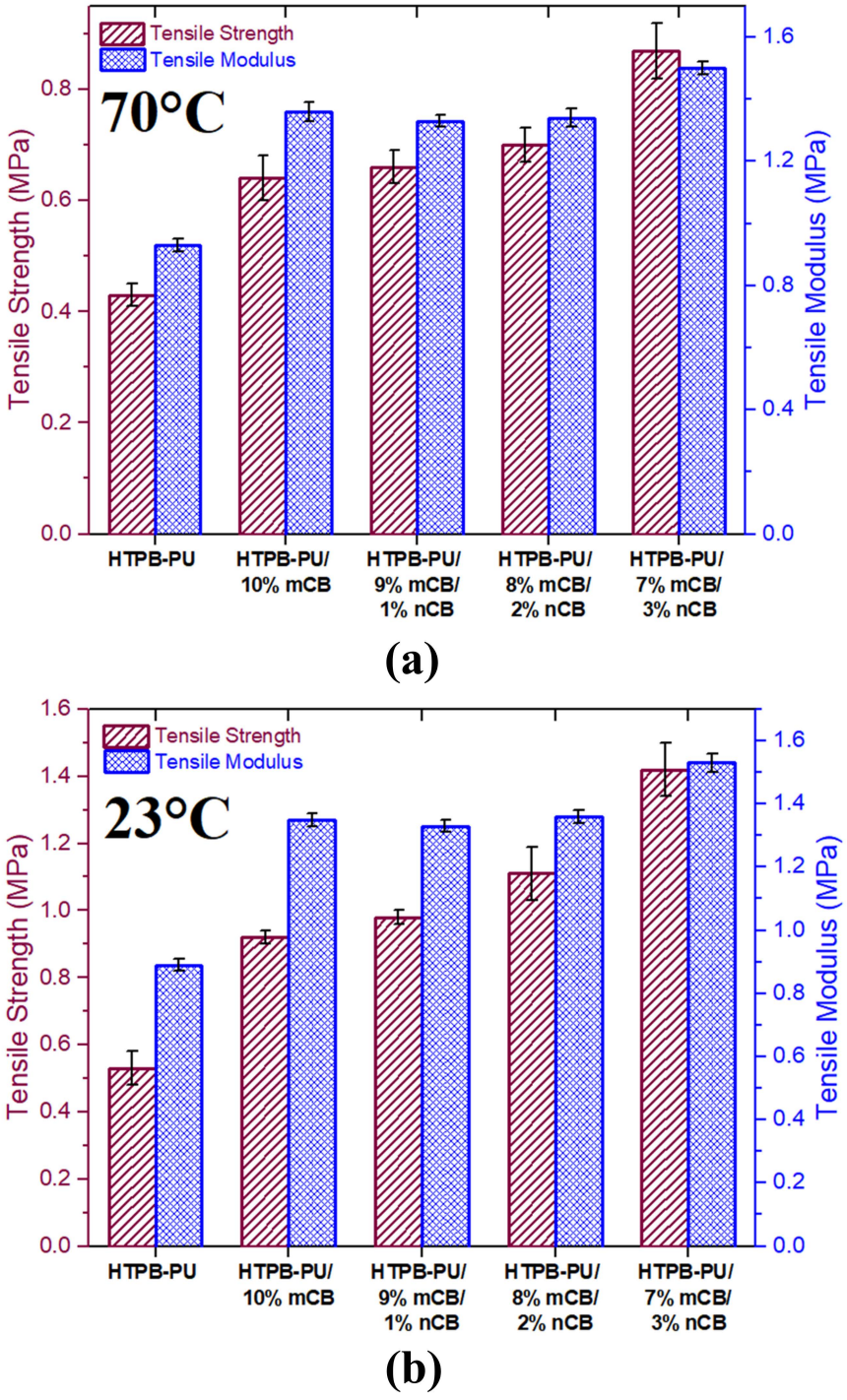

Figure 3.4 Effects of mCB and nCB replacement on the Tensile Strength and Tensile Modulus values at (a) 70°C, (b) 23°C, and (c) -40°C.

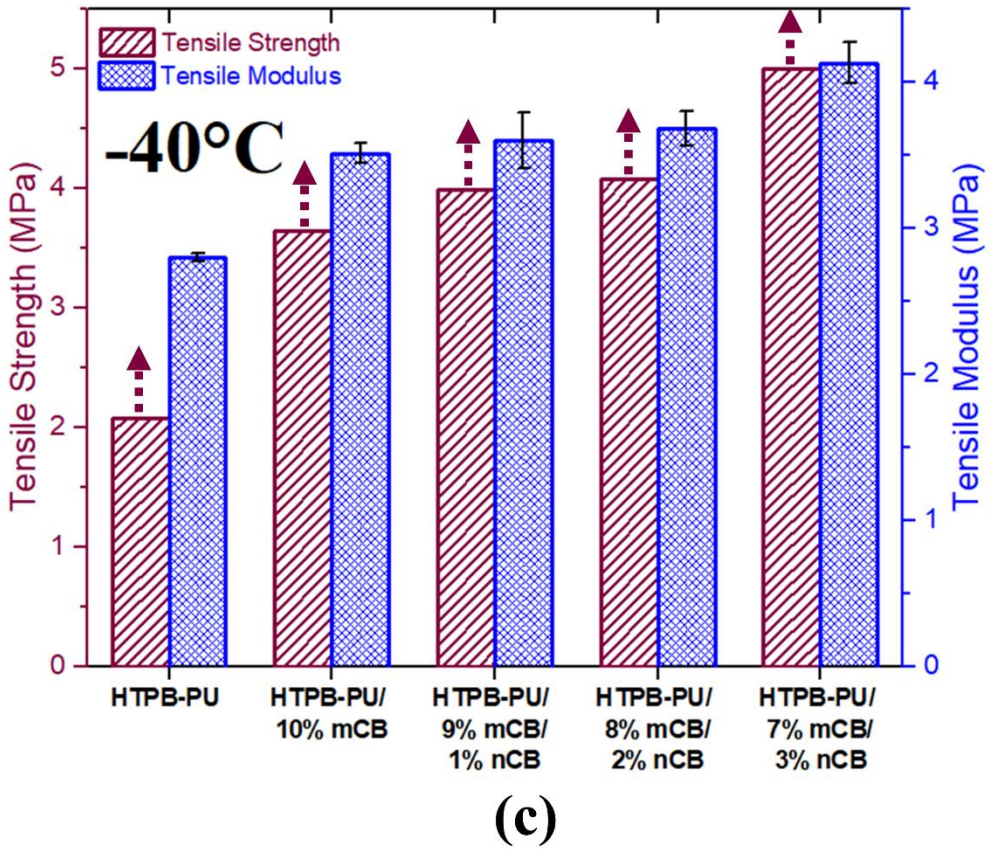

Figure 3.4 Contn'd.

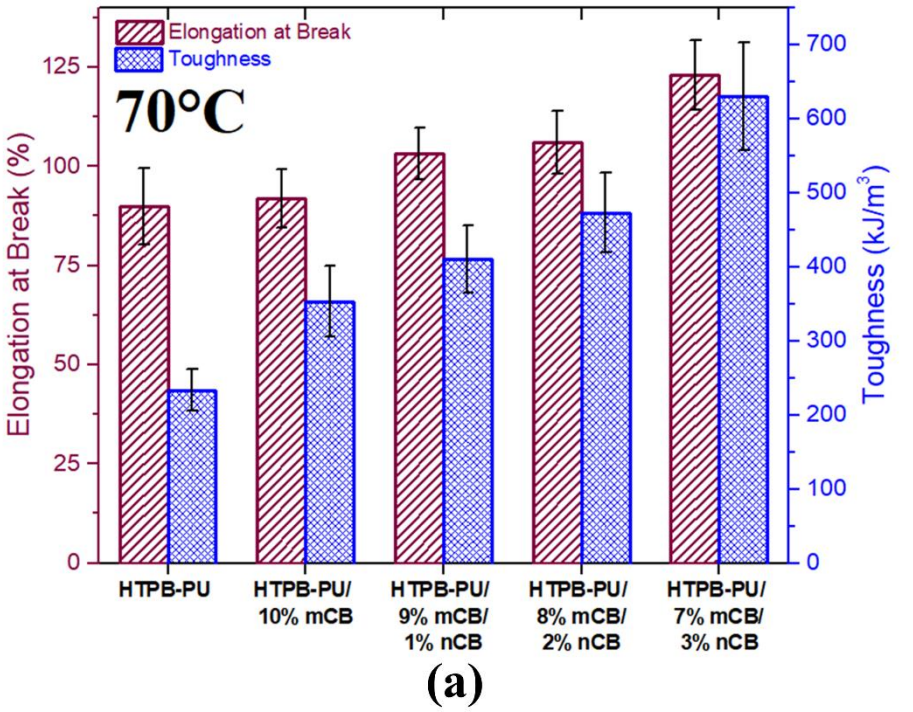

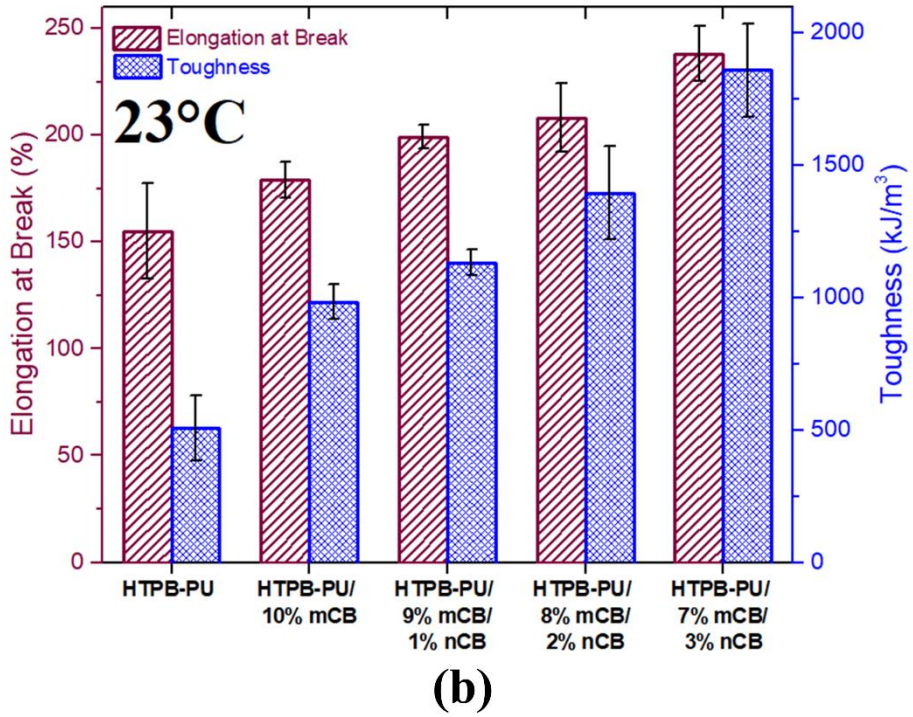

Figure 3.5 Effects of mCB and nCB replacement on the Elongation at Break and Toughness values at (a) 70°C, (b) 23°C, and (c) -40°C.

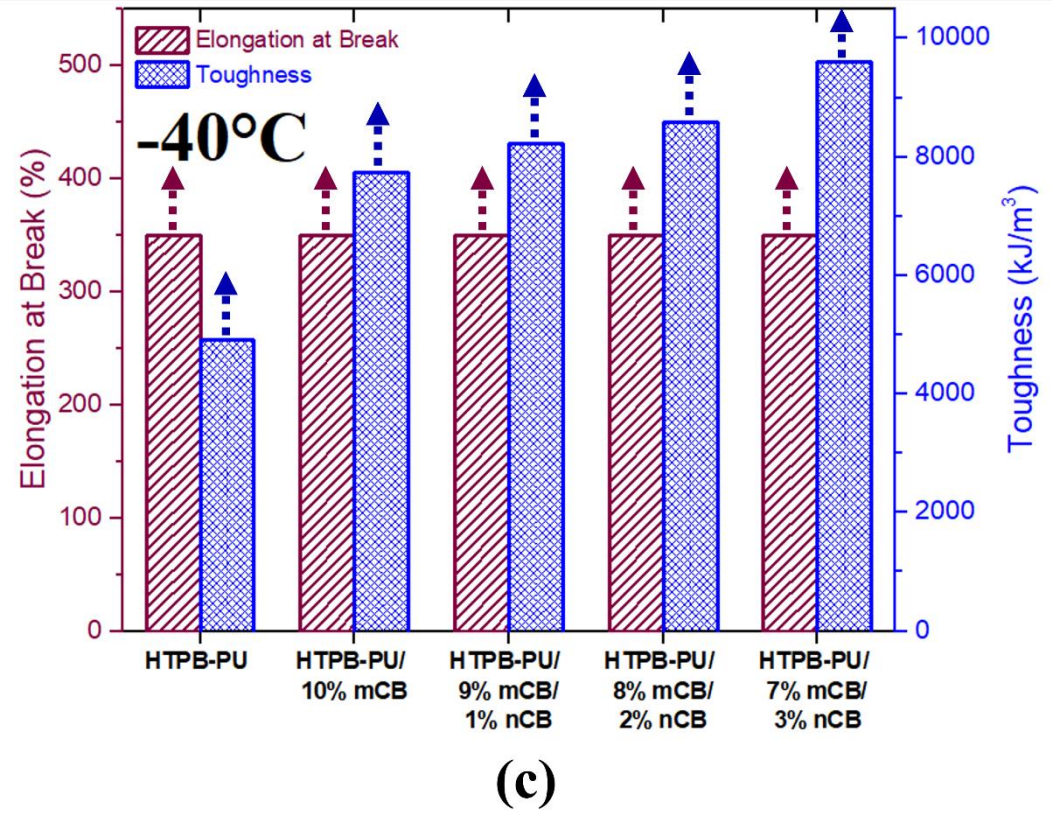

Figure 3.5 Contn'd.

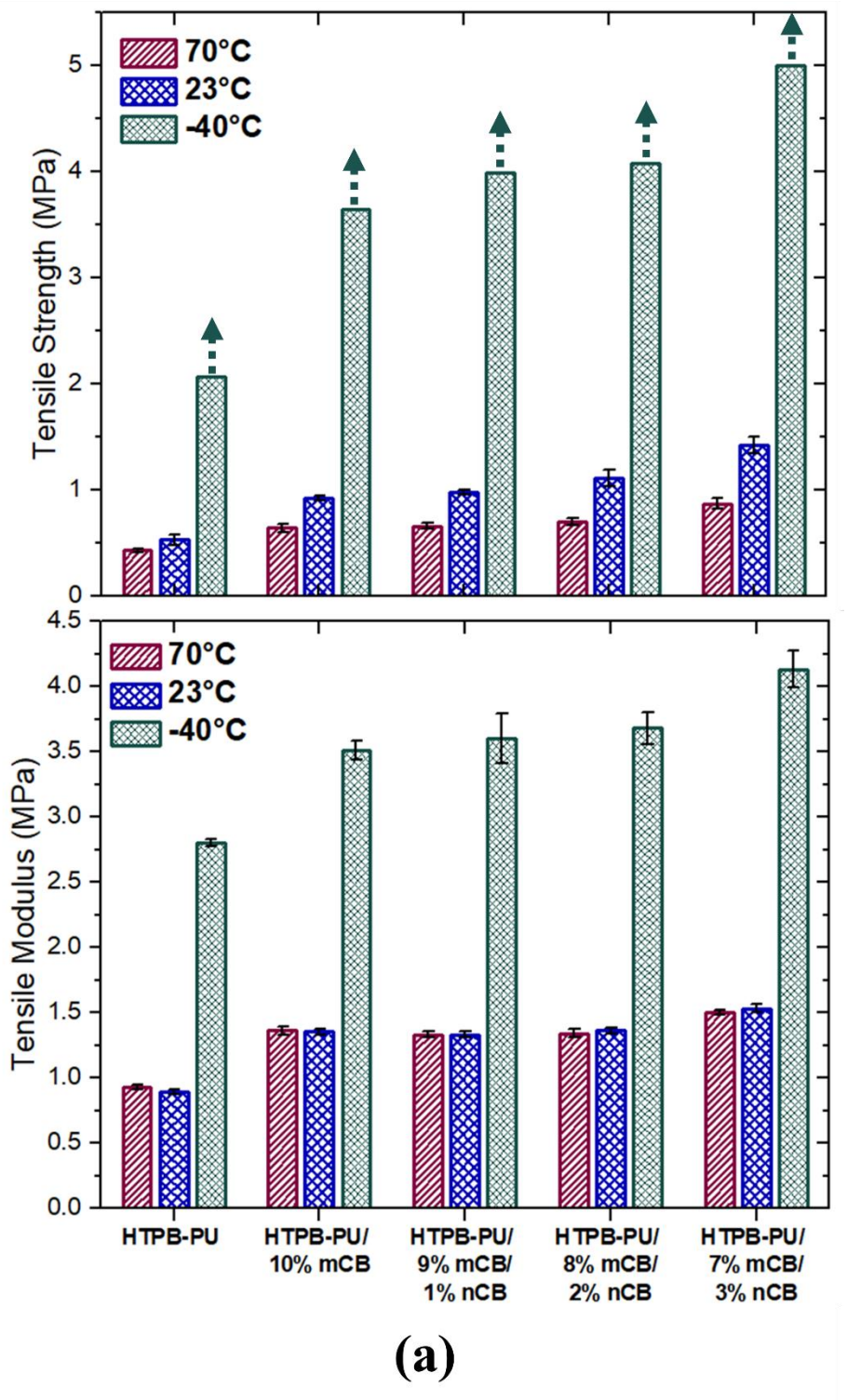

Figure 3.6 Effects of Temperature on the values of (a) Tensile Strength and Tensile Modulus, and (b) Elongation at Break and Toughness

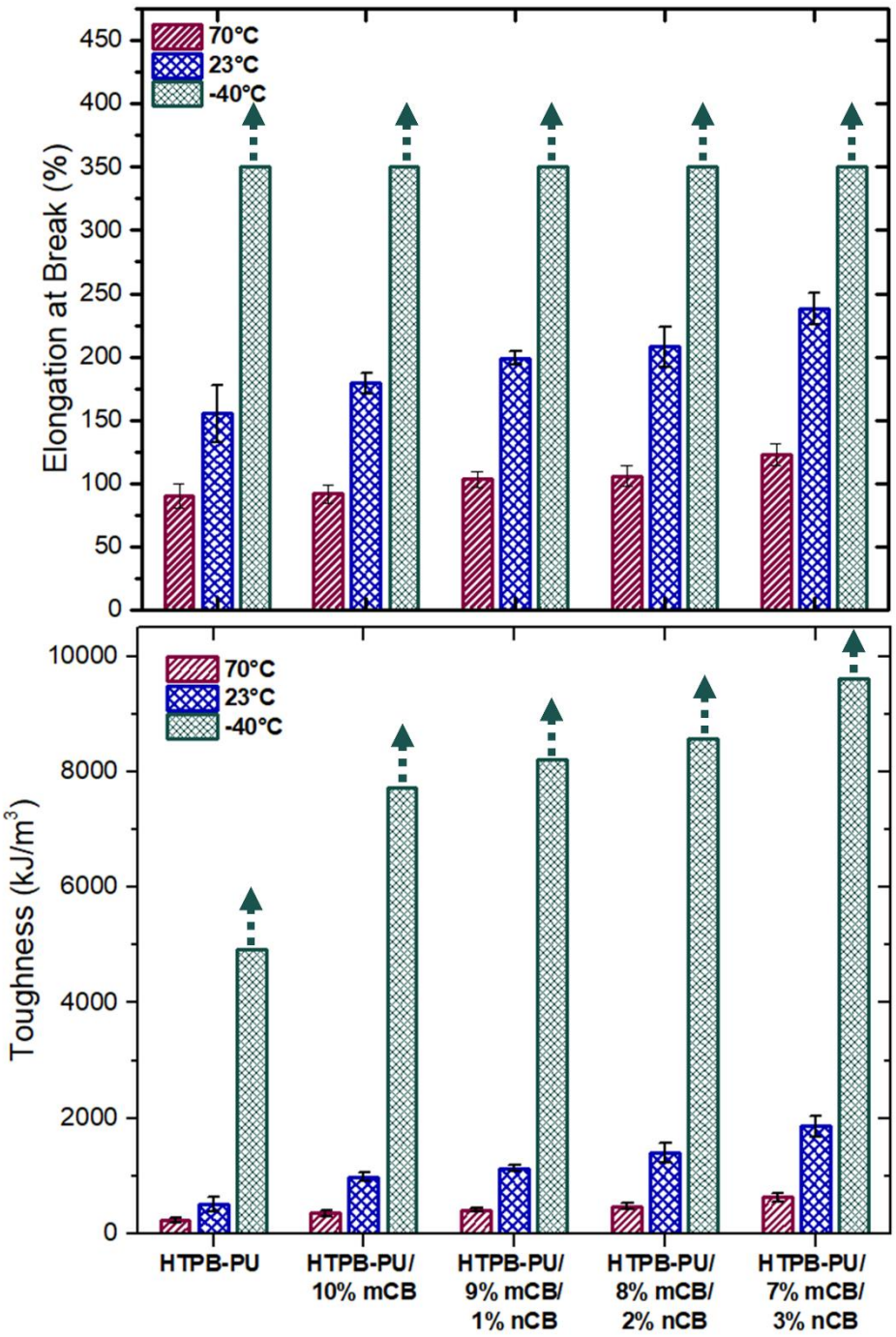

(b)

Figure 3.6 Contn'd.

(i) Effects of Temperature on All Mechanical Properties

Since HTPB-PU based elastomers are especially used as the main material in the liner and/or insulator layer of the solid propellant rocket motor cases; it was important to determine mechanical performance of the specimens in the design temperature range of (-40°C)-(+70°C). Thus, in this study, all specimen formulations were tested at -40°C, room temperature (23°C), and 70°C. As stated above, effects of temperature on the mechanical performance of the specimens were evaluated clearly in Figure 3.3, Figure 3.6, and Table 3.1

These figures and the table indicated that temperature level had very significant effects on all mechanical properties of the specimens. For instance at 23°C, unfilled HTPB-PU elastomer has Tensile Strength of 0.53 MPa; which decreased to 0.43 MPa (i.e. 19% decrease) at 70°C; while increased to 2.07 MPa (i.e. 290% increase) at -40°C. This behavior was seen for all mechanical properties and for all unfilled and filled specimen compositions; that is increasing temperature degraded all properties significantly.

The main reason for this behavior was of course related to the "Glass Transition Temperature, T_g" of the elastomer materials having extremely high "rubbery" behavior above this transition. As will be discussed in the Thermal Properties Section later, T_g of HTPB-PU elastomer was determined as around -79°C. Since test temperature of -40°C is the closest temperature to the T_g of the elastomer (only 39°C above T_g), specimens had much higher mechanical properties compared to test temperatures of 23°C (i.e., 102°C above T_g) and 70°C (i.e., 149°C above T_g).

Because at -40°C; not only hard segments of isocyanate groups, but also soft segments of hydrocarbon butadiene groups have higher structural stability leading to higher mechanical performance. When temperature was increased to 23°C and 70°C being much above the T_g of the material, all soft and hard segments in the structure become extremely rubbery with much lower stability leading to very low mechanical performance.

It should be pointed out that during tension tests at -40°C, due to the more stable structure, enormous level of strain values was observed. However, the height of the testing chamber was not sufficient to continue pulling until fracture of the specimens. Height of the chamber was sufficient to record strain values only up to 350%, thus tensile pulling of the specimens during tests were stopped at that position. Then, tensile strength and toughness values of the specimens at -40°C were determined by taking the maximum final strain value as 350%. Therefore, these properties at -40°C were tabulated with greater symbol ">" in Table 3.1, and with continuing arrow symbol " --→ " in the related figures.

(ii) Effects of mCB and nCB Replacement on Tensile Strength and Tensile Modulus

As shown in Figure 3.4 and Table 3.1, when HTPB-PU matrix was filled with 10% mCB, both Tensile Strength and Tensile Modulus values increased significantly at all temperatures. For example at -40°C, strength increased from 2.07 MPa to 3.64 MPa (i.e., 76% increase), modulus increased from 2.80 MPa to 3.51 MPa (i.e., 25% increase). These increases at 23°C were 74% and 52%; while at 70°C increases were 49% and 46%, respectively.

When certain amounts of mCB were replaced with nCB particles, i.e., 1%, 2%, and 3% without changing the total filler content of 10 wt%, it was seen that nCB particles had further contribution to the strength and modulus values of the HTPB-PU matrix; the highest contribution being with 3% nCB. For example, at -40°C, strength and modulus values increased to 5.00 MPa (i.e., 142% increase) and 4.13 MPa (i.e., 48% increase) respectively. These increases at 23°C were 168% and 72%; while at 70°C, increases were 102% and 61%, respectively.

It is known that there are two main mechanisms for the increase in strength and modulus values of filled polymer materials, named as "load transfer" and "molecular mobility decrease" mechanisms. According to the first mechanism, when the filled

HTPB-PU elastomer was loaded, the applied tensile forces on the macromolecules of both hard segments and soft segments would be transferred to the stronger and stiffer Carbon Black particles leading to higher strength and modulus values.

According to the second strengthening mechanism, the presence of Carbon Black particles would decrease macromolecular mobility of again both hard segments and soft segments of the elastomer matrix, thus resulting in higher strength and modulus values.

Figure 3.4 and Table 3.1 indicated that when certain amounts of mCB particles were replaced with nCB particles, the effectiveness of these two strengthening mechanisms were much more pronounced leading to much higher strength and modulus values. Because, when the fillers were used in nano-sizes, their specific surface area increases considerably leading to much more molecular level interaction between the fillers and the matrix material.

(iii) Effects of mCB and nCB Replacement on Elongation at Break and Toughness

As shown in Figure 3.5 and Table 3.1, when HTPB-PU matrix was filled with 10% mCB particles, both Elongation at Break and Toughness values increased at all temperatures. For example at 23°C, elongation at break increased from 155% to 179%, at -40°C it was more than 350%. Increases in toughness were much more significant, for example, at -40°C, it increased from 4910 kJ/m^3 to 7730 kJ/m^3 (i.e., 57% increase). Toughness increases at 23°C and 70°C were 94% and 52%, respectively.

When certain amount of mCB were replaced with nCB particles, it was again seen that nCB particles had further contribution to the Elongation at Break and Toughness values, highest contribution being again with 3% nCB. For instance, elongation at break increased to 123% at 70°C, 238% at 23°C, and more than 350% at -40°C. Toughness values become 630 kJ/m^3 at 70°C, 1860 kJ/m^3 at 23°C, and more than

9610 kJ/m^3 at -40°C, i.e., increases compared to the elastomer matrix were more than 2 times.

It is known that when an elastomer material was pulled, there would be possibilities of formation of cavities, crazes, microvoids and microcracks. During loading, if growth of these defects were not prevented, then Elongation at Break and Toughness values could not be improved. According to the main "toughening" mechanism, reinforcement of elastomer matrices with fillers such as Carbon Black particles might prevent or decrease the propagation rate of those defects via toughening submechanisms of "crack deflection" and "crack bowing". Again, higher level of effectiveness of nCB compared to mCB particles would be higher level of interfacial microstructural interaction of nCB particles having much higher specific surface area values.

3.3 Dispersion of mCB Together with $mZrO_2$, $nTiO_2$, and $nSiO_2$ in the Matrix

As discussed above, 3 wt% nCB replacement resulted in highest mechanical performance. Therefore, in the second step of this study, effects of 3 wt% replacement of $mZrO_2$, $nTiO_2$, and $nSiO_2$ fillers were investigated again keeping the total filler content as 10 wt%. Before mechanical testing and thermal analyses of these specimens, their dispersion state in the matrix together with 7% mCB particles were investigated under SEM (Figure 3.7).

As shown in Figure 3.7(a), mCB and $mZrO_2$ fillers were rather uniformly dispersed which might be due to their micron-range particle sizes. On the other hand, nano-sized fillers of $nTiO_2$ and $nSiO_2$ resulted in certain degree of agglomeration, as seen in Figure 3.7(b) and (c), respectively.

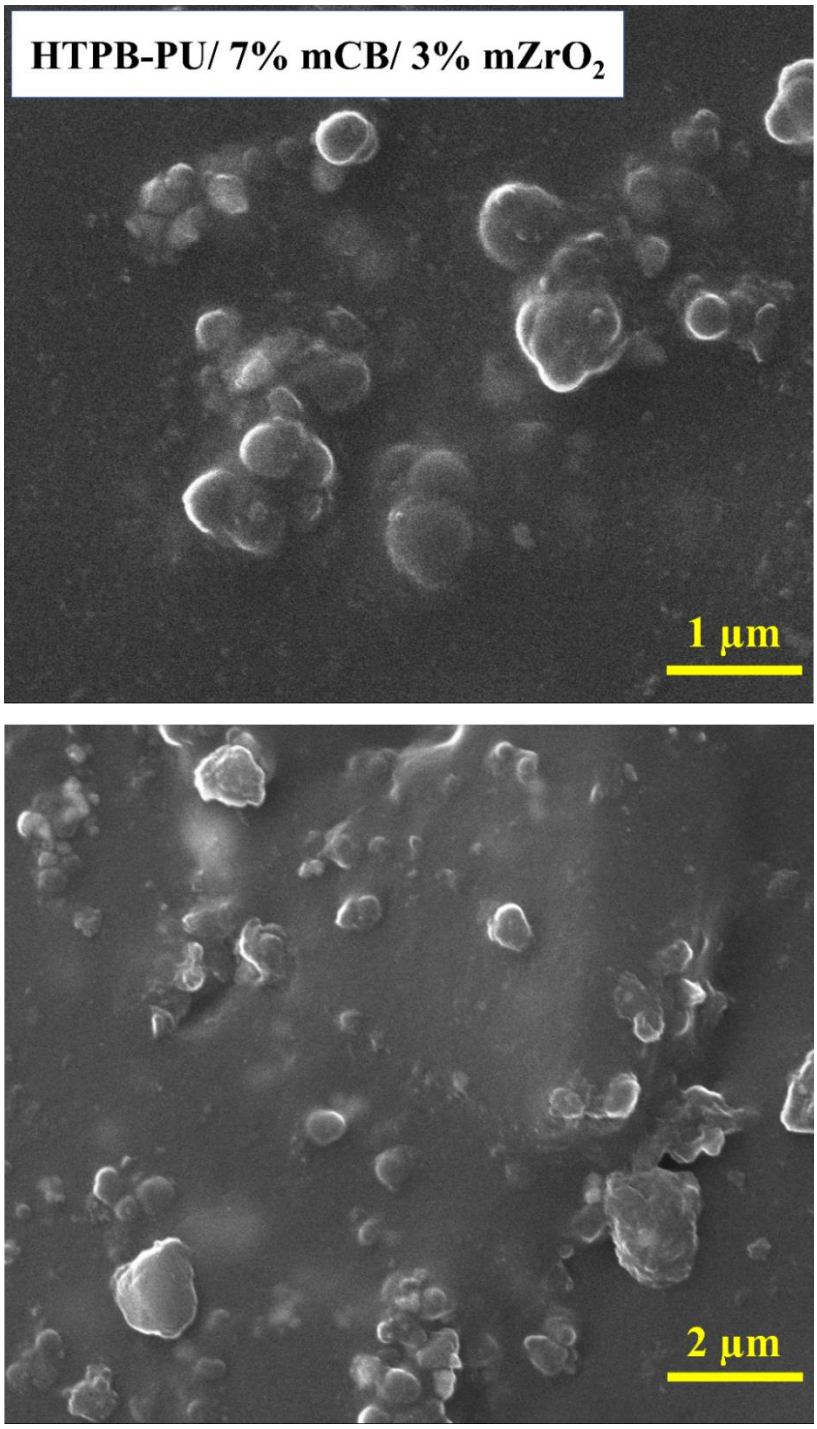

(a)

Figure 3.7 SEM images showing dispersion state of 7% mCB together with 3% (a) $mZrO_2$, (b) $nTiO_2$, and (c) $nSiO_2$fillers in the HTPB-PU matrix.

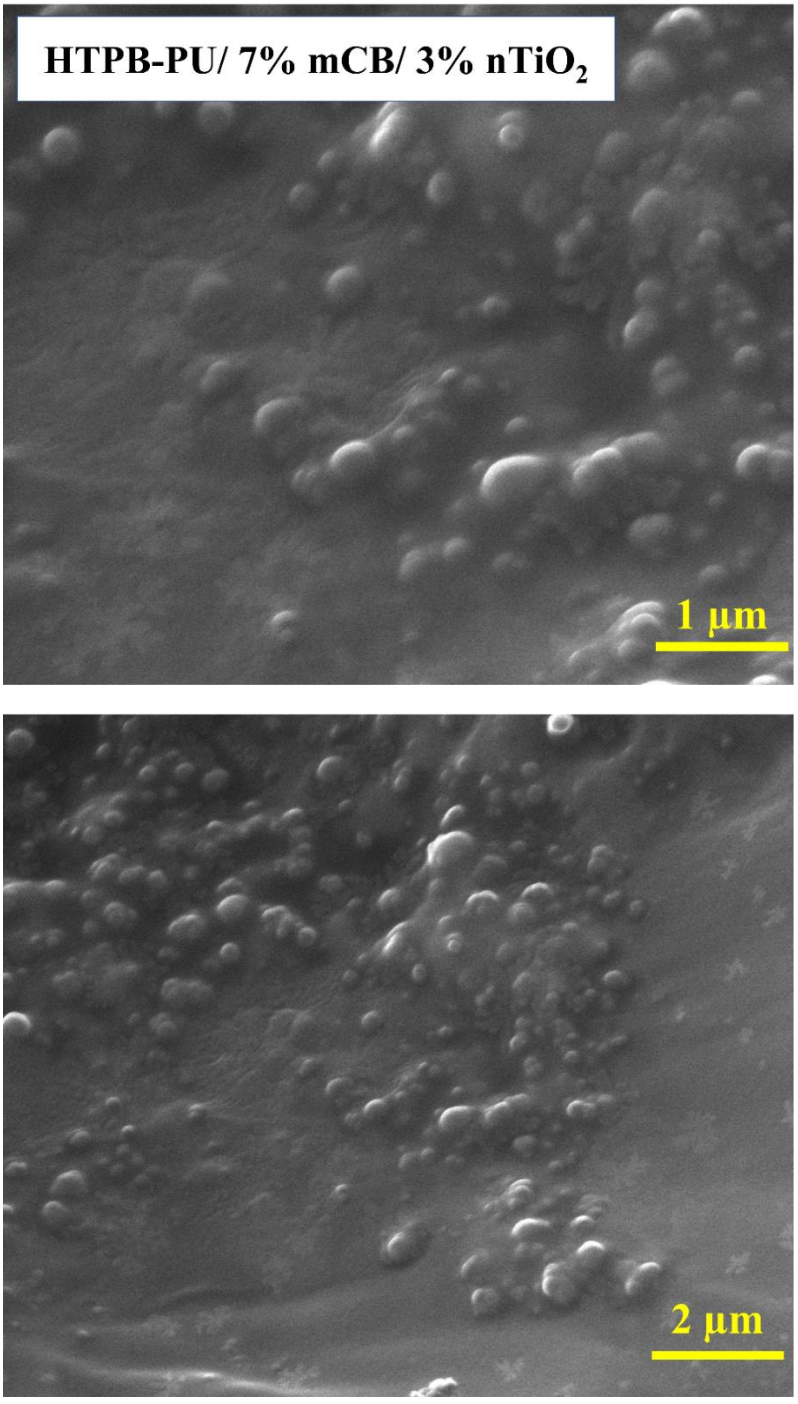

(b)

Figure 3.7 Contn'd.

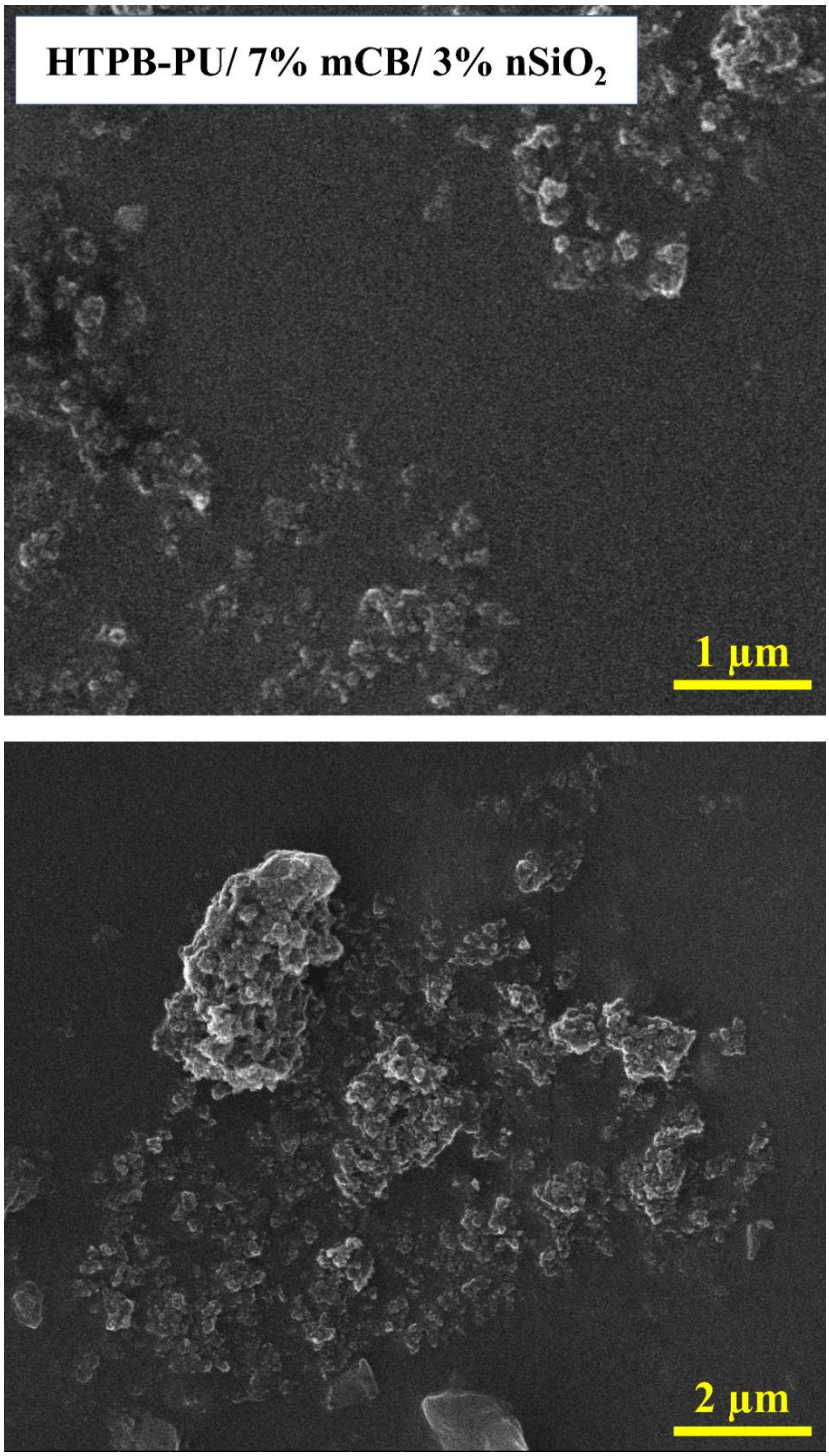

(c)

Figure 3.7 Contn'd.

3.4 Effects of $mZrO_2$, $nTiO_2$, and $nSiO_2$ Replacements on the Mechanical Properties

Stress-strain curves obtained by the tension tests of unfilled HTPB-PU matrix and filled formulations with 3 wt% replacement of nCB, $mZrO_2$, $nTiO_2$, and $nSiO_2$ were given in Figure 3.8 at three different temperatures (70, 23, -40°C). Then, these curves for all specimen compositions at each temperature were used to determine the four mechanical properties as tabulated in Table 3.2 with average values and standard deviations.

In order to compare effects of 3% nCB replacement with the 3% replacements of $mZrO_2$, $nTiO_2$, and $nSiO_2$ fillers on the mechanical properties; data were re-evaluated for the Tensile Strength and Tensile Modulus in Figure 3.9, while for the Elongation at Break and Toughness in Figure 3.10.

Just like in the first step of this study, these figures and the table indicated that temperature level had very significant importance on all mechanical properties of the specimens; i.e., increasing the temperature degraded all properties significantly. Since the main reason for this discrepancy was discussed in Section 3.2 before, it would be not mentioned in this section.

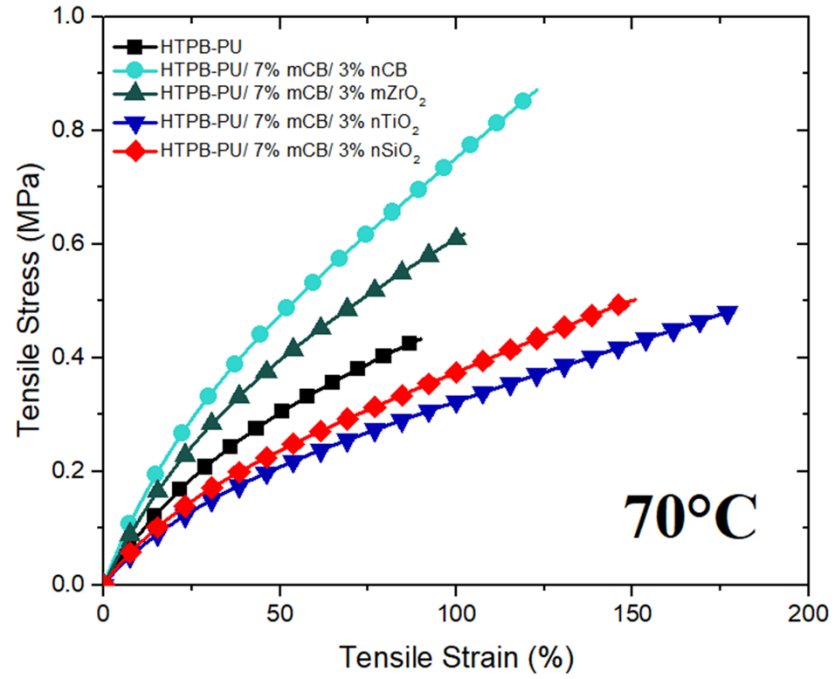

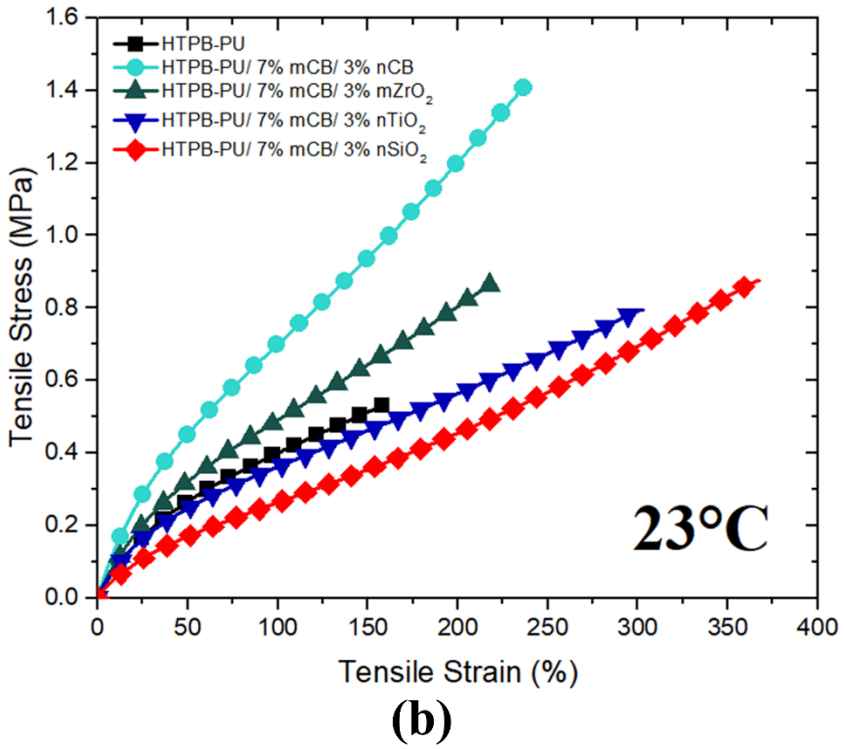

Figure 3.8 Effects of nCB, $mZrO_2$, $nTiO_2$, and $nSiO_2$ replacements on the Tensile Stress versus Tensile Strain curves at (a) 70°C, (b) 23°C, and (c) -40°C.

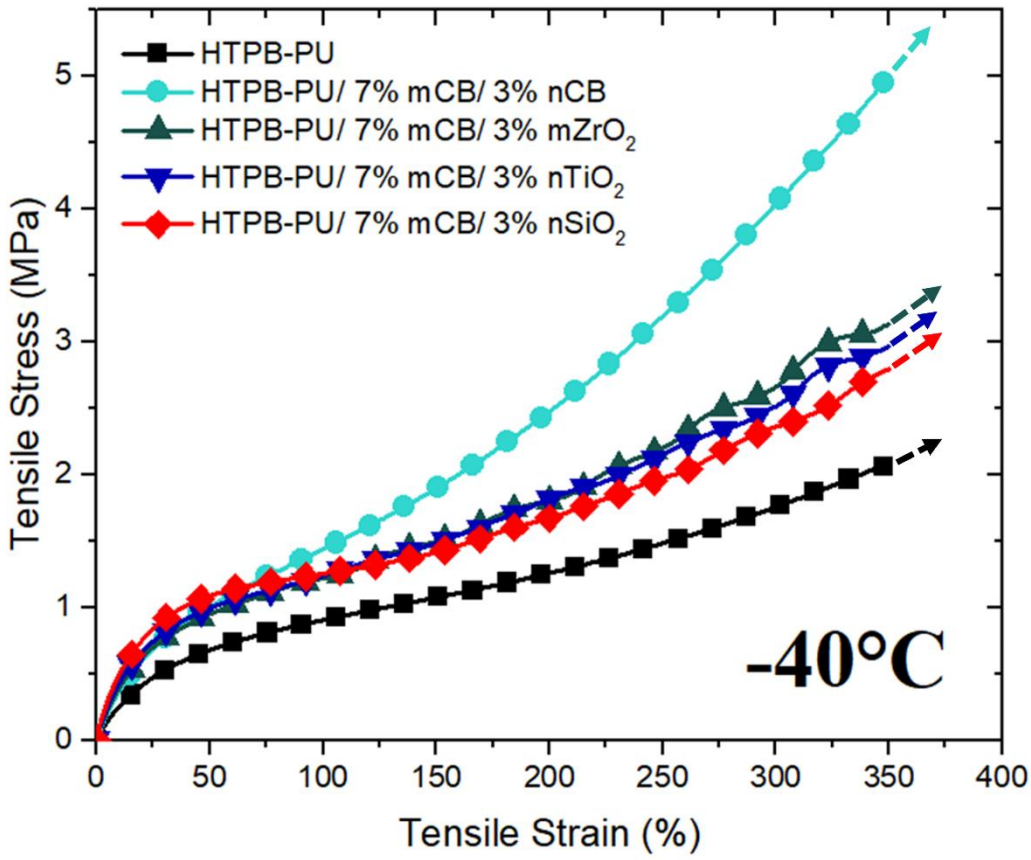

(c)

Figure 3.8 Contn'd.

Table 3.2. Mechanical properties of unfilled and filled HTPB-PU elastomer materials at three different testing temperatures

Temperature (°C)	**Specimens**	**Tensile Strength** (MPa)	**Tensile Modulus** (MPa)	**Elongation at Break** (%)	**Toughness** (kJ/m^3)
70	HTPB-PU	0.43±0.02	0.93±0.02	90±9	233±38
	HTPB-PU/ 7% mCB/ 3% nCB	0.87±0.05	1.50±0.02	123±9	630±73
	HTPB-PU/ 7% mCB/ 3% $mZrO_2$	0.62±0.03	1.23±0.02	102±5	382±36
	HTPB-PU/ 7% mCB/ 3% $nTiO_2$	0.48±0.05	0.68±0.03	177±22	510±70
	HTPB-PU/ 7% mCB/ 3% $nSiO_2$	0.56±0.03	0.79±0.03	151±10	446±50
23	HTPB-PU	0.53±0.05	0.89±0.02	155±22	508±123
	HTPB-PU/ 7% mCB/ 3% nCB	1.42±0.08	1.53±0.03	238±13	1860±176
	HTPB-PU/ 7% mCB/ 3% $mZrO_2$	0.87±0.06	1.08±0.03	220±18	1110±149
	HTPB-PU/ 7% mCB/ 3% $nTiO_2$	0.80±0.15	0.92±0.06	303±56	1399±225
	HTPB-PU/ 7% mCB/ 3% $nSiO_2$	0.88±0.08	0.59±0.04	368±29	1617±286
-40	HTPB-PU	>2.07	2.80±0.03	>350	>4910
	HTPB-PU/ 7% mCB/ 3% nCB	>5.00	4.13±0.14	>350	>9610
	HTPB-PU/ 7% mCB/ 3% $mZrO_2$	>3.13	4.45±0.40	>350	>7562
	HTPB-PU/ 7% mCB/ 3% $nTiO_2$	>2.96	4.90±0.67	>350	>8277
	HTPB-PU/ 7% mCB/ 3% $nSiO_2$	>2.79	5.59±0.73	>350	>7419

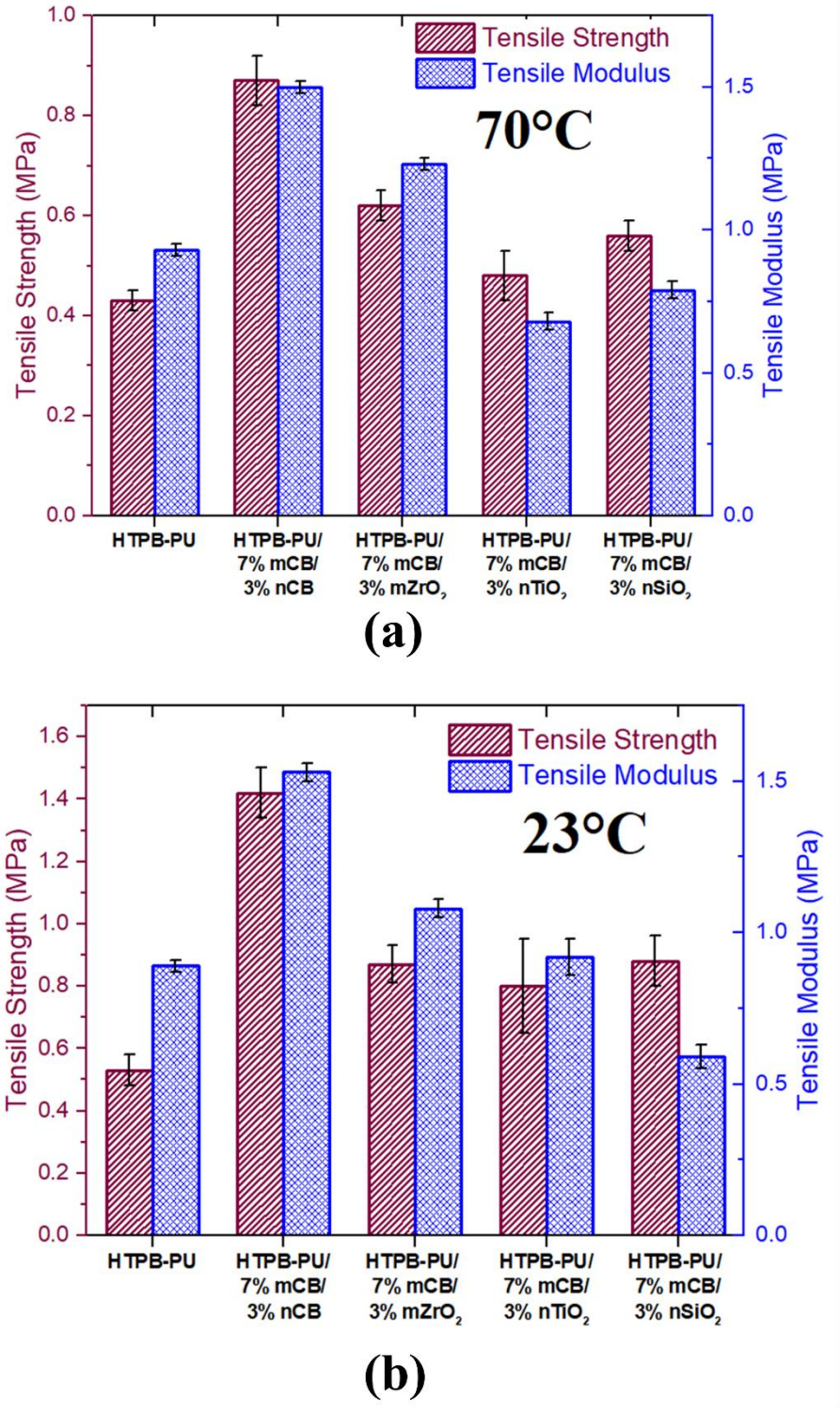

Figure 3.9 Effects of nCB, $mZrO_2$, $nTiO_2$, and $nSiO_2$ replacements on the Tensile Strength and Tensile Modulus values at (a) 70°C, (b) 23°C, and (c) -40°C.

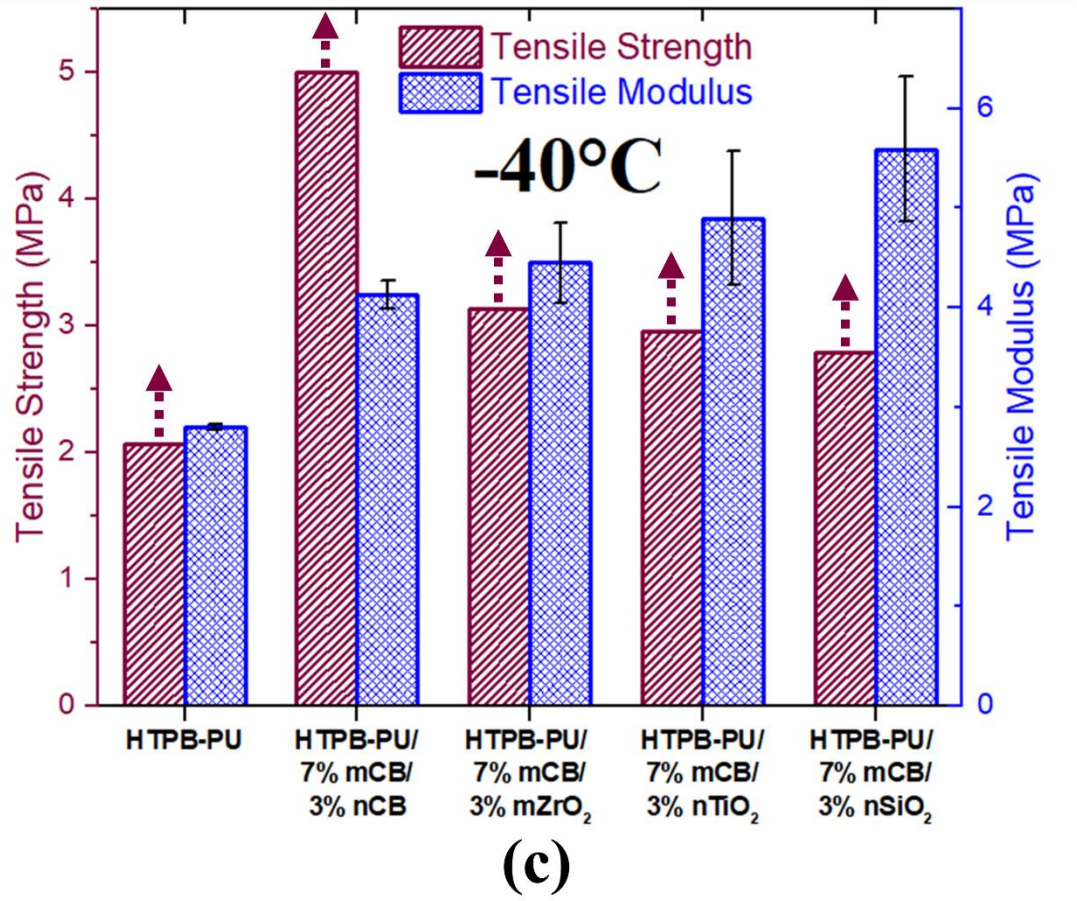

Figure 3.9 Contn'd.

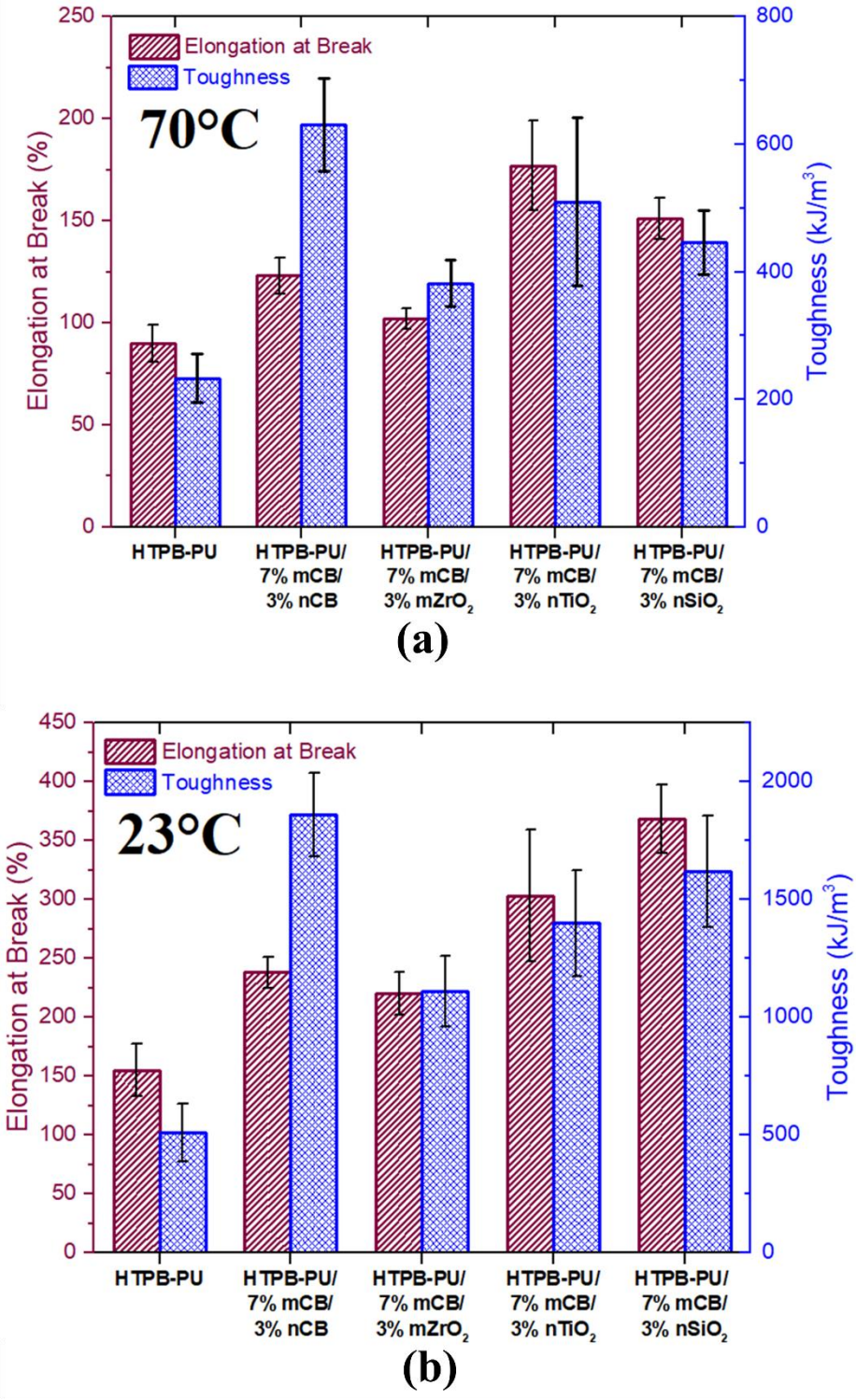

Figure 3.10 Effects of nCB, $mZrO_2$, $nTiO_2$, and $nSiO_2$ replacements on the Elongation at Break and Toughness values at (a) 70°C, (b) 23°C, and (c) -40°C

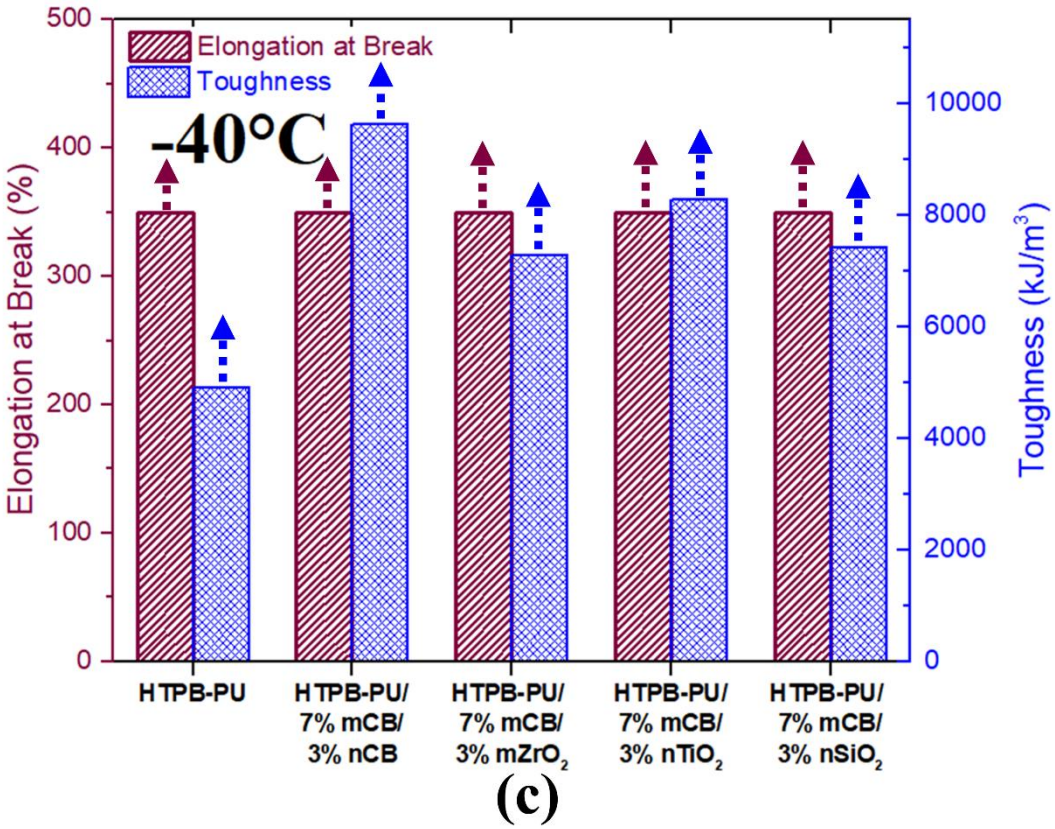

Figure 3.10 Contn'd.

Just like 7% mCB plus 3% nCB specimen formulation; Table 3.2, Figure 3.9, and Figure 3.10 indicated that when HTPB-PU matrix was filled with 7% mCB together with 3% $mZrO_2$, $nTiO_2$, and $nSiO_2$ particles, all mechanical properties improved significantly at all temperatures. Because, as discussed in Section 3.2 in detail before, the same strengthening mechanisms and the same toughening mechanisms mentioned for nCB particles would be also valid for the $mZrO_2$, $nTiO_2$, and $nSiO_2$ particles.

On the other hand, Figures 3.9, 3.10, and Table 3.2 also revealed that the degree of improvements in all mechanical properties in the nCB replacement were higher compared to the improvements in the $mZrO_2$, $nTiO_2$, and $nSiO_2$ replacements.

Thus, it could be generally concluded that replacement of total 10 wt% mCB particles with 3 wt% nCB particles would be an optimum composition for the highest level of mechanical properties at all temperatures.

The reason for the higher performance of nCB particles compared to the $mZrO_2$, $nTiO_2$, and $nSiO_2$ particles would be higher possibility of chemical interactions at the interface between HTPB-PU matrix and nCB surfaces. Because, it is known that [13, 18, 21] normally there are active hydroxyl groups (—OH) on the surface of Carbon Black particles, both mCB and nCB. Then, it would be easier to interact with the hydroxyl end groups (—OH) of the butadiene structure (soft segments), and with the isocyanate groups (—NCO) of the urethane structure (hard segments) of the HTPB-PU matrix. It is also reported that [13, 18] reinforcing effects of Carbon Black particles would take place not only by the physical interaction but also formation of chemical bonds and interactions at the interface between the Carbon Black particles and macromolecular structure of HTPB-PU elastomer.

Therefore, compared to the $mZrO_2$, $nTiO_2$, and $nSiO_2$ particles, higher possibility of chemical interactions between the HTPB-PU matrix and nCB particles would result in higher effectiveness in the strengthening mechanisms and toughening mechanisms leading to better mechanical properties.

3.5 Thermal Behavior of Unfilled and Filled HTPB-PU Elastomer

Thermal behavior of the unfilled and filled HTPB-PU with total filler content of 10 wt% mCB, and 3 wt% replacements of nCB, $mZrO_2$, $nTiO_2$, and $nSiO_2$ fillers were investigated by thermogravimetric analysis (TGA), differential scanning calorimetry (DSC), dynamic mechanical analysis (DMA), thermomechanical analysis (TMA) and thermal conductivity measurements.

(i) Thermal Degradation Temperatures of the Specimens

Thermogravimetric analysis (TGA) of all specimens were conducted first to investigate their thermal decomposition behaviors. Results of these analyses were given in Figure 3.11 in the form of % weight loss and derivative of weight loss per degrees.

It is known that application of thermal stress to polymers causes vibration and rotation of covalent bonds within their structure, and excessive excitation leads to breakage of these bonds to form radicals and small molecules. These fragments are then vaporized or diffused out, and a non-volatile char is formed at the end.

Generally, decomposition of polyurethane structures take place at three stages [42]. Derivative curves for the HTPB-PU matrix in Figure 3.11 indicated that the peak temperature for the “First Decomposition Step” was around 209°C, while for the “Second Decomposition Step” the peak was around 330°C. It was discussed that [28, 43] the first and the second decomposition steps belong to the rather weak bonds of C-N, C-O, N-H, etc. present in the isocyanate based hard segments of the structure. It was shown in the Figure 3.11 that the highest peak took place around 448°C, which is the “Third Decomposition Step”. It was indicated that [42, 43] this most significant step belongs to the stronger bonds of C-C, C-H, C=C, etc. present in the butadiene based soft segments of the structure. It was observed that there were no significant influences of the fillers on the Thermal Decomposition Steps of the HTPB-PU elastomer matrix.

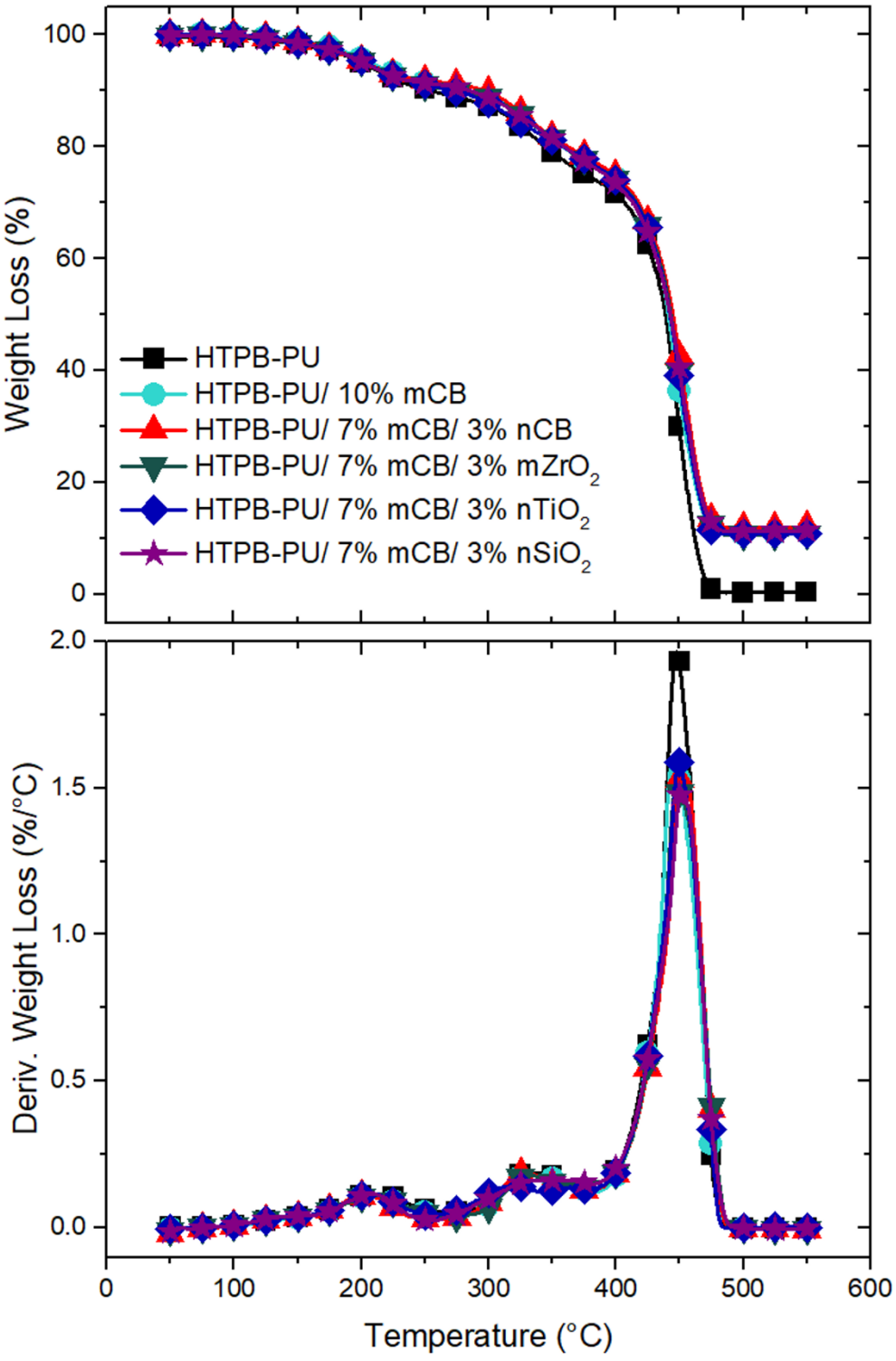

Figure 3.11 TGA curves as % Weight Loss and its Derivative for the unfilled and filled HTPB-PU specimens.

Table 3.3 Thermal Degradation Temperatures ($T_{5\%}$, $T_{10\%}$, $T_{25\%}$, T_{max}) and % Residue at 550°C for the unfilled and filled HTP-PU specimens.

Specimens	$T_{5\%}$ (°C)	$T_{10\%}$ (°C)	$T_{25\%}$ (°C)	T_{max} (°C)	**% Residue at 550°C**
HTPB-PU	203	270	389	445	0.81
HTPB-PU/ 10% mCB	208	282	396	445	10.84
HTPB-PU/ 7% mCB/ 3% nCB	204	298	399	448	12.14
HTPB-PU/ 7% mCB/ 3% $mZrO_2$	203	274	395	447	11.07
HTPB-PU/ 7% mCB/ 3% $nTiO_2$	203	274	395	450	10.79
HTPB-PU/ 7% mCB/ 3% $nSiO_2$	203	286	392	452	11.57

TGA curves were than used to determine "Thermal Degradation Temperatures" $T_{5\%}$, $T_{10\%}$, and $T_{25\%}$ for the 5, 10, 25 wt% weight losses, and T_{max} for the maximum mass loss in the specimens as tabulated in Table 3.3. In the table, % Residue of each specimen determined at 550°C was also included, which was consistent with the 10 wt% total filler content used.

Table 3.3 indicated that when HTPB-PU matrix was filled with 10 wt% mCB or replacement of this content with 3 wt% of nCB, $mZrO_2$, $nTiO_2$, and $nSiO_2$ particles, Thermal Degradation Temperatures of the matrix were not improved significantly.

These increases would be especially due to the heat barrier effects of the fillers at all stages of the thermal decomposition of the matrix. Because, compared to the matrix; mCB, nCB, $mZrO_2$, $nTiO_2$, and $nSiO_2$ particles have much higher thermal stability and shielding effect against transportation of heat and volatile products formed during thermal decomposition of the matrix.

(ii) Glass Transition Temperature of the Specimens

Differential scanning calorimetry (DSC) analyses were conducted in order to determine Glass Transition Temperature (T_g) of all specimens as given in Figure 3.12. Thermograms in Figure 3.12 revealed that there was only one endothermic change corresponding to the Glass Transition regime. Therefore, T_g of the materials were determined via half-height midpoint method by drawing the onset line on the upper plateau and the endset line on the lower plateau of the transition region, and midpoint of the liner connecting them was taken as T_g of the specimens and the values were tabulated in Table 3.4.

Figure 3.12 and Table 3.4 pointed out that T_g of the HTPB-PU elastomer matrix was around -78.6°C. It was also observed that when HTPB-PU matrix was filled with mCB, nCB, mZrO_2, nTiO_2, and nSiO_2 particles as the total filler amount of 10 wt%, there were no significant changes in the value of T_g.

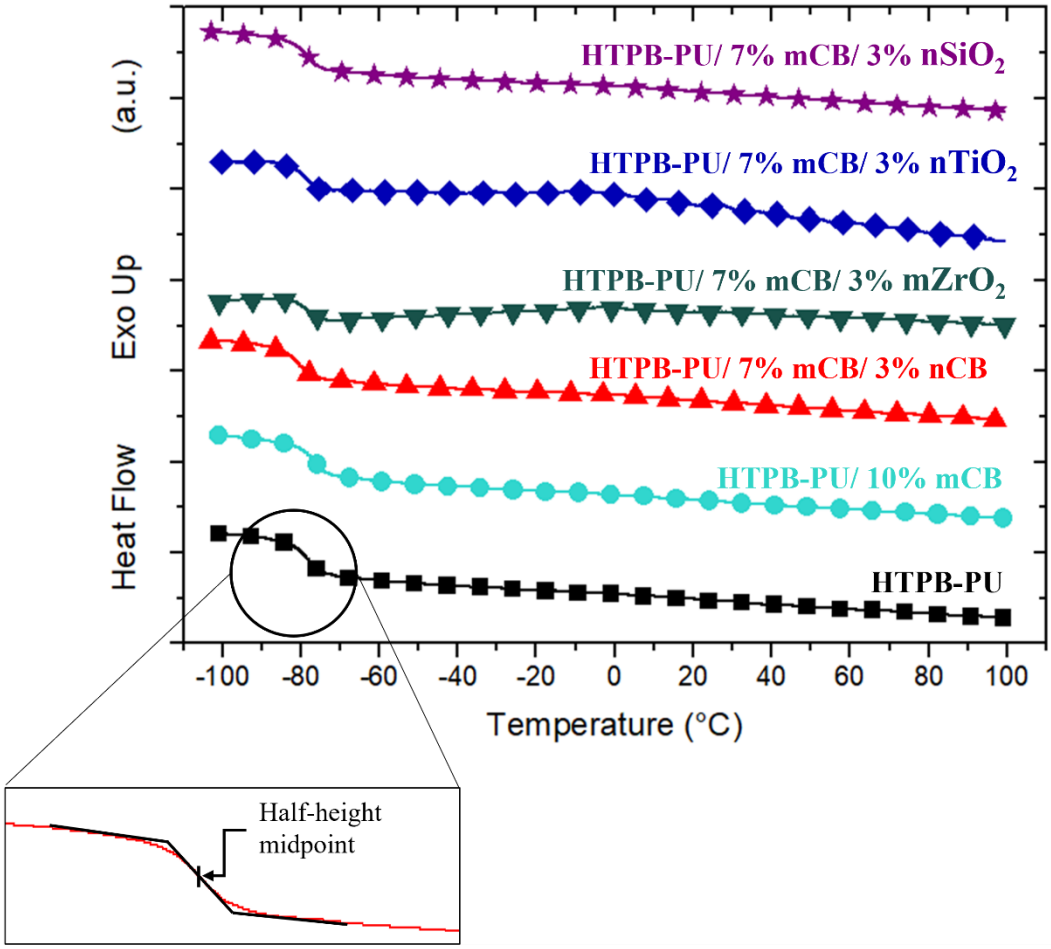

Figure 3.12 DSC thermograms of the unfilled and filled HTPB-PU specimens, including the T_g determination method used.

Table 3.4 Glass Transition Temperature (T_g) determined by DSC, Onset and Peak of *tan δ* temperatures determined by DMA of the unfilled and filled HTPB-PU specimens

Specimens	DSC	DMA	
	T_g (°C)	Onset of *tan* δ_{peak} (°C)	*tan* δ_{peak} (°C)
HTPB-PU	-78.6	-78.6	-57.8
HTPB-PU/ 10% mCB	-78.5	-77.7	-55.7
HTPB-PU/ 7% mCB/ 3% nCB	-78.8	-76.7	-56.3
HTPB-PU/ 7% mCB/ 3% $mZrO_2$	-78.6	-79.1	-57.2
HTPB-PU/ 7% mCB/ 3% $nTiO_2$	-79.6	-80.0	-58.2
HTPB-PU/ 7% mCB/ 3% $nSiO_2$	-79.1	-80.3	-57.8

(iii) Storage Modulus and *tan δ* of the Specimens

Dynamic mechanical analyses (DMA) were carried out in order to determine Storage Modulus values and *tan δ* peaks of all specimens (Figure 3.13). In order to compare T_g values of the specimens determined by DSC analyses, first of all *tan δ* curves were evaluated; and determined temperature values at the "onset of *tan* δ_{peak}" and temperature values for the "*tan* δ_{peak}" of all specimens were tabulated in Table 3.4 together with the T_g values determined from DSC analyses.

Table 3.4 revealed that T_g value of the HTPB-PU matrix from DSC was the same with the value of Onset Temperature of *tan* δ_{peak}, i.e., -78.6°C. For the HTPB-PU matrix, temperature at the *tan* δ_{peak} was -57.8°C. Again, no significant influences of fillers were observed for these *tan* δ_{peak} temperatures.

Then, storage modulus curves in Figure 3.13 were evaluated to observe effects of fillers on the Storage Modulus values of HTPB-PU matrix at four different temperatures (-95°C, -85°C, -75°C, -65°C) being all lower than the *tan* δ_{peak} of -57.8°C. The data were tabulated in Table 3.5.

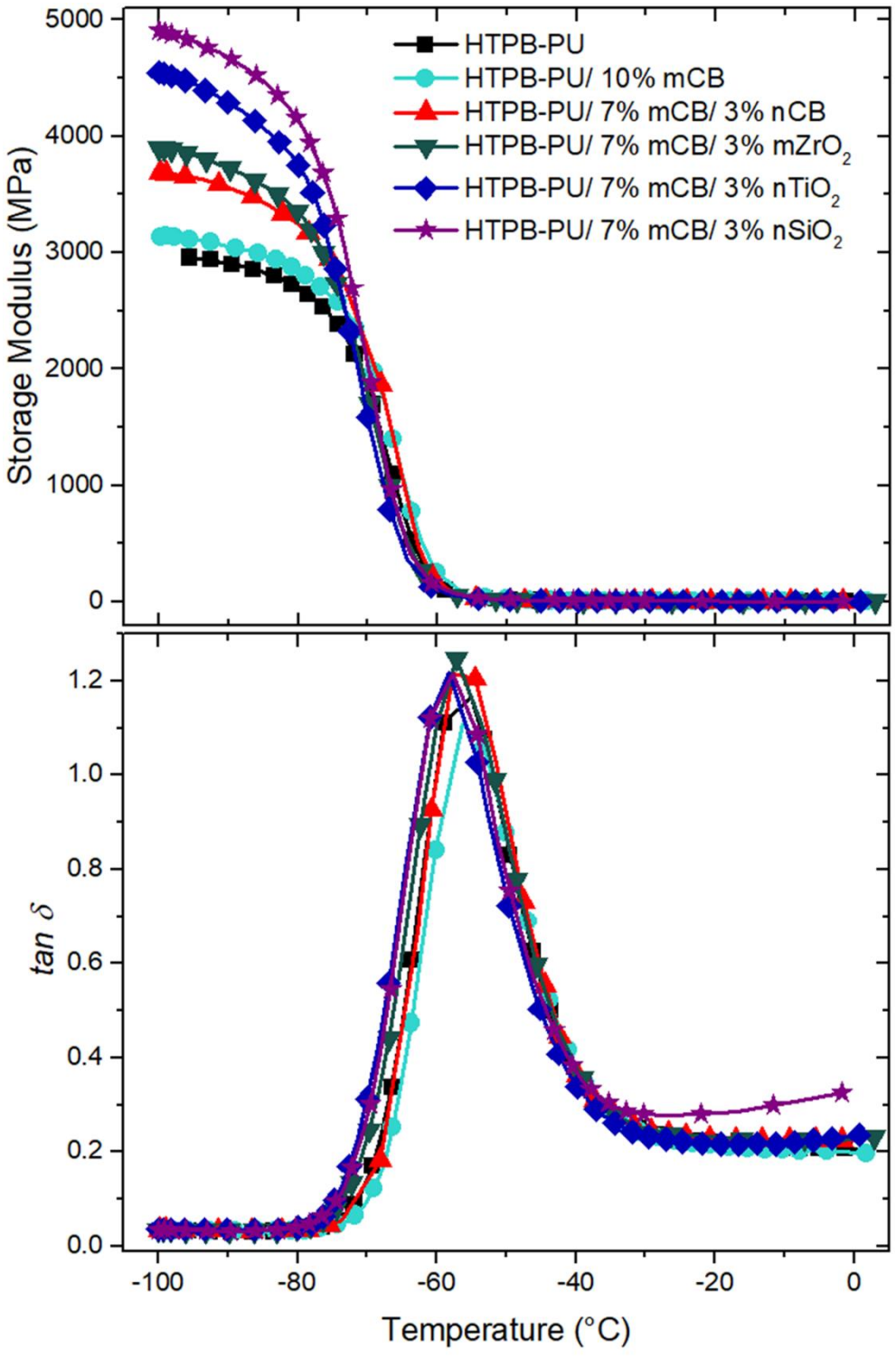

Figure 3.13 DMA curves as Storage Modulus and *tan δ* for the unfilled and filled HTPB-PU specimens.

Table 3.5 Storage Modulus values determined at four different temperatures for the unfilled and filled HTPB-PU specimens.

Specimens	**Storage Modulus** (MPa)			
	at -95°C	**at -85°C**	**at -75°C**	**at -65°C**
HTPB-PU	2952	2828	2443	793
HTPB-PU/ 10% mCB	3108	2982	2618	1079
HTPB-PU/ 7% mCB/ 3% nCB	3642	3432	2919	1050
HTPB-PU/ 7% mCB/ 3% $mZrO_2$	3839	3582	2813	624
HTPB-PU/ 7% mCB/ 3% $nTiO_2$	4449	4075	2938	478
HTPB-PU/ 7% mCB/ 3% $nSiO_2$	4812	4475	3412	642

Since it is closer to the *tan* δ_{peak} (-57.8°C), Table 3.5 indicated that at -65°C, there was almost no improvement when the matrix was filled with $mZrO_2$, $nTiO_2$, and $nSiO_2$ particles; mCB and nCB particles resulted in certain improvement.

On the other hand, at -95°C, -85°C, -75°C, being much lower than the *tan* δ_{peak}, significant improvements in the Storage Modulus value of HTPB-PU matrix were observed by the addition of all fillers (mCB, nCB, $mZrO_2$, $nTiO_2$, and $nSiO_2$). For instance, the improvement in the Storage Modulus value of the matrix at -95°C started from 5% up to 63%, while at -85°C the improvement was up to 58%; at -75° up to 40%, respectively.

Because, at these low temperatures, “load transfer” strengthening mechanism and “crack bowing”, “crack deflection” toughening mechanisms discussed in Section 3.2 would be also operative resulting in significant improvements in the Storage Modulus values of the filled specimens.

(iv) Thermal Expansion Coefficient and Thermal Conductivity of the Specimens

Thermomechanical Analyses (TMA) were used to determine Thermal Expansion Coefficient of all specimens in the range from -50°C to 100°C. Dimension change curves for the specimens were given in Figure 3.14. It was seen that these curves were almost linear. Then, by taking the slope of these curves, Thermal Expansion Coefficient of the specimens were determined and tabulated in Table 3.6.

As expected, Table 3.6 showed that the highest Thermal Expansion Coefficient value (258 μm/m·°C) was determined for the unfilled HTPB-PU matrix. Filling with mCB, nCB, $mZrO_2$, $nTiO_2$, and $nSiO_2$ particles decreased the Thermal Expansion Coefficient of the elastomer matrix. Compared to the others, higher level of reduction was obtained with the mCB and nCB particles being around 13%.

It can be stated that the reduction in the Thermal Expansion Coefficient of the matrix would be due to the decreased macromolecular expansion of the hard and soft segments of the HTPB-PU matrix by the mobility retardation effects of the fillers.

Thermal conductivity measurements of all specimens were carried out at four different temperatures of 0°C, 30°C, 60°C, and 90°C. Data for each specimen at each temperature were compared in Figure 3.15. Then, the average of the values determined at these temperatures were tabulated in Table 3.6 with standard deviations for all specimens.

Table 3.6 indicated that the lowest Thermal Conductivity value (0.230 W/m·K) was obtained for the unfilled HTPB-PU matrix, because polymers have extremely low Thermal Conductivity values. Addition of mCB, nCB, $mZrO_2$, $nTiO_2$, and $nSiO_2$ particles increased the Thermal Conductivity of the matrix, because these particles have higher Thermal Conductivity compared to the polymer matrices. For example, the increases started from 13% up to 22%.

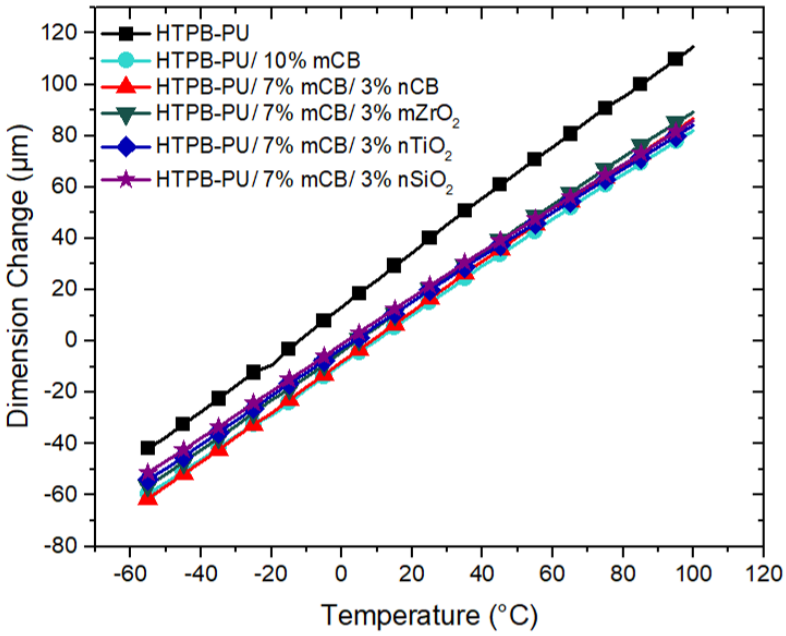

Figure 3.14 TMA dimension change curves for the unfilled and filled HTPB-PU specimens

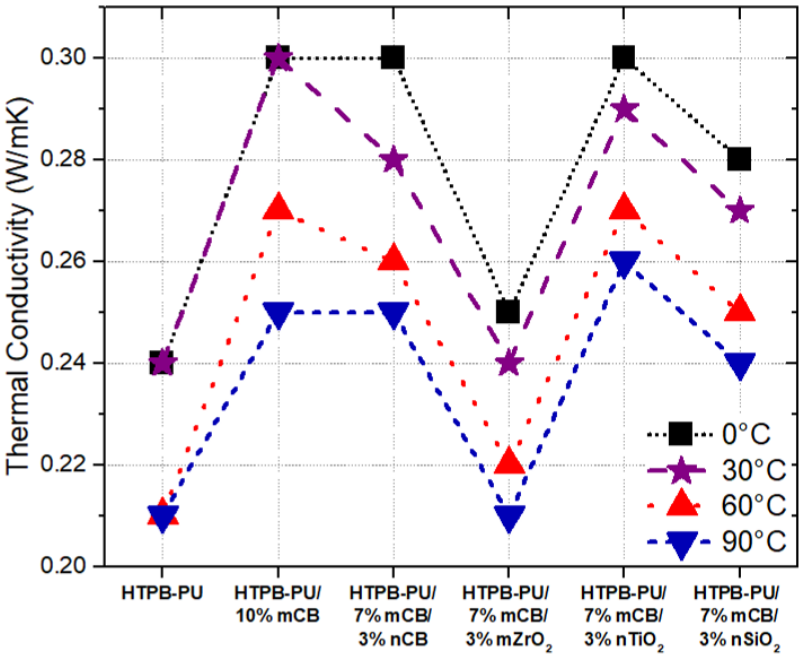

Figure 3.15 Thermal Conductivity values for the unfilled and filled HTPB-PU specimens determined at four different temperatures

Table 3.6 Thermal Expansion Coefficient and Thermal Conductivity values for the unfilled and filled HTPB-PU specimens.

Specimens	**Thermal Expansion Coefficient** (between -50°C and 100°C) (μm/m·°C)	**Thermal Conductivity** (average of values determined at 0°C, 30°C, 60°C, 90°C) (W/m·K)
HTPB-PU	258.64	0.225±0.017
HTPB-PU/ 10% mCB	224.50	0.280±0.024
HTPB-PU/ 7% mCB/ 3% nCB	227.90	0.273±0.022
HTPB-PU/ 7% mCB/ 3% mZrO_2	243.68	0.228±0.015
HTPB-PU/ 7% mCB/ 3% nTiO_2	240.20	0.280±0.018
HTPB-PU/ 7% mCB/ 3% nSiO_2	241.24	0.260±0.018

CHAPTER 4

CONCLUSIONS

Main conclusions on the performance of unfilled and filled HTPB-PU elastomer materials investigated were as follows.

- Tension tests conducted at 70°C, 23°C and -40°C revealed that all mechanical properties of the unfilled and filled specimens enhanced by decreasing the temperature. For instance, Tensile Strength of unfilled HTPB-PU at 23°C increased as much as 290% at -40°C. Because, it has more stable structure when loaded at temperatures closer to its Glass Transition Temperature determined as -79°C.

- When HTPB-PU matrix was filled with 10 wt% mCB, all mechanical properties improved significantly at all temperatures. For example, at 23°C, the increase in Tensile Strength was 74%.

- When certain amounts of mCB were replaced with nCB particles, e.g., 3 wt% without changing the total filler content of 10 wt%, it was seen that nCB particles had further contribution to all mechanical properties of the HTPB-PU matrix. For example, at 23°C, Tensile Strength value increased by 145%.

- Two main “strengthening” mechanisms proposed were “load transfer” and “molecular mobility decrease” mechanisms. The main “toughening” mechanism proposed was the prevention or retardation of the defects via “crack deflection” and “crack bowing” sub-mechanisms.

- When certain amounts of mCB particles were replaced with nCB particles, the effectiveness of these strengthening and toughening mechanisms were much more pronounced. Because, when the fillers were used in nano-sizes, their specific surface area increases considerably leading to much more molecular level interaction between the fillers and the matrix material.

- When HTPB-PU matrix was filled with 7 wt% mCB together with 3 wt% $mZrO_2$, $nTiO_2$, and $nSiO_2$ particles, all mechanical properties again enhanced significantly at all temperatures. On the other hand, the degree of improvements in all mechanical properties in the nCB replacement were higher compared to the improvements in the $mZrO_2$, $nTiO_2$, and $nSiO_2$ replacements.

- Main reason proposed for the higher performance of nCB particles compared to other fillers would be higher possibility of chemical interactions at the interface between HTPB-PU matrix and active hydroxyl groups present on the surface of CB particles, leading to higher effectiveness in the strengthening and toughening mechanisms.

- Various thermal analyses conducted for all specimen compositions indicated that use of 10 wt% total filler content had slight influences on the thermal properties of the HTPB-PU elastomer matrix.

To compare the results acquired in this study to those reported in the literature, obtained properties were retabulated in Table 4.1. In this table, only mechanical properties obtained at 23°C are tabulated for comparison.

Table 4.1 Comparison of mechanical properties of HTPB-PU elastomer materials filled with various particles reported in the literature and obtained in this study.

Main Filler	Main Filler Content (wt%)	Additional Filler	Additional Filler Content (wt%)	Tensile Strength (MPa)	Tensile Modulus (MPa)	Elongation at Break (%)	Source
No Filler	-	-	-	0.53	0.89	155	*This study*. (Test results at 23°C testing temperature)
Carbon Black (200-500 nm)	10	-	-	0.92	1.35	179	
Carbon Black (200-500 nm)	7	Carbon Black (40-90 nm)	3	1.42	1.53	238	
Carbon Black (200-500 nm)	7	ZrO_2 (100-350 nm)	3	0.87	1.08	220	
Carbon Black (200-500 nm)	7	TiO_2 (10-100 nm)	3	0.80	0.92	303	
Carbon Black (200-500 nm)	7	SiO_2 (20-60 nm)	3	0.88	0.59	368	
No Filler	-	-	-	0.50	-	250	Aslan, *MSc. Thesis* (2021) [44]
Carbon Black (300 nm)	10	-	-	0.77	-	260	
Carbon Black (25 nm)	10	-	-	1.75	-	375	
Carbon Black (25 nm)	5	Carbon Black (300 nm)	5	1.35	-	278	
No Filler	-	-	-	1.06	-	707	Quagliano *et. al*. (2019) [31]
TiO_2	20	-	-	0.67	-	500	
ZrO_2	20	-	-	1.33	-	186	
ZnO	20	-	-	1.81	-	237	
Nanoclay (Cloisite 20A)	5	-	-	1.48	-	636	
No Filler	-	-	-	-	0.50	-	Ross *et. al*. (2017) [32]
TiO_2 (10-15 μm)	20	-	-	-	1.08	-	
ZnO (0.4 μm)	20	-	-	-	1.81	-	
Lithophone (2-4 μm)	20	-	-	-	1.68	-	
$CaCO_3$ (1.5 μm)	20	-	-	-	2.17	-	
Carbon Black (1.5 μm)	20	-	-	-	2.82	-	
Nanoclay (Cloisite 20A)	5	-	-	-	3.3	-	
Silanized Nanoclay (Cloisite 20A)	5	-	-	-	0.5	-	

Table 4.1 Contn'd.

Main Filler	Main Filler Content (wt%)	Additional Filler	Additional Filler Content (wt%)	Tensile Strength (MPa)	Tensile Modulus (MPa)	Elongation at Break (%)	Source
No Filler	-	-	-	0.51	-	-	Kim *et. al.* (2013) [33]
Octaisobutyl POSS	50	-	-	0.13	-	-	
trans-cyclohexanediol isobutyl POSS	23	-	-	1.19	-	-	
1,2-propanediol isobutyl POSS	33	-	-	0.97	-	-	
SiO_2	2.5	-	-	0.792	-	136.6	Dubois *et. al.* (2006) [34]
Bisphenol-A coated SiO_2	2.5	-	-	0.919	-	128.5	
Carbon Black	10	Sb_2O_3	10	2.6-2.9	-	-	Navale *et. al.* (2004) [4]
Carbon Black	10	Sb_2O_3	24	2.8-3.3	-	-	
Carbon Black (N550)	48	-	-	5.60	-	-	Kakade *et. al.* (2001) [18]
Carbon Black (N550)	40	SiO_2 (2-10 μm)	8	5.24	-	-	
Carbon Black (N550)	40	TiO_2 (2-10 μm)	8	4.88	-	-	
Carbon Black (N550)	40	Sb_2O_3 (2-10 μm)	8	4.92	-	-	
No Filler	-	-	-	0.567	-	-	Benli *et. al.* (1998) [21]
Carbon Black (300 nm)	10	-	-	0.858	-	-	
Carbon Black (25 nm)	10	-	-	2.010	-	-	
Carbon Black (25 nm)	10	SiO_2 (500 nm)	16	2.658	-	-	
Carbon Black (25 nm)	10	Al_2O_3 (5 μm)	16	2.075	-	-	
Carbon Black (25 nm)	10	ZrO_2 (10 μm)	16	1.983	-	-	

REFERENCES

[1] Merriam-Webster. (n.d.). Propulsion definition & meaning. Merriam-Webster. Retrieved April 2, 2022, from https://www.merriam-webster.com/dictionary/propulsion

[2] Sutton, G. P., & Biblarz, O. (2017). *Rocket Propulsion Elements*. John Wiley & Sons.

[3] NASA. (n.d.). *Beginner's Guide to Propulsion*. NASA. Retrieved April 2, 2022, from https://www.grc.nasa.gov/www/k-12/airplane/bgp.html

[4] Navale, S. B., Sriraman, S., Wani, V. S., Manohar, M. V., & Kakade, S. D. (2004), "Effect of additives on liner properties of case-bonded composite propellants", *Defence Science Journal*, 54(3), 353–359, https://doi.org/10.14429/dsj.54.2049

[5] Zhou, Q. C., Xu, J. S., Chen, X., & Zhou, C. S. (2016), "Review of the adhesively bonded interface in a solid rocket motor", *Journal of Adhesion*, 92(5), 402–428, https://doi.org/10.1080/00218464.2015.1040155

[6] Huang, Z. P., Nie, H. Y., Zhang, Y. Y., Tan, L. M., Yin, H. L., & Ma, X. G. (2012), "Migration kinetics and mechanisms of plasticizers, stabilizers at interfaces of NEPE propellant/HTPB liner/EDPM insulation", *Journal of Hazardous Materials*, 229–230, 251–257, https://doi.org/10.1016/j.jhazmat.2012.05.103

[7] Gustavson, C., Greenlee, T. W., & Ackley, A. W. (1966), "Bonding of composite propellant in cast-in-case rocket motors", *Journal of Spacecraft and Rockets*, 3(3), 413–418, https://doi.org/10.2514/3.28461

[8] Morais, Ana & Holanda, Sabóia & Pinto, Juliano. (2006), "Optimization of bondline's properties of solid rocket motors", In, *Energetic Materials*

Insensitivity, Ageing, Monitoring-37th International Annual Conference of ICT, Fraunhofer-Institut für Chemische Technologie (ICT).

[9] Rodic, V. (2007), "Case Bonded System for Composite Solid Propellants", *Scientific Technical Review,* LVII(3-4).

[10] Libardi, J., Ravagnani, S. P., Morais, A. M. F., & Cardoso, A. R. (2009), "Study of plasticizer diffusion in a solid rocket motoŕs bondline", *Journal of Aerospace Technology and Management*, 1(2), 223–229. https://doi.org/10.5028/jatm.2009.0102223229

[11] Horine, C. L., & Madison, E. W. (1971), "Solid propellant processing factors in rocket motor design", *NASA Space Vehicle Design Criteria (Chemical Propulsion) Monograph,* NASA SP-8075.

[12] Twitchell, S. E. (1976), "Solid rocket motor internal insulation", *NASA Space Vehicle Design Criteria (Chemical Propulsion) Monograph*, NASA SP-8093.

[13] Chen, G. H., Tian, J., Liu, C., Li, D., & Lu, X. H. (2014), "Analysis on the bonding property of the propellant and liner", *Advanced Materials Research,* 912–914, 44–47, https://doi.org/10.4028/www.scientific.net/AMR.912-914.44

[14] Hemminger, C. S. (1997), "Surface characterization of solid rocket motor HTPB liner bond system", *33rd Joint Propulsion Conference and Exhibit*, https://doi.org/10.2514/6.1997-2995

[15] Gupta, D. C., Divekar, P. K., & Phadke, V. K. (1997), "HTPB-based polyurethanes for inhibition of composite-modified double-base (CMDB) propellants", *Journal of Applied Polymer Science,* 65(2), 355–363, https://doi.org/10.1002/(sici)1097-4628(19970711)65:2<355::aid-app16>3.3.co;2-x

[16] Schloss, H. R. (1972), “Applied Research and Development of Adhesives for Bonding Filled Carboxyl Terminated Polybutadienes to Various Substrates”, *The Journal of Adhesion*, 4:4, 333-351, DOI:10.1080/00218467208075012.

[17] Liang, B., Zhang, N., Zhang, Z.-bo, Ren, R., & Luo, Y.-jun. (2021), “Study on the properties of the liner of HTPE propellant”, *Science and Technology of Energetic Materials*, 82(3), 70–74, https://doi.org/https://doi.org/10.34571/stem.82.3_70

[18] Kakade, S. D., Navale, S. B., Kadam, U. B., & Gupta, M. (2001), “Effect of fillers and fire-retardant compounds on hydroxy-terminated polybutadiene-based insulators”, *Defence Science Journal*, 51(2), 133–140, https://doi.org/10.14429/dsj.51.2213

[19] Gupta, D. C., Deo, S. S., Wast, D. V, Raomore, S. S., & Gholap, D. H. (1995), “HTPB-Based Polyurethanes for Inhibition”, *Journal of Applied Polymer Science*, 55, 1151–1155.

[20] Haska, S. B., Bayramli, E., Pekel, F., & Özkar, S. (1997), “Mechanical properties of HTPB-IPDI-based elastomers”, *Journal of Applied Polymer Science*, 64(12), 2347–2354, https://doi.org/10.1002/(sici)1097-4628(19970620)64:12<2347::aid-app9>3.3.co;2-c

[21] Benli, S., Yilmazer, Ü., Pekel, F., & Özkar, S. (1998), “Effect of fillers on thermal and mechanical properties of polyurethane elastomer”, *Journal of Applied Polymer Science*, 68(7), 1057–1065, https://doi.org/10.1002/(sici)1097-4628(19980516)68:7<1057::aid-app3>3.3.co;2-e

[22] Libardi, J., Ravagnani, S. P., Morais, A. M. F., & Cardoso, A. R. (2010), “Diffusion of plasticizer in a solid propellant based on hydroxyl-terminated polybutadiene”, *Polimeros*, 20(4), 241–245, https://doi.org/10.1590/S0104-14282010005000048

[23] Grythe, K. F., & Hansen, F. K. (2006), "Diffusion rates and the role of diffusion in solid propellant rocket motor adhesion", *Journal of Applied Polymer Science*, 103(3), 1529–1538, https://doi.org/10.1002/app.25086

[24] Haska, S. B., Bayramli, E., Pekel, F., & Özkar, S. (1997), "Adhesion of an HTPB-IPDI-based liner elastomer to composite matrix and metal case", *Journal of Applied Polymer Science*, 64(12), 2355–2362, https://doi.org/10.1002/(sici)1097-4628(19970620)64:12<2355::aid-app10>3.3.co;2-7

[25] Gercel, B.O., Üner, D.O., Pekel, F. and Özkar, S. (2001), "Improved adhesive properties and bonding performance of HTPB-based polyurethane elastomer by using aziridine-type bond promoter", *Journal of Applied Polymer Science*, 80: 806-814, https://doi.org/10.1002/1097-4628(20010502)80:5<806::AID-APP1158>3.0.CO;2-G

[26] Gottlieb, L. and Bar, S. (2003), "Migration of Plasticizer between Bonded Propellant Interfaces", *Propellants, Explosives, Pyrotechnics*, 28: 12-17, https://doi.org/10.1002/prep.200390000

[27] Hori, K., Iwama, A., & Fukuda, T. (1985), "On the adhesion between Hydroxyl-Terminated Polybutadiene Fuel-Binder and Ammonium Perchlorate. Performance of bonding agents", *Propellants, Explosives, Pyrotechnics*, 10(6), 176–180, https://doi.org/10.1002/prep.19850100604

[28] Szycher, M. (2013), *Szycher's Handbook of Polyurethanes*, 2nd Edition, CRC Press. Florida.

[29] Quagliano, J., Wittemberg, V., Gonzalez, J., & Bacigalupe, A. (2015), "Mechanical and rheological properties of polyurethane elastomers from hydroxy-terminated polybutadiene and isophorone diisocyanate used as liners for composite propellants", *Journal of Research Updates in Polymer Science*, 4(1), 50–55. https://doi.org/10.6000/1929-5995.2015.04.01.6

[30] Giants, T.W, (1991), “Case-bond liner systems for solid rocket motors”. The Aerospace Corporation, El Segundo, California, USA, Aerospace Corporation Report No.TR 0090(5935-02)-1.

[31] Quagliano, J., Bocchio, J., & Ross, P. (2019), “Mechanical and Swelling Properties of Hydroxyl-Terminated Polybutadiene-Based Polyurethane Elastomers”, *Jom*, 71(6), 2097–2102, https://doi.org/10.1007/s11837-019-03417-8

[32] Ross, P., Escobar, G., Sevilla, G., & Quagliano, J. (2017), “Micro and nanocomposites of polybutadienebased polyurethane liners with mineral fillers and nanoclay: Thermal and mechanical properties”, *Open Chemistry*, 15(1), 46–52, https://doi.org/10.1515/chem-2017-0006

[33] Kim, H. J., Kwon, Y., & Kim, C. K. (2013), “Thermal and mechanical properties of hydroxyl-terminated polybutadiene-based polyurethane/polyhedral oligomeric silsesquioxane nanocomposites plasticized with DOA”, *Journal of Nanoscience and Nanotechnology*, 13(1), 577–581, https://doi.org/10.1166/jnn.2013.6944

[34] Dubois, C., Rajabian, M., & Rodrigue, D. (2006), “Polymerization compounding of polyurethane-fumed silica composites”, *Polymer Engineering and Science,* 46, 360-371.

[35] Jiqiao, L., & Baiyun, H. (2001), “Particle size characterization of ultrafine tungsten powder”, *International Journal of Refractory Metals and Hard Materials*, 19(2), 89–99, https://doi.org/10.1016/s0263-4368(00)00051-2

[36] P. Bowen (2002), “Particle Size Distribution Measurement from Millimeters to Nanometers and from Rods to Platelets”, *Journal of Dispersion Science and Technology,* 23(5), 631-662, DOI: 10.1081/DIS-120015368

[37] B. Akbari, M. Pirhadi Tavandashti, & M. Zandrahimi (2011), "Particle size characterization of nanoparticles – A practical approach", *Iranian Journal of Materials Science and Engineering*, 8(2), 48-56.

[38] Gregg, S.J. and Sing, K.S.W. (1982), *Adsorption, Surface Area and Porosity*, 2nd Edition, Academic Press, London.

[39] ASTM. (2014), "*Standard Test Method for Tensile Properties of Plastics"* (ASTM D638-14), ASTM International, https://www.astm.org/

[40] Military Agency for Standardization, NATO. (2002), "*Explosives: Thermal Characterization by Differential Thermal Analysis, Differential Scanning Calorimetry and Thermogravimetric Analysis"* (STANAG 4515).

[41] Military Agency for Standardization, NATO. (2001), "*Explosives, Physical/Mechanical Properties, Thermomechanical Analysis for Determining the Coefficient of Linear Thermal Expansion (TMA)"* (STANAG 4525).

[42] Gupta, T., & Adhikari, B. (2003), "Thermal degradation and stability of HTPB-based polyurethane and polyurethaneureas", *Thermochimica Acta*, 402(1-2), 169–181, https://doi.org/10.1016/s0040-6031(02)00571-3.

[43] Chattopadhyay, D. K., & Webster, D. C. (2009), "Thermal stability and flame retardancy of polyurethanes", *Progress in Polymer Science*, 34(10), 1068–1133, https://doi.org/10.1016/j.progpolymsci.2009.06.002.

[44] Aslan, O., (2021), "*Improvement of rheological, mechanical and interface properties of solid rocket motor liner*" MSc. Thesis, Middle East Technical University.